Dissertation

on

THE TIME-VARIATION OF COSMIC RAY INTENSITY NEAR THE GEOMAGNETIC EQUATOR

presented

by

RAJARAM P. KANE

of the

Physical Research Laboratory

Ahmedabad

for the degree of

Doctor of Philosophy

of the

University of Bombay.

MAY 1952.

PREFACE.

The work described in the present thesis forms part of a wider investigation planned by the Physical Research Laboratory, Ahmedabad, for studying the time-variation of the various cosmic ray components in low latitudes. The investigation was carried out both at Kodaikanal and Ahmedabad. The work at Kodaikanal was done by the author and is described in the present thesis. The work at Ahmedabad has been carried out by my colleague Mr. U. D. Desai.

During the building of the apparatus for the present investigation, described in Chapter II, the author received assistance from Mr. Desai, for which he is deeply grateful. The entire running of the apparatus at Kodaikanal, as well as the computation and analysis of data, described in Chapters III and V, was conducted by the author. In the discussions and conclusions given in Chapters IV and VI, the interpretation of the overall data collected at both Kodaikanal and Ahmedabad has been made in collaboration with Mr. U. D. Desai and Dr. V. A. Sarabhai.

Facilities at Kodaikanal were generously provided by the India Meteorological Department for which the author is obliged to Mr. Sohoni, Dr. A. K. Das, Dr. Ananthkrishnan and Mr. Bhargava of the India Meteorological Department.

The project under which the present investigation was carried out, was supported by the Atomic Energy Commission of India. I take this opportunity to express my gratitude to the Commissioners for their help.

My thanks are also due to all my colleagues in the laboratory for their kind cooperation during the course of the investigation. Mr. J. V. Dave has rendered assistance in making the diagrams for this thesis.

I express my deep gratitude to Dr. V. A. Sarabhai for his continuous guidance throughout the course of this investigation. I am indebted to Dr. K. R. Ramanathan for guidance and helpful discussions especially on the meteorological aspect of the problem.

CONTENTS.

I. INTRODUCTION.

The time-variation of cosmic ray intensity has been studied systematically during the last two decades. The variations can be divided into two distinct groups viz. the non-periodic variations and the periodic variations. The former consist of variations due to changes in meteorological factors, magnetic activity, solar flares, etc. The periodic variations can be classified according to the length of the period, namely, annual and daily, reckoned on solar time as well as sidereal and lunar times.

1. Non-periodic variations :-

The non-periodic variations have been studied extensively by using both ionization chambers and G-M counters as detecting devices. The results have proved the existance of a mass-absorption effect as well as an effect due to changes in heights of isobaric levels in the upper atmosphere. Recently a positive temperature effect due to temperature variations in the upper atmosphere has been observed. Magnetic storms and solar flares are occasionally found to cause large changes in cosmic ray intensity which occur sometimes simultaneously all over the world.

1.1. Effect of meteorological factors :-

Day-to-day changes in ground pressure are found to be negatively correlated with the variations of the daily

means of cosmic ray intensity. The pressure coefficient as found by many workers for the total and the meson intensities, varies between -1.0 % and -5.0 % per cm.Hg. (Refer to Table 26 p.119-120). As pointed out by Duperier,[1] this may be due to the fact that the overall pressure coefficient is not purely a mass-absorption effect but also includes a factor due to meson decay, since the height of the meson formation layer is related to the ground pressure by the hypsometric formula. Duperier found that the partial correlation $r_{CH.P}$ between cosmic ray intensity 'C' and height of any isobaric level 'H', the ground pressure remaining constant, increased for higher levels and was highest for H = 16.1 km., the maximum level for which radiosonde data were then available.

These results were obtained for the total intensity of the cosmic rays. Later on, the experiment was repeated with a narrower angle of the counter telescope and a lead absorber of 25 cm. thickness was interposed in between the counter trays. The partial correlation $r_{CH.P}$ then increased upto the height corresponding to the 200 mb. level but decreased rapidly for heights between 200 and 100 mb. levels. Additional factors were looked into for explaining the variations of meson intensity. Duperier[2] calculated the partial correlations $r_{C\theta.PH}$ between cosmic ray intensity 'C' and the temperature 'θ' just below an isobaric level, the ground pressure 'P' and the height of that isobaric level 'H' remaining constant. The partial correlation had

a high positive value (+ 0.68) for the region between 200 and 100 mb. levels but was insignificant for any lower level. In a recent paper, Duperier[3] has shown that the correlation is still better if the temperature between 200 and 50 mb. levels is considered instead of that between 200 and 100 mb. levels.

It can be concluded therefore, that the ground pressure, the height of the 100 mb. level and the temperature between the 200 and 50 mb. levels are all effective in causing the variations of the meson intensity at ground level. The 'positive temperature effect' is interpreted by Duperier[2] as being due to competitive processes of nuclear capture and decay of π- mesons. The π- mesons produced by cosmic ray primaries, either decay into μ- mesons or get captured in a nuclear collision. The probability of capture is increased for greater densities. Hence, a decrease in temperature is instrumental in increasing the probability of nuclear capture and correspondingly decreasing the number of μ- mesons which are produced by decay. This interpretation explains the positive effect of temperature qualitatively; but numerical calculations[3] show that the observed temperature effect is about 3 times greater than the temperature effect calculated on the basis of the values of $T_\pi = 2.6 \times 10^{-8}$ sec. and R = 60 gm.cm^{-2}, where T_π is the life-time and R the mean free path for a nuclear interaction for a π- meson. Duperier's interpretation seems therefore to be somewhat doubtful.

1.2 Effects connected with magnetic and solar activity:-

It has been observed by several workers that the intensity of cosmic rays decreases during some magnetic storms. The relationship between the two has not however been found to be quite consistent. Large magnetic storms are sometimes found to be unconnected with any observable change of cosmic ray intensity.

Hoge[4] has shown that the variations of cosmic ray intensity during magnetic storms are broadly similar to the storm-time variations of H (horizontal component of earth's magnetic field) which are characterised by sudden initial changes followed by a slow recovery. It is also found that the cosmic ray changes, especially when they are very large, are delayed by a few hours relative to the large changes of H.

Explanation of the changes of cosmic ray intensity during magnetic storms has been attempted notably by Chapman[5], Forbush[6], Johnson[7] and Alfven[8,9]. Existence of ring currents at several earth radii and the creation of electric fields by the motion of charged particles in the solar magnetic field have been looked into for an understanding of the problem; but the theories are still beset with a number of difficulties.

The increase of cosmic ray intensity with solar flares has been observed by several workers e.g. Lange and Forbush,[10] Duperier,[1] Ehmert,[11] Clay,[12] etc. The main characteristics of such variations are :

(a) The variations are not always world-wide.

(b) The maximum of the cosmic ray intensity and solar flare occur at about an hour's interval.

(c) The magnitude of the effect differs for stations at different latitudes and increases rapidly with altitude.

(d) The effect is greatly reduced near the geomagnetic equator, suggesting that the primaries responsible for these variations have momenta less than 10 BeV/c.

In order to explain this effect, different mechanisms have been suggested for the acceleration of particles upto energies of about 10 BeV. near the sun. The arguments can be summarized as follows :

(1) Alfven[8,9] - Acceleration of such particles in the electric fields associated with solar corpuscular streams polarised due to their motion through the solar magnetic field.

(2) Ehmert[11] - Acceleration by the betatron action of the changing magnetic field of a growing sunspot. This possibility was also suggested by Swann[52] earlier in 1933.

(3) Menzel and Salisbury[13] - Electro-magnetic waves of low frequencies (1000 to .01 cycles/sec.) may be produced because of fluctuations in sunspot magnetic fields due to turbulence in the solar atmosphere. These waves are propagated outwards from the sun and produce electric fields

which accelerate charged particles to energies upto 10 BeV.

(4) Forbush, Gill and Vallarta[14] - The magnetic bi-polar field of a sunspot group may reduce the effective solar field to such a value as to allow comparatively low energy particles to be emitted from the surface of the sun.

The experimental data are still insufficient to decide if any of these suggestions is valid.

It may be remarked that occasionally, such variations of cosmic ray intensity, either due to solar flares or due to magnetic storms, are found to occur simultaneously all over the world. World-wide changes have been notably reported by Forbush[15].

2. Periodic variations :-

2.1 Seasonal variation :-

A seasonal variation in cosmic ray intensity has been reported by many workers e.g. Forbush[15,16], Hess and Graziadei[17], Hogg[18], etc. The maximum of the intensity is found to be in winter and the minimum in summer. The variation is thus opposite in phase to the ground temperature.

An explanation of this negative temperature effect has been given by Blackett[19] on the basis of the instability of the μ -meson. A warming of the atmosphere as a whole increases the height of the meson formation layer. The mesons have therefore to travel a greater distance before

they reach the ground and their probability of decay is increased. This results in a reduction of the meson intensity at ground.

The temperature coefficient is found to vary by as much as 2 : 1 from winter to summer. (Hogg[18], Hess[17]). The discrepency is reduced to some extent when average temperature upto 16 km. is considered. This can be understood since it is this temperature rather than the ground temperature which is really effective in causing the expansion and contraction of the atmosphere as a whole.

Vallarta and Goddart[20] had suggested an alternative explanation connected with the solar magnetic field. They had assumed a dipole moment of 10^{34} gauss cm^3 for the sun and had taken into consideration (a) the yearly change in the heliomagnetic latitude of the earth due to the angle between the sun's dipole and the plane of the ecliptic (b) the periodic change in the distance of the earth from the sun and (c) the effect due to the angle between the earth's axis and the plane of the ecliptic. The variation calculated in this way does not agree with the results of Forbush and Gill. In any case, there is strong experimental evidence denying the existence of a permanent solar magnetic field at the present time[21,22,23].

Elliot and Dolbear[24] have studied the seasonal variation with G-M counter telescopes. The monthly means of cosmic ray intensity, after correcting for barometric

effect, show a high negative correlation with the height of the 100 mb. level. The decay coefficient is -3.55 % /km. and differs significantly from the value -5.70 % /km. obtained from day-to-day values for the same data. However, there are slight discrepencies between the variation of cosmic ray intensity and the variation of the height of the 100 mb. level for some months. The authors therefore conclude that some additional factor is operative in causing these variations. The possibility of a positive temperature effect reported by Duperier is considered by the authors.

2.2 Daily variation :-

Variations of cosmic ray intensity with a period of one sidereal day have been reported by some workers[24,25,26]. The variation is not however fully established so far. Such a variation, if it exists, is of great importance from the point of view of getting a clue to the origin of cosmic radiation.

Variations with local solar time have been investigated under different atmospheric conditions and for places differing in latitude and longitude. A summary of the work done upto 1947 has been given by Nicolson and Sarabhai[27]. The following table includes additional data from work published subsequently. The notations used are :-

λ = geomagnetic latitude of the station,

h = altitude of station in metres above sea level,

ϕ = angle of cone of measured radiation (classified in general as wide and narrow),

θ = inclination of axis of observed cone to the vertical,

D(b,c);S(b,c) = diurnal (semi-diurnal) variation of amplitude b % and maximum at c hours.

+S;-S imply that the maximum of the variation is displaced by less than one hour from the maximum (minimum) of the semi-diurnal pressure variation.

I.C.;G.C. indicate use of ionization chamber; Geiger counter apparatus.

B.; E.T.;I.T. indicate correction for barometer effect; external temperature effect; internal temperature effect.

2.21 The diurnal variation :-

It can be seen from Table 1 that the diurnal variation has an amplitude of about .2 % at places in the temperate zone. However, the phase seems to vary widely from station to station and is different for stations on the same latitude. Even allowing for the fact that the different workers have applied different corrections to their data, the results are difficult to understand. The only definite conclusion that can be drawn about the diurnal variation is that the maximum occurs sometime during the sunlit hours and the minimum during the dark hours.

Also one can say in general that the percentage amplitudes of the variations observed with ionization chambers are less than those measured by counter telescopes. This can be understood in terms of the wideness of the effective solid angle in which cosmic rays are recorded by the two devices. As is clear from the results of Alfven and Malmfors, Kolhorster and Elliot and Dolbear, the phase of the diurnal variation is not the same for all zenith angles. If therefore a measuring device is measuring cosmic rays in a wide angle, the variation of intensity incident in directions on opposite sides of the zenith but equally inclined to it will have different phases. The resultant amplitude will therefore get reduced. This effect will be more prominent in an ionization chamber where the solid angle is very wide. The percentage amplitudes measured by

counter telescopes (specially those with narrow angles) would thus be larger than those measured by ionization chambers.

Another thing worthy of note is that the hour of maximum of the diurnal variation for higher altitudes is in general shifted towards earlier hours in the day. This is quite clear from the results obtained at Cheltenham, Christchurch and Godhavn which are within an altitude of 100 metres above sea-level as compared with those from Hafelekar and Huyancayo which are at altitudes of 3350 m. and 2300 m. respectively above sea-level. The hours of maxima for the two groups are about 1500 hrs. and 1100 hrs. respectively. The variations obtained by other workers at sea-level show the hours of maxima sometime in the afternoon.

In most attempts at exphaining the diurnal variation, the changes in the phase of the variation from station to station are neglected. The diurnal variation is assumed to have a maximum at about midday. As an example, Vallarta and Godart[20] have suggested that such a variation can be produced at high latitudes by a heliomagnetic field and at low latitudes by variations of the geomagnetic field. Obviously, this explanation cannot account for the changes in phase of the diurnal variation for stations on the same latitude. Moreover, Malmfors[48] has shown that the results he has obtained with Alfven in Stockholm are not compatible with this explanation. His results are particularly

interesting because they cannot be explained by meteorological effects. As Malmfors suggests, the results may be due to small disturbances in the isotropy of the primary radiation.

The results obtained recently by Elliot and Dolbear[24,35] with directional counter telescopes show a marked difference between the diurnal variation for cosmic rays coming in the north and south directions. The hour of maximum for the former is shifted earlier by about 2 hrs. The two telescopes are inclined to the vertical by 45°. Since the latitude of Manchester is 53° N, the north telescope is pointing approximately to a fixed direction in space, whereas the south telescope sweeps across the sky in the equatorial plane of the earth. The atmospheric effects for both the telescopes are alike since the particles from both the north and south have travelled the same amount of atmosphere under approximately similar conditions. The difference in the two variations may therefore be attributed to a non-isotropy of primary radiation, a measure of which is obtained by the difference curve between the two.

The difference curve so obtained can be represented by the sum of a 24 hourly and a 12 hourly component and shows a maximum at about 18 hrs. and a minimum at about 10 hrs.

Elliot and Dolbear have suggested that the non-isotropy may be connected with the emmission of corpuscular streams by the sum. According to Alfven[9], such streams get

polarised during their passage through the sun's magnetic field. Transverse electric fields are therefore produced. Elliot and Dolbear[24] point out that the direction of this field as seen from the earth will be opposite for particles emitted from the east and west limbs of the sun and would lead to a decrease of intensity in the late morning and an increase during the early afternoon, provided the solar dipole is oriented in the same way as that of the earth. This seems to be in qualitative agreement with the experimentally observed difference curve. A rough quantitative agreement is obtained by assuming a solar equatorial field of about 8 gauss. The assumption of the existance of a solar magnetic field is however doubtful as already pointed out.

2.22 The semi-diurnal variation :-

As is evident from Table 1, the nature of the semi-diurnal variation, like the diurnal variation, is widely varying from place to place and is different for different cosmic ray components. Amongst the results that may be considered to be statistically significant are firstly those of Rau which were obtained from two ionisation chambers susponded in a narrow vertical fissure of rock, 40 metres under the surface of Lake Constance. The variation is purely semi-diurnal with an amplitude of about .16 % and phase almost coinciding with that of the semi-diurnal variation of daily barometric pressure. In Rau's experiment, the

variation measured was only of mesons which could penetrate through 50 metres of water equivalent (including the atmosphere) and hence had an initial energy greater than 10^{10} eV. Moreover, the solid angle was narrow because of the presence of the fissures of rock. The intensity measured was thus almost vertical and was unaffected by magnetic variations.

The other results are those of Duperier for the total intensity of cosmic rays as measured by a counter telescope. Duperier obtained a daily variation with a diurnal component of amplitude .25 % and hour of maximum at about 17 hrs., and a semi-diurnal component with amplitude .18 % and hour of maximum at about 03 hrs. The latter was thus negatively correlated with the daily variation of ground pressure.

An explanation for both these effects is sought in terms of the Pekeris[49,50] theory of atmospheric oscillations, the implications of which have been examined by Nicolson and Sarabhai[27]. The main feature of the oscillation is the reversal of phase after a height of about 30 km. above ground. Thus for heights upto 30 km. the pressure variation has got the same phase as at ground. At 30 km. there exists a nodal surface. The pressure variations above this surface have a phase in opposition to the pressure variations below it.

These pressure variations are directly connected to the variations Δ H in the height of an isobaric level

situated at a mean height 'H' For levels upto 30 km. an increase of ground pressure would correspond to an elevation in the different isobaric levels. However for levels above 30 km. the phase of the variation would be reversed and an increase in ground pressure would lower all the isobaric levels. The values of Δ H corresponding to a pressure change of amplitude 1 mm. at sea-level are given in Table 2 for various heights 'H'. The amplitude of the oscillation increases with decreasing latitudes by a factor of about $\cos^3 \lambda$. The values given are for $\lambda = 0$ and $\lambda = 50^0$.

Table 2.

H (km.)		0	10	20	30	40	50
Δ H (km.)	λ=0	.010	.012	.012	-.002	-.086	-.272
	λ=50	.003	.003	.003	-.001	-.023	-.072

H (km.)		60	70	80	90	100
Δ H (km.)	λ=0	-.490	-.510	-.60	-1.05	-2.22
	λ=50	-.129	-.135	-.16	-0.28	-0.59

The positive or negative correlation with the semi-diurnal component of ground pressure can therefore be explained by assuming the meson formation layer to be either above or below 30 km. respectively. Nicolson and Sarabhai have shown that the positive pressure effect in Rau's results can be explained by assuming that the mesons are formed at an average height of about 65 km. above ground. Above the nodal surface at 30 km. the amplitude of the pressure

variation increases rapidly and attains at about 70 km.,a value of the right order to explain the ground variation of meson intensity. However, the portion of atmosphere left above 70 km. is only 1/8000 th of the whole atmosphere. The primary radiation has therefore to traverse only this much mass before it produces the secondary meson component. Such an assumption leads to an abnormally high value for the cross-section of meson formation, if the primary radiation is supposed to be composed of protons. Even for heavy nuclei in the primary radiation, such as are found by Freier[51] et al., the discrepency would not be removed.

The negative pressure effect observed by Duperier can be explained qualitatively by assuming the meson formation layer to be below 30 km. The height variation is in phase with the pressure variation below 30 km. An increase of ground pressure is associated with an increase in height of the various isobaric levels. The cosmic ray intensity is therefore decreased because of an increased probability of meson decay. Since an increase in ground pressure also increases the mass absorption effect, both these effects are in the same direction. Duperier has got a pressure coefficient of -3.5 % per cm.Hg.,out of which 60 % is attributed by him to mass absorption and the remainder to the decay process.This requires an amplitude of height variation of about 22 metres at the height of 16 km. As is seem from Table 2, the maximum displacement of isobaric levels below 30 km. is only about 3 metres at 50^{0} latitude.

It is evident, therefore, that the positive and negative pressure effects obtained by Rau and Duperier cannot be explained quantitatively on the basis of variations of the heights of isobaric levels, produced by the Pekeris oscillation. On the other hand, it is difficult to imagine an alternative process which can produce such variations in cosmic ray intensity.

3. Statement of the problem :-

The broad features of the problem of the time-variation of cosmic ray intensity can be summarised as follows :

(1) Dependence on the latitude and altitude of the station — The semi-diurnal component of the daily variation of atmospheric pressure is expected to produce variations in the meson intensity. The amplitude of the pressure variation increases rapidly for decreasing latitude. On the other hand, the day-to-day changes in barometric pressure are more prominent in higher latitudes as compared to the tropics. A study of the day-to-day variations would therefore be more revealing in higher latitudes whereas a study of the daily variation would be more reliable and conclusive in lower latitudes. Also, the amplitude of the variation of cosmic ray intensity is more pronounced at higher altitudes. A study of the variation at mountain stations and at low latitudes is, therefore, desirable.

(2) Dependence on the nature of the particles — The nature of the daily variation of cosmic ray intensity depends largely upon the nature of particles under consideration, because (a) the interactions of the various types of fundamental particles in cosmic rays with the constituents of the atmosphere are different and (b) certain components of cosmic

ray intensity are produced primarily in certain strata of the atmosphere and there is a great deal of difference in the variations of the meteorological factors at different elevations. The nature of the daily variation depends, therefore, upon the component studied. To resolve the complications due to these factors, it is desirable to separate the various components.

(3) Dependence upon the angle of incidence — The phase and amplitude of the daily variation are dependent upon the angle of incidence of the observed particles with respect to the zenith. Measurement of the intensities within restricted angles is, therefore, expected to bring out more clearly the amplitude and phase of the true variation. It is desirable, therefore, to use counter telescopes (with narrow angles) instead of ionisation chambers which measure intensity from all directions.

Taking these factors into account, a special apparatus was designed to study the time-variation of the various cosmic ray components in low latitudes. The apparatus consisted of a number of triple coincidence telescopes with varying amounts of absorber. The instrument thus measured the total and the meson intensities restricted in narrow vertical cones.

Duplicate units of this apparatus were constructed and installed, one at the Solar Physics Observatory, Kodaikanal (mag.lat. 1°N, alt.7688 ft.) and the other at Ahmedabad (mag. lat.13°N, alt.180 ft.).

The results obtained at Kodaikanal by the author are described in this thesis. The nature of the variations at Kodaikanal and Ahmedabad is discussed in chapter IV.

II. THE APPARATUS.

The main components of the apparatus used for the present investigation are Geiger counters with their associated electronic units and an automatic photographic unit. All these were prepared in the laboratory.

Section 1 of this chapter deals with the experimental arrangement and the photographic unit for taking automatic hourly exposures of the dials of the mechanical recorders. Sections 2 and 3 give detailed accounts of the Geiger counter and electronic units used in the experiment.

1. Experimental arrangements and the automatic photographing device:-

1.1 Experimental arrangement for measuring the total and the meson intensities :-

The apparatus consists essentially of two sets of three triple coincidence counter telescopes. Following is a schematic diagram of the counter arrangement and the electronic units associated with it:-

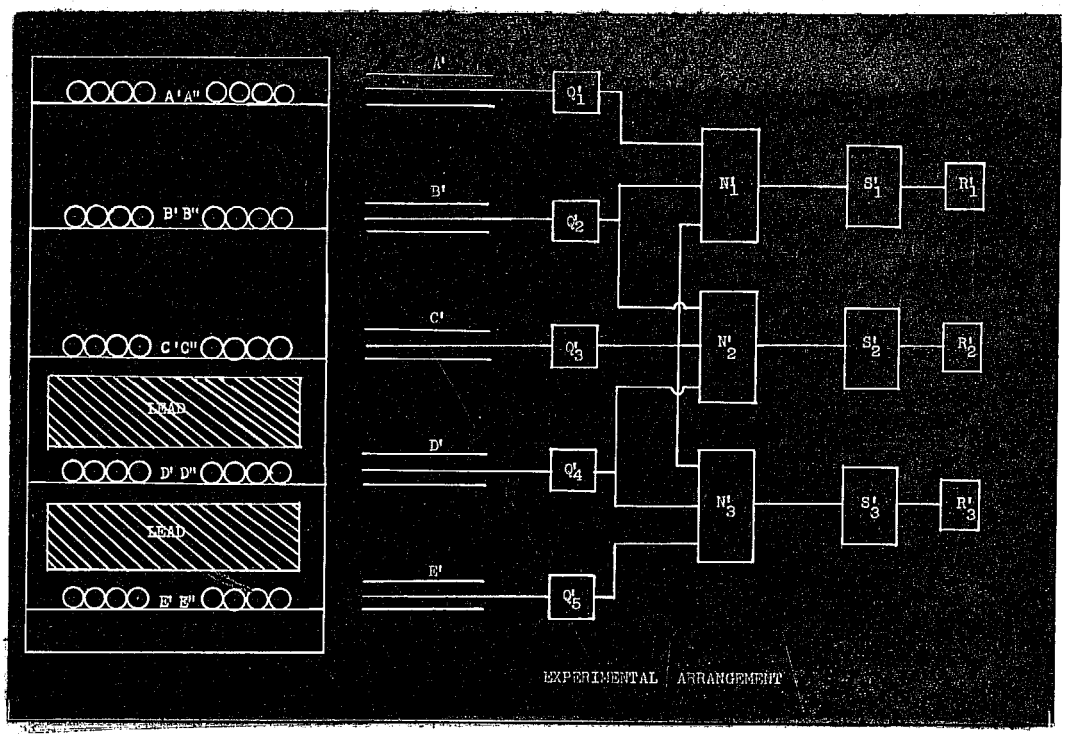

Fig. 1. Experimental arrangement for measuring the total and the meson intensities.

Five counter trays A', B', C', D', E' each containing four G-M counters in parallel, are arranged one above the other and the triple coincidences A'B'C', B'C'D' and C'D'E' are measured. A similar set of trays A", B", C", D", E" is arranged alongside of them and coincidences A"B"C", B"C"D" and C"D"E" are measured independantly.

The output of each of the trays A', B', C', D', E' is fed to a separate quenching unit (Q'_1 etc.). The outputs of quenching units Q'_1, Q'_2 and Q'_3 are fed to the coincidence unit N'_1 which gives an output pulse only when Q'_1, Q'_2, and

Q'_3 are triggered simultaneously. The output of N'_1 is fed first to a scaler S'_1 and thence to a mechanical recorder R'_1. The recorders R'_1, R'_2 and R'_3 thus record the scaled coincidence rates A'B'C', B'C'D' and C'D'E'. Similar recorders R''_1, R''_2 and R''_3 (not shown in the figure) record the coincidence rates A"B"C", B"C"D" and C"D"E".

The sensitive area of each of the trays is about 500 sq. cms. (length = 30 cms., breadth = 16 cms.) and the vertical separation between any two trays is 20 cms. The semi angles of the telescopes A'B'C' etc. are thus 37^0 in the lengthwise and 22^0 in the breadthwise direction. All the counters are arranged with their axes in the north-south direction. Thus the telescopes measured particles in a wider angle in the N-S direction than in the E-W direction. Since one of the primary objects of the experiment was to study the daily solar time variation which is produced by the rotation of the earth from West to East, a narrower angle of the telescopes in this direction was expected to be advantageous. In between the trays C'-C" and D'-D" and also between D'-D" and E'-E" lead plates of 38 cm. x 30 cm. and thickness of about 1 cm. are piled up one above the other. They intercept the solid angles of the telescopes B'C'D', B"C"D" and C'D'E' , C"D"E" completely and give an effective lead thickness of 7 cm. between trays C'-C" and D'-D" and 8 cms. between trays D'-D" and E'-E".

II.

1.

The coincidence rates R_1' and R_1'' thus represent the total cosmic ray intensity and are designated by T' and T'' respectively. The rates R_2' and R_2'' correspond to the intensity of particles, which can penetrate through 7 cm. of lead and are designated as M_1' and M_1'' respectively. The rates R_3', R_3'' correspond to the intensity of cosmic ray particles capable of penetrating through 15 cm. of lead and are designated as M_2', M_2''.

The counter assembly as a whole is enclosed in a box with walls of sheets made of a thermally insulating compressed fibre. At Kodaikanal, where the investigation was carried out, the daily range of ground temperature is very small ($\sim 10^0$ F). The use of an insulating material for the walls reduces the range of the temperature variation inside the box still further. Actual measurements showed it to be always less than 4^0 F during the course of the day. No special temperature controlling device was therefore needed for the present investigation.

The advantage of having two similar telescopes running independently side by side is in providing a comparison with respect to each other. In case a telescope stops functioning because of any counter failure, the rate of the adjoining telescope serves for standardising the counting rate of the corrected telescope in terms of its original rate. Even otherwise, two independent telescopes showing similar trends of variation for any cosmic ray component increase the reliability of both observations.

II.

The advantage of a triple coincidence arrangement over a double coincidence arrangement is firstly to reduce the effect of side-showers. As estimated by Greisen and Neresson[54], the contribution due to side showers to a vertical coincidence rate at sea level is about 15 % for double coincidence and 7 % for triple coincidence for a separation of 35 cm. between the extreme counters.

Secondly, a multiple coincidence set-up helps in reducing the percentage of chance coincidences. If a tray of counters is measuring cosmic rays at the rate of 'n_1' per sec., the probability that a count will occur during a time interval 't' (viz. the resolving time of the coincidence circuit) is

$$P_1 = n_1 \cdot t \quad \ldots\ldots\ldots\ldots (1)$$

For other trays with counting rates n_2, n_3 etc. the probabilities will be P_2, P_3 etc. A chance coincidence occurs when independent particles pass through the different trays all in the same time-interval 't'. The probability that two independent counts will occur during the same interval 't' is

$$P_{1,2} = 2 P_1 \cdot P_2 = 2 n_1 \cdot n_2 \cdot t^2 \ldots\ldots (2)$$

The product of the individual probabilities is multiplied by 2 because the time interval is overlapping.

For m-fold coincidences

$$P_{1,2,\ldots m} = m \cdot n_1 \cdot n_2 \ldots n_m \cdot t^m \quad \ldots\ldots\ldots (3)$$

If the tray rates n_1, n_2 etc. are all alike

$$P = m \cdot n^m \cdot t^m \quad \ldots\ldots\ldots\ldots\ldots (4)$$

This represents the probability of a chance coincidence during an interval 't'. The rate of chance coincidences is given by

$$R = P/t = m \cdot n \cdot (nt)^{m-1} \quad \ldots\ldots\ldots\ldots (5)$$

$$\therefore \% \text{ Rate} = \frac{100\ R}{n} = 100 \cdot m \cdot (nt)^{m-1} \quad \ldots\ldots (6)$$

The resolving time 't' of a coincidence circuit is usually of the order of a few microseconds. The factor $(nt)^{m-1}$ therefore, decreases very rapidly with increasing values of 'm' and more than compensates for the increase of 'R' due to the factor 'm'. Thus multiple coincidence arrangements are instrumental in reducing the percentage of chance coincidences. The percentage can also be reduced by reducing the individual counting rate 'n' which is however not desirable, since high counting rates are necessary to get statistically significant results within a reasonable period.

The use of a scaling stage between the coincidence and recording stage serves two purposes. Firstly, it

reduces the counting rate and the wear of the mechanical recorder which has got an optimum usable range of about one million counts before deterioration. Secondly, it reduces the losses due to the finite resolving time of the mechanical recorder.

When the resolving time of the mechanical recorder is T (of the order of 10^{-1} sec.) it can count only those pulses which are separated from each other by at least a time interval T. Pulses following each other within this interval would only be counted as one. If the recorder be now subjected to a random counting rate averaging 'n' per second, the average number of pulses arriving during the interval T is given by

$$\bar{n} = n \cdot T = T/t, \text{ where } n = 1/t \quad \ldots\ldots (7)$$

For a random distribution the probability that 'x' number of particles will arrive when an average rate of 'n' is expected is given by

$$P_x = \frac{(\bar{n})^x}{x!} e^{-\bar{n}} \quad \ldots\ldots\ldots\ldots\ldots (8)$$

For proper counting, the rate 'x' coming during the interval T should not exceed unity. Hence the probability of losing counts is given by

$$P = \sum_{x=1}^{x=\infty} \frac{(\bar{n})^x}{x!} e^{-\bar{n}} \quad \ldots\ldots\ldots$$

$$= 1 - e^{-\bar{n}}$$

$$= 1 - (1-\bar{n} + \frac{\bar{n}^2}{2!} - \frac{\bar{n}^3}{3!} \ldots\ldots)$$

$$= (\bar{n} - \frac{\bar{n}^2}{2!} + \frac{\bar{n}^3}{3!} \ldots\ldots\ldots\ldots) \quad \ldots\ldots\ldots (9)$$

For low counting rates 'n', the fraction 'nT' is small and the fractional loss given by (9) can be taken to be $\bar{n} = T/t$ to a first approximation.

If a scaling stage is now introduced, the output of the scaler willnot remain a Poisson distribution. For a scale of two, the losses will occur when the number of particles arriving in the interval T will exceed 2. The fractional loss is therefore given by

$$P = \sum_{x=2}^{x=\infty} \frac{(\bar{n})^x}{x!} e^{-\bar{n}}$$

$$= e^{-\bar{n}} \cdot (e^{\bar{n}} - 1 - \bar{n})$$

$$= 1 - (1-\bar{n} + \frac{\bar{n}^2}{2!} \ldots\ldots) - \bar{n}\ (1-\bar{n} + \frac{\bar{n}^2}{2!} \ldots\ldots)$$

$$= \frac{\bar{n}^2}{2} - \frac{\bar{n}^3}{3} + \quad \ldots\ldots\ldots\ldots\ldots\ldots (10)$$

The fractional loss is thus reduced by a factor of about $\bar{n}/2$. For higher scaling stages the losses can be shown to be almost neglibible. The only limitation then is the resolving time of the scaling stages themselves which is generally of the order of a few microseconds.

At Kodaikanal, each scaler consisted of three scales of two connected in cascade giving thus a reduction in the rate by a factor of 2^3 or 8.

The voltages given to the various electronic units are from four voltage terminals viz. 420V, 210V, 150V and -70V each obtained from a separate electronically regulated power supply. The high voltage for the counters is obtained from a common high voltage power supply provided with tappings differing by 50 Volts in the range 1000-1400 volts. All the counters are operated at about 75 volts above their respective threshold voltages.

In the initial stages of the experiment lot of trouble arose due to interfeeding in the electronic circuits at Various stages. To overcome this, systematic measures had to be adapted. Firstly, shielded cable for interconnecting the counters, the quenching units and the coincidence units was used. Adequate earthing of the shields of the cables was very essential. Secondly, decoupling condensers were put across all the voltages terminals viz. high voltage 1000-1400 volts, 420V, 150V and -70V. Thirdly the bias voltages of all quenching units were properly adjusted.

The electric supply at Kodaikanal was found to be extremely unsatisfactory. The mains voltage used to fluctuate between 160 and 210 volts. This had no effect on the power supplies which were highly stabilised to take

care of input variations from 150 to 250 volts. When however, the mains voltage dropped down to 160, the filament supply was affected and the filaments used to get much less than 5 V. instead of 6.3 V. A constant voltage transformer was therefore used. This was capable of giving a constant output of 210 volts for a fluctuation of 160 to 250 volts of the mains voltage, for a total current drainage of about 4 amperes. In the present investigation the overall current drain was only 3 amperes.

1.2 The automatic photographing device :-

The mechanical recorders are mounted on a panel and photographed every hour by an automatic photographing device which is shown with the camera unit in the following diagram :

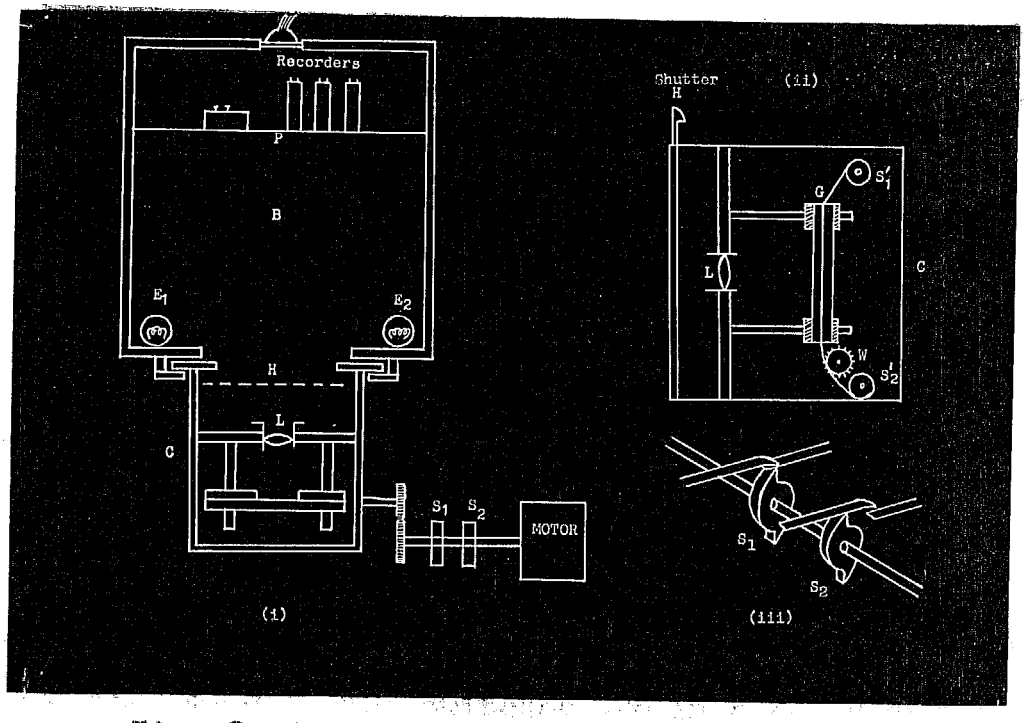

Fig. 2. Automatic photographing device.

The panel P (Fig.2.(i)) on which all the recorders R_1', R_2' etc. are mounted, forms the end side of a light tight box B. C is a detachable camera(Fig.2 (ii))in which the lens L is adjusted so as to focus the image of the panel P on the photographic film running in the groove G. The film is wound on the spool S_1' and gets collected on the spool S_2' after being pulled by the sprocket wheel W. The shaft of the sprocket protrudes outside the camera box and is driven by an electric motor. With the help of a relay arrangement triggered by an electrical contact of a few seconds duration made hourly by a clock, the following sequence of operations is achieved at regular hourly intervals:

(i) Momentarily lighting of the bulbs E_1 and E_2 which exposes the film.

(ii) Moving the exposed portion of the film in front of the lens by a distance equal to the size of the image on the film and thus making the camera ready for a fresh exposure.

The electric motor has an internal gearing arrangement so that its main shaft rotates with a very slow speed viz. one revolution per minute. Two ebonite cams each pressing against a separate switch S_1 and S_2 are mounted on the shaft. It is so arranged that S_1 is on when S_2 is off and vice versa (Fig.2.(iii)). The shaft of the motor rotates the wheel W. The switches are in a relay circuit

shown schematically in the following diagram :

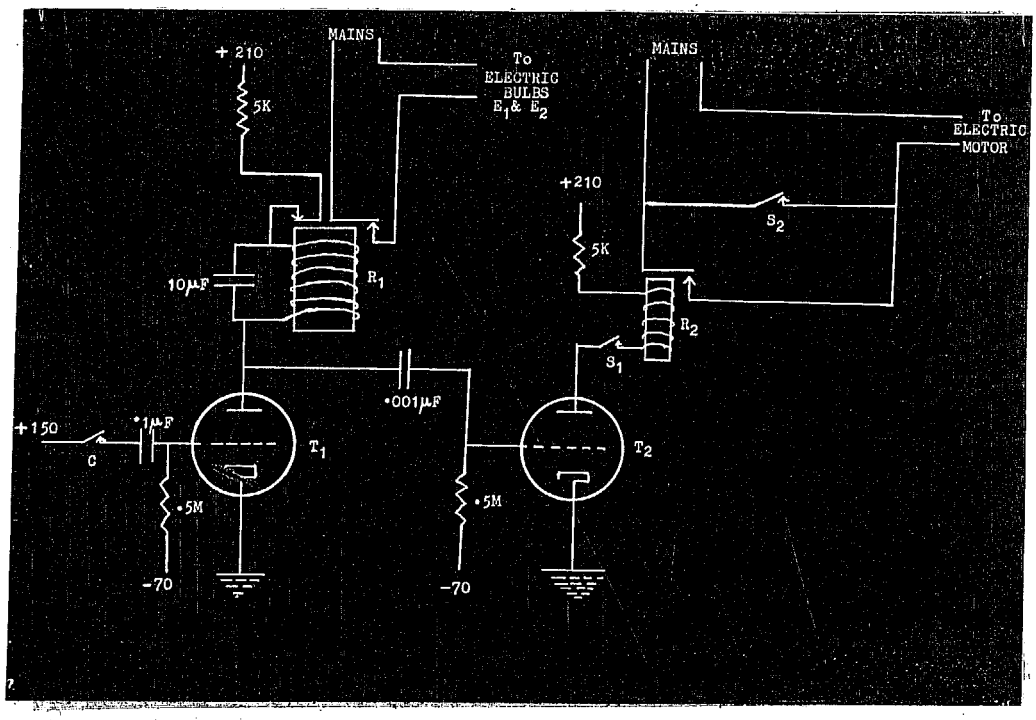

Fig. 3. Sequence control circuit.

The motor circuit is made either when S_2 is closed or when relay R_2 is closed. In the normal position of the shaft of the motor, the switch S_2 is open while S_1 is closed.

(a) Every hour, the minute hand of a pendulum clock closes the contact C and the grid of the thyratron T_1, which is normally biassed negatively, receives a positive pulse of 150 V.

(b) The thyratron T_1 passes current and relay R_1 closes whereby the lamp circuit is made. Simultaneously the plate circuit of T_1 gets open and T_1 becomes non-conducting. The relay R_1 opens and the lamps get switched off. The plate of T_1 gets a positive voltage but does not become conducting as the grid is now negatively biassed.

(c) The positive pulse from the plate of T_1 is fed to the grid of another thyratron T_2 which becomes now conducting and operates the relay R_1 since switch S_1 is on.

(d) The motor circuit is thus completed and the main shaft starts rotating. The switch S_1 is soon opened by the cam, and the thyratron circuit gets broken. But the switch S_2 is now on and hence the motor keeps running till the main shaft rotates through 180^0 and the other half of the segment under S_2 again switches it off. The size of the wheel W is adjusted so as to pull just the proper length of film during half a revolution of the shaft. Switch S_2 is thus left open while switch S_1 is closed.

The sequence of operations is now complete and cannot be repeated until the grid of thyratron T_1 again receives a positive pulse. This occurs only after an hour's interval when the clock operates the contact C.

The panel P consists of an alluminium sheet with slits for the dials of the mechanical recorder and a circular opening for a time-piece. A piece of paper with the date of the day is mounted in one corner of the panel. In Fig.4

is reporduced a typical photograph taken hourly by the camera unit.

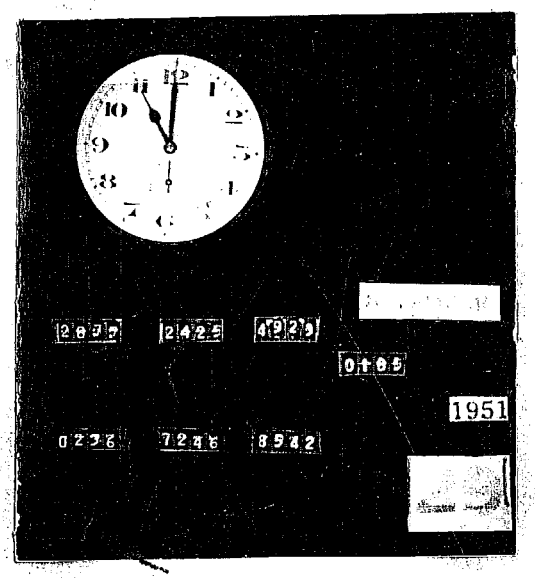

Fig. 4. Enlargement of an hourly exposure.

The film used is of the standard Kodak Super XX type. The spool S_1' can hold about 30 ft. of the film at a time. The camera unit C is detached from the rest of the apparatus every day just after the 9 A.M. exposure, and opened in darkness. The film collected on the spool S_2' is cut so as to include the 9 o'clock exposure. The loose end of the stock film is then attached once again to the take up spool S_2' and the camera unit replaced in its position in the apparatus. The cut out portion of the film is developed and washed. The hourly data is noted down and analysed as described in Chapter III.

1.3 Experimental arrangement for measuring the hard component which can penetrate 36 cm. of lead :-

The counting rates M_2' and M_2'' in 1.1 correspond

to the intensity of cosmic rays that can penetrate through 15 cm. of lead. An additional unit was set up as shown below for studying the variation of the intensity H_c that could penetrate 36 cm. of lead.

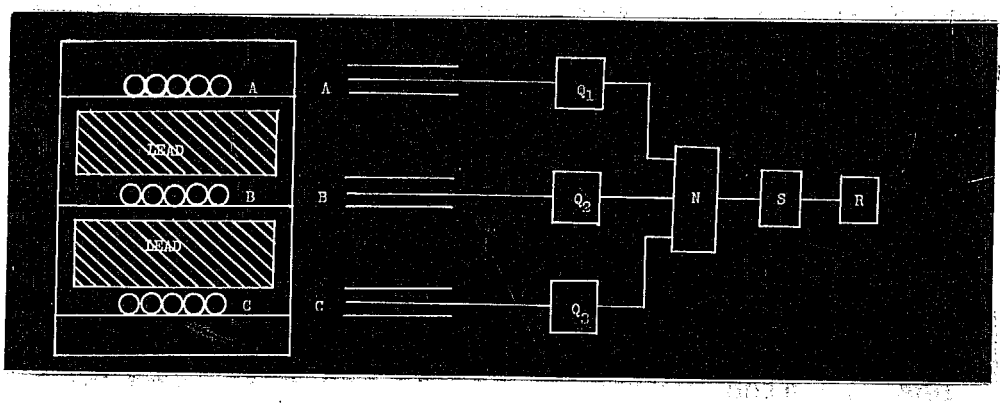

Fig. 5. Experimental arrangement for measuring the hard component.

Each of the trays A, B, C contains five counters in parallel. The counters are of the same dimensions as described earlier. The outputs of the three trays are fed to the three quenching units Q_1, Q_2 and Q_3 and the coincidences ABC are registered by the mechanical recorder R after scaling by a factor of 8 by the scaler S. The assembly of counters is enclosed in a box with walls of heat insulating material.

The axes of the counters are along the north-south direction and the trays are separated by a vertical distance of 30 cm. The semi-angles of the telescope are thus 22^0 in the north-south and 15^0 in the east-west direction. The total thickness of lead between the end

trays A and C is 36 cm. The recorder R is mounted on the panel P of the camera box and is photographed hourly.

1.4 Variation of atmospheric shower intensity :-

The variation of the intensity of atmospheric showers was studied for a short period by a modification of the apparatus described in 1.1. Alternate counters of tray C' are connected in parallel and the triple coincidence rate of tray A' and the two sections of tray C' is measured. The arrangement thus registers only atmospheric showers without any absorber. Trays B' and B'' are removed. The output of tray A' is fed to the quenching unit Q_1' and that of the two sections of C' to the quenching units Q_2' and Q_3'. The outputs of Q_1', Q_2' and Q_3' are fed to the coincidence unit N_1' as before. Since both sides are used for this purpose, the recorders R_1' and R_1'' give the independent coincidence rates scaled by a factor of 8. The combined variation is designated by S.

2. Geiger Counter :-

2.1 Counter tube technique :-

The passage of a charged particle through a gas, produces ionisation. If there is an electric field, the electrons travel towards the anode and are collected by it. The positive ions drift towards the cathode, at a

slower speed because of their heavier mass. In the case of a Geiger counter, generally the cathode is a copper cylinder and the anode is a tungsten wire stretched along the axis of the cylinder. The electrodes are enclosed in a glass envelope which is filled with a gas.

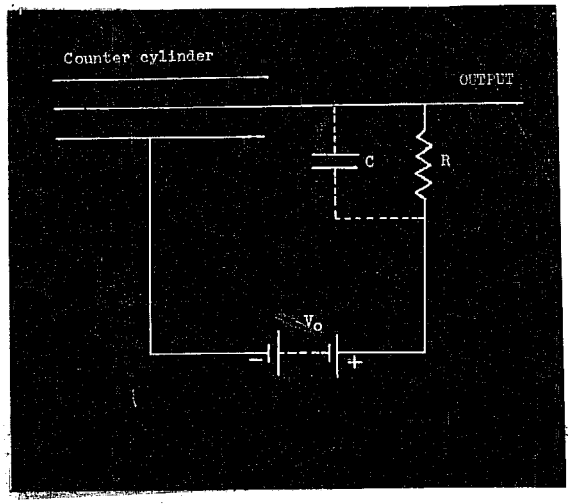

Fig. 6. Fundamental counter circuit.

Consider an experimental arrangement as shown in Fig. 6. A voltage V_o is applied across the electrodes of the counter through a resistance R having an associated capacity C in parallel. The size of the pulse developed on the central wire (anode) is determined by the charge collected by it and the effective capacity. For particles of unit electronic charge (1.60×10^{-19} coulombs) the rise of the potential of the central wire is given by

$$dV = \frac{dq}{C} = 1.60 \times 10^{-7} \times \frac{n}{C} \quad \ldots\ldots\ldots\ldots (1)$$

where 'n' = No. of electrons collected, C = the effective capacity in micromicro farads and dV = the rise in potential in volts. For low applied voltages Vo, the number of electrons 'n' arriving at the central wire is equal to

that produced in the initial ionising event minus the number which has disappeared by recombination. The counter is then operating in the ionisation chamber region.

An increase of the voltage Vo initiates the production of secondary electrons by collision. This process starts first in the neighbourhood of the central wire where the field is strongest and is sufficient to permit over a mean free path of the electron an acceleration adequate to cause further ionisation by collision i.e. the kinetic energy of the electron exceeds the ionisation potential of the gas. At this stage the original electron precipitates an 'avalanche' of secondary electrons. If each initial ion-pair produces 'A' ion-pairs by this process,

$$dV = 1.6 \times 10^{-7} \times \frac{An}{C} \quad \ldots\ldots\ldots\ldots\ldots (2)$$

'A' is termed the gas amplification. Depending upon the voltage Vo , it varies from 1 to 10^7 in the 'proportional region' which is characterised by a constant value of 'A' for a particular applied voltage V_o. The pulse size in this region is proportional to the number of ions produced in the initial ionising event.

For a further increase of V_o, the counter operates in the region of limited proportionality where the factor 'A' is not constant any more. Its value depends upon the size of the initial ionising event and is smaller for higher initial ionisation.

When the applied voltage V_o is increased still more, the size of the pulse dV on the central wire becomes independent of the number of ions formed in the initial ionising event. The product 'An' thus attains saturation and the counter is said to be operating in the 'Geiger region'. The minimum voltage at which the saturation occurs is termed as the 'threshold voltage' V_G. For any voltage V greater than V_G, all the pulses arriving on the central wire are of a particular size, proportional to the overvoltage ($V - V_G$). The number of ion-pairs produced in the initial ionising event is largely dependent upon the nature of the particles. Thus, in the non-relativistic region, an α - particle is several times more ionising than an electron or other lighter and singly charged particle of similar energy. The pulse size dV developed on the central wire due to an α - particle and an electron for different applied voltages, is shown in Fig.7 (originally given by Montogomery and Montogomery[55]).

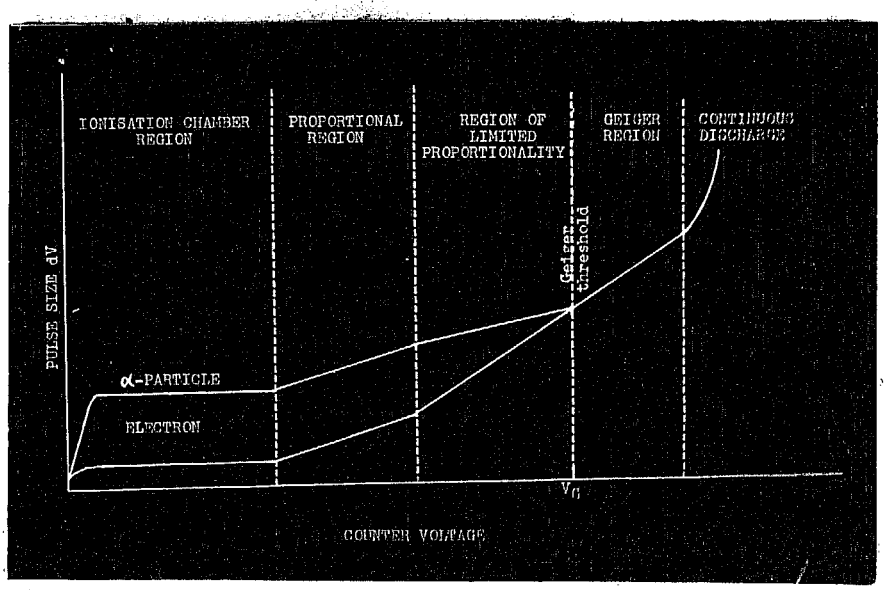

Fig. 7.

Operating characteristics of a counter in various regions for large and small ionising events.

At the end of the Geiger region the counter goes into apparently a continuous discharge which actually consists of a number of fast multiple pulses.

In the earliest experiments counters were used both in the proportional and the Geiger region. However, in most contemporary experiments, especially in coincidence work, counters are operated only in the Geiger region. The present investigation has been carried out with Geiger counters. Our discussion will therefore be confined only to this type of counter.

The mechanism of a Geiger counter discharge has been investigated by several authors and the work has been summarised by Korff[56] in his book 'Electron and Nuclear Counters- Theory and Use.' Fig. 8 gives the 'corona' or continuous discharge characteristics of a counter in the circuit of Fig. 6. It is evident that the discharge cannot be maintained unless the voltage and the current exceed minimum values V_{min} and I_{min} respectively. The current I_{min} flows through the resistance R.

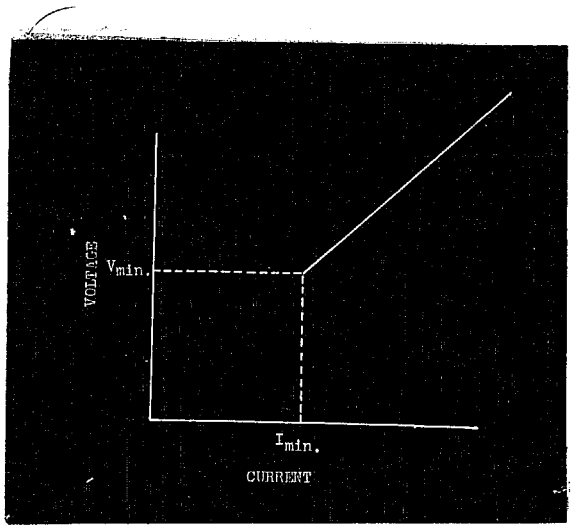

Fig. 8. Corona characteristic of a counter.

When the counter is operating at a voltage $V_o > V_{min}$, the

overvoltage on the counter is $V_o - V_{min}$. If the voltage drop $R \cdot I_{min}$ exceeds this overvoltage, the applied voltage across the counter electrodes drops down below V_{min} and the discharge stops. If V_o is increased sufficiently so that the overvoltage exceeds $R \cdot I_{min}$ by an appreciable amount, the counter tends to go into a continuous discharge. $R \cdot I_{min}$ is thus the effective range of operation or the 'plateau' of such a counter and the resistance 'R' serves the purpose of 'quenching' the discharge and keeping the counter ready for detecting the next event. This interpretation is not however strictly accurate and should be accepted with reservations.

The value of the resistance R cannot be increased indefinitely as it would increase the recovery time (RC) of the circuit and thus put a limitation to its use for fast counting. Resort is therefore made to electronic circuits which serve the purpose of quenching the discharge within a period of about 10^{-4} sec.

The same purpose can be achieved by introducing some heavy organic vapour inside the counter. Such counters are termed 'Self-quenched counters'. To understand the role of a polyatomic molecule in the process of quenching the discharge, it is first necessary to discuss the mechanism of counter discharge in greater detail.

The general picture of the atomic mechanism as examined by Montogomery and Montogomery[57] is as follows.

An electron formed somewhere in the interior of the counter due to ionisation by some ionising event, is accelerated towards the central wire and forms the 'Townsend avalanche' in this process. Because of the high mobility of the electrons, their collection at the central wire is over within a fraction of a micro-second. By then, the positive ions have hardly moved any distance and hence form a positive ion sheath around the central wire. The effect is to reduce the field strength there and thus stop the discharge. The positive ion sheath serves the purpose of actually quenching the discharge, whereas the resistance R helps in leaking the original voltage back to the central wire and thus serves the purpose of a 'recovery resistance'.

The discharge remains quenched so long as no further electrons are produced by any subsequent process. When the positive ion sheath reaches the cathode it may produce secondary electrons by positive ion bombardment. These electrons neutralize the positive ions and the neutral molecule emits its characteristic recombination radiation (photons) while returning to its ground state. These photons may emit secondary electrons on reaching the cathode, depending upon the photoelectric efficiency and work function of the material of the cathode. The voltage V_{min} can therefore be interpreted as the voltage at which every ion sheath produces at least one electron after reaching the cylinder. The secondary electron then produces another 'avalanche' and the counter goes into a continuous discharge.

The function of the 'quenching resistance' or external quenching circuit is therefore to keep the potential of the wire below V_{min} until all the positive ions reach the cylinder and are neutralised there.

The initial avalanche may not always be strong enough to produce a positive ion sheath capable of reducing the wire potential below I_{min}. However, there are photons formed in the initial avalanche itself, which on reaching the cylinder eject secondary electrons which form further avalanches. The wire thus attains its full drop of potential not in one electron avalanche but in several stages in quick succession. The subsequent recovery to a new operating potential is as usual controlled by the external quenching circuit or resistance.

This analysis by Montogomery and Montogomery is extended further by Stever[58] to interpret the 'dead-time' and 'recovery time' of a counter in terms of the motion of the positive ion sheath. 'Dead -time' is the time interval during which quenching mechanism is in operation and hence no new ionising event can be detected. For an event occuring just after the deat time interval, a small pulse of a barely detectable size is developed. For later and later instants the pulse developed is bigger and bigger till finally it regains its normal size. The phenomenon as seen on a oscilloscope screen is shown in Fig. 9.

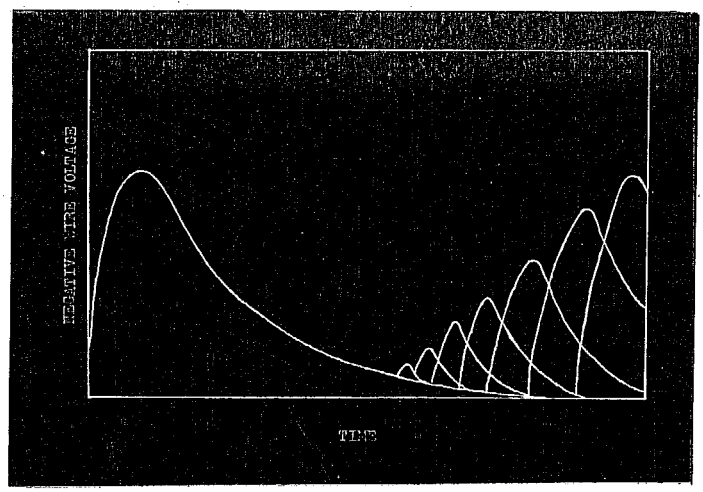

Fig. 9. Oscilloscope pattern of the dead-time and recovery time phenomena.

The recovery time is then the minimum interval after which a new pulse will be developed of the full size. Now, the positive ion sheath reduces the potential of the wire below V_{min}. As the sheath moves out the wire starts regaining its potential and returns to normal when the sheath has travelled a distance r_c (critical radius) which is related to the cylinder radius 'r' and overvoltage V as

$$r_c = r^{-V/2q} \quad \ldots\ldots\ldots\ldots\ldots (3)$$

where 'q' = the positive ion space charge per unit length. 'Dead - time' is therefore the time taken by the positive ion sheath to travel the distance 'r_c' while 'recovery time' is the time required to reach the cathode and get neutralised there. Both these are functions of the mobility of the positive ions.

As is evident by now, the process of quenching in a Geiger counter tube is of three distinct types :

(a) quenching of photons in the initial avalanche,

(b) electrostatic quenching of the avalanche by the positive ion space charge and

(c) quenching of the secondary emission when the positive ions reach the cathode.

Out of these, (b) is a process occuring in the counter independent of the presence of any polyatomic molecule. The role played by a polyatomic molecule so far as (a) and (c) are concerned is as follows.

The absorption of energy by a molecule raises it to an excited state. The reverse (de-excitation) process can occur in three different ways viz.

(1) Decomposition (dissociation),
(2) Radiation (fluorescence) and
(3) Deactivation by collision.

Out of these, (3) is negligible since this process cannot occur within 10^{-8} sec. which is the collision time in an ordinary counter. The process (1) when possible can occur within 10^{-11} to 10^{-13} sec. while process (2) has a radiation life-time of 10^{-8} sec. Diatomic molecules and some of the light polyatomic molecules have well-defined

vibrational-rotational structures and possess discrete stable electronic states well above the dissociation limit of the molecule. The de-excitation process, therefore, results mostly in re-emission of the absorbed photons and rarely in dissociation. The case of the polyatomic molecules is altogether different. Spectroscopic and photochemical data show that dissociation is more a rule than an exception in their case and their absorption spectra at low pressures show a continuous absorption in the invisible ultra-violet region. Their decomposition products are usually free radicles which combine to form some other simpler organic molecules which in some cases can act as quenching agents thus prolonging the life of a counter.

It is clear therefore that a polyatomic molecule plays a substantial role in the process (a) of quenching of the photons in the initial avalanche. One can also understand why self-quenched counters 'go bad' after use. By decomposition the large vapour molecules are all reduced to non-quenching gases and heavy hydrocarbons, which get deposited on the cathode. For the same reason, some vapours give longer life than others because their initial decomposition products are again some quenching gases.

Let us consider now the neutralisation process and the subsequent secondary emission. The non-quenching gaseous ion (e.g. an argon ion) , on approaching the cathode surface within 10^{-7} cm. can produce a field strong enough to extract an electron from the cathode. The metal surface is actually

a potential barrier which separates the electrons from the vacant energy levels of the positive ion. But there is a definite probability of the electrons leaking out through these potential barriers. If φ is the work-function of the metal, the electrons are φ volts below the top of the barrier. If the vacant energy levels of the ion are 'I' volts below the top where I = Ionisation potential of the gas, the resulting neutralised atom formed after the extraction and absorption of the electron, radiates energy equal to $(I - \varphi)$ volts. If this energy is still greater than φ, an additional photo-electron is ejected from the cathode and a secondary avalanche starts in the gas. It is in this way that a continuous discharge is maintained in the absence of any quenching device. Consider now a poly-atomic ion (e.g. methane) in place of the argon ion. Since the Ionisation energy of methane is 14.5 eV., the neutralised atom carries an excitation energy equivalent to a photon of 1200 A^{o}. For such low wave-lengths, the excited methane molecule has a life-time against decomposition of the order of 10^{-13} sec. Thus, almost all the molecules get decomposed before they are able to reach the cathode surface. Even if they do reach, the ejection of a secondary electron is most improbable because of their several bond structure. The discharge is therefore completely quenched. Any gas or vapour having a diffuse or continuous absorption spectrum corresponding to the region $(I - \varphi)$, is thus a good quenching agent. This condition is fulfilled by most heavy polyatomic molecules.

However, mixtures of quenching and non-quenching gases also exhibit similar quenching characteristics. The reason is as follows. The non-quenching gases have got higher Ionisation potentials than the quenching gases. During the time the ions of the non-quenching gas move across the counter to its cathode, they suffer $\sim 10^5$ collisions with the quenching vapour molecules. Electrons are therefore transferred from the quenching gas to the non-quenching gas in this process and the latter get neutralised, liberating photons of energy equal to the difference of the Ionisation potentials of the two gases. These photons are then absorbed by the quenching vapour. The vapour molecules which are converted into positive ions because of the transfer of electrons, reach the cathode in due course but get decomposed there as already stated.

A heavy polyatomic molecule is therefore a very good quenching agent for both the processes (a) and (c).

We have surveyed till now the actual mechanism of a Geiger counter, especially the one of the self-quenched type. Let us consider now the various operation characteristics of a Geiger counter in general.

(1) Starting potential : The starting potential is the threshold voltage of the Geiger region. For non-self-quenched counters the threshold voltages are generally lower.

(2) Flatness of the plateau : An important characteristic of a Geiger counter is its 'plateau'. For a constant source of initial ionising radiation the counting rate as measured by the counter should remain constant. The voltage region in which the rate is constant, is called the 'plateau' of a Geiger counter. Fig. 10 below give the plateau characteristics of a self-quenched counter.

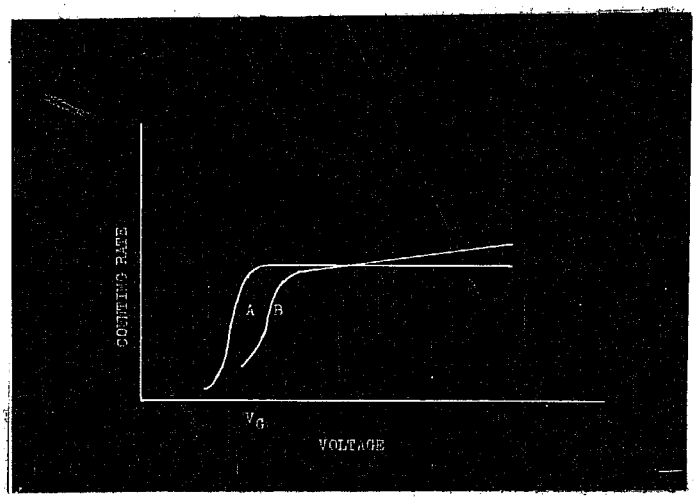

Fig. 10. Plateau characteristics of a self-quenched counter.

The curve A is for a mixture of pure gases. Curve B is for the same mixture with 2 % of air.

It is obvious that the flatness of the plateau is largely dependent upon the purity of the gases used. The impurities that are most detrimental are (i) Air and (ii) water vapour, because of the spurious counts they produce due to negative ion-formation. A plateau with a slope of

less than 3-4 % rise of counting rate per 100 volts is generally considered to be good. The advantage in having a good plateau is twofold. Firstly it ensures a proper working of the counter in the Geiger region. Secondly, the counting rate remains unaltered for small fluctuations in the applied voltage V_o.

(3) Efficiency : This is defined as the probability that the counter will record an event, which is tantamount to the formation of at least one ion-pair in the sensitive volume of the counter. The efficiency can be expressed by the formula :

$$G = (1 - e^{-slp}) \times 100 \% \quad \ldots\ldots\ldots\ldots \quad (4)$$

where s = specific ionisation of the gas mixture,
l = average path length in the counter and
p = the gas pressure.

For counters arranged in a coincidence set-up, the inefficiency of the arrangement is multiplicative. It is desirable, therefore, to have counters of very high individual efficiencies.

(4) Stability or life : Because of the decomposition of the larger vapour molecules, a self-quenched counter can be used only for a limited period, depending upon the actual number of vapour molecules. This sets up a 'life to a counter of the self-quenching type.

In case of the non-self-quenched type counter the quenching is done by external sources and hence the life of the counter is unlimited.

2.2 Selection of the type of counters :-

Since the present investigation was mainly concerned with the time variation of cosmic ray intensity, the most important requisite of a Geiger counter from our point of view was the stability of the counters. It was therefore advisible to use counters of the non-self-quenching type to avoid counters 'going bad' during the course of the investigation.

Counters were initially filled with pure (99.9 %) Argon, pure Hydrogen as well as their mixtures in different proportions. However, we did not succeed in preparing non-self-quenched counters with good plateau characteristics and hence resort was taken to the self-quenching type.

The mixture used for the self-quenched type consisted of Argon and Ethyl acetate vapour in the proportion 9 : 1 respectively and the total pressure in the counter was $\sim$ 10 cm. of Hg. The efficiency of such a counter, as calculated from eq.(4), is nearly 99.8 %. The efficiency of a triple coincidence set thus comes to nearly 99.2 % which is adequate for our purposes.

Counters of these specifications have their starting potentials near about 1200 volts and give a plateau of about 200 volts with a slope of less than 2-3 % in 100 volts.

These counters contain about 10^{20} vapour molecules when newly filled. As each discharge consumes about 10^{10} molecules, the life of the counter is of the order of 10^{10} counts. The counter could therefore be safely used for a period of about 8 or 9 months in Ahmedabad and about 6 months in Kodaikanal.

To provide greater stability to the counters, they were used with external quenching units (for circuit diagram, refer to section 3). The essential purpose of an external quenching unit is to keep the counter voltage V_o below V_{min} until the positive ion sheath gets neutralised near the cathode. This ensures a complete suppression of any secondary avalanche. It was found that the counters gave better plateau when used with external quenching units. The deteoriation of the plateau with use was also very much reduced.

The exclusion of impurities like Air and Water vapour from the gas mixture is taken due care of as will be seen in the following section where the method adopted for cleaning and filling the counters is described in detail.

2.3 Preparation of a Geiger counter :-

The counter tube used in the present investigation consists essentially of two electrodes. The cathode is a hollow cylinder of copper sheet and the anode is a thin tungsten wire stretched along the axis of the cylinder. The electrodes are assembled in a glass envelope as shown in Fig. 11 below.

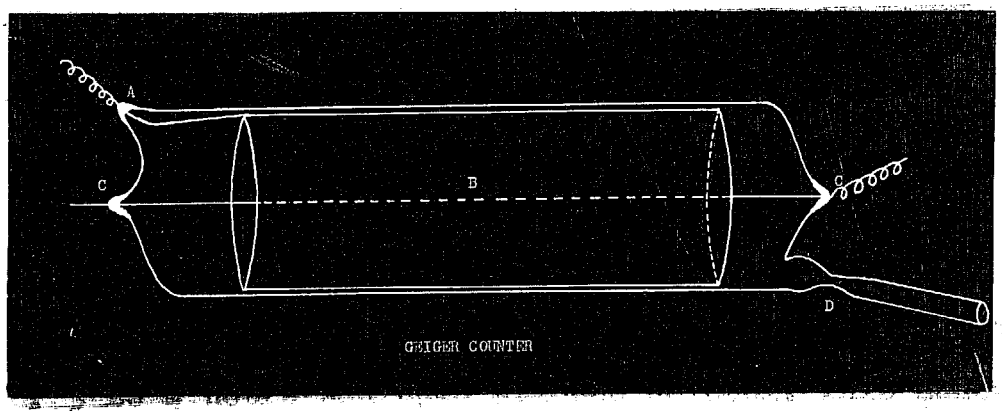

Fig. 11. Geiger counter.

The copper sheet used for the cathode is .15 mm. thick. It is first hammered to remove all sharp edges and points on its surface, and then rolled into a cylinder of length 30 cms. The diameter is adjusted so as to fit in the glass envelope which is of diameter 4 cm. The envelope is made out of pyrex glass tubing.

A thick tungsten wire is silver-soldered to the outer surface of the copper cylinder at one end. The other

end of the wire is fused to the glass envelope and protrudes out of it at the point A. It thus serves the double purpose of holding the cylinder in position and providing an external electrical contact for it.

The (4 ml.) tungsten wire B serves as the anode and is stretched along the axis of the cylinder and sealed through the tapered ends C,C of the glass envelope. The end adjoining the cathode terminates in the glass while the other end is fused through an intermediate nickel bead to a copper wire serving as an external electrical contact for the anode. A constricted neck D is provided in the glass envelope for washing and evacuating the counter and for filling the required gas mixture in it.

After the glass-blowing process is over, the counter is heated to about 300° C. in an electric oven for 3 to 4 hours and then allowed to cool. This annealing process is necessary for the prevention of strains in the glass envelope which often lead to cracks especially when medium or thick walled glass tubing is used. The cathode at this stage is very heavily coated with copper oxide. To remove this and any other grease or dirt, the counters are required to be thoroughly washed.

The apparatus used for washing the counters is shown in the following diagram :

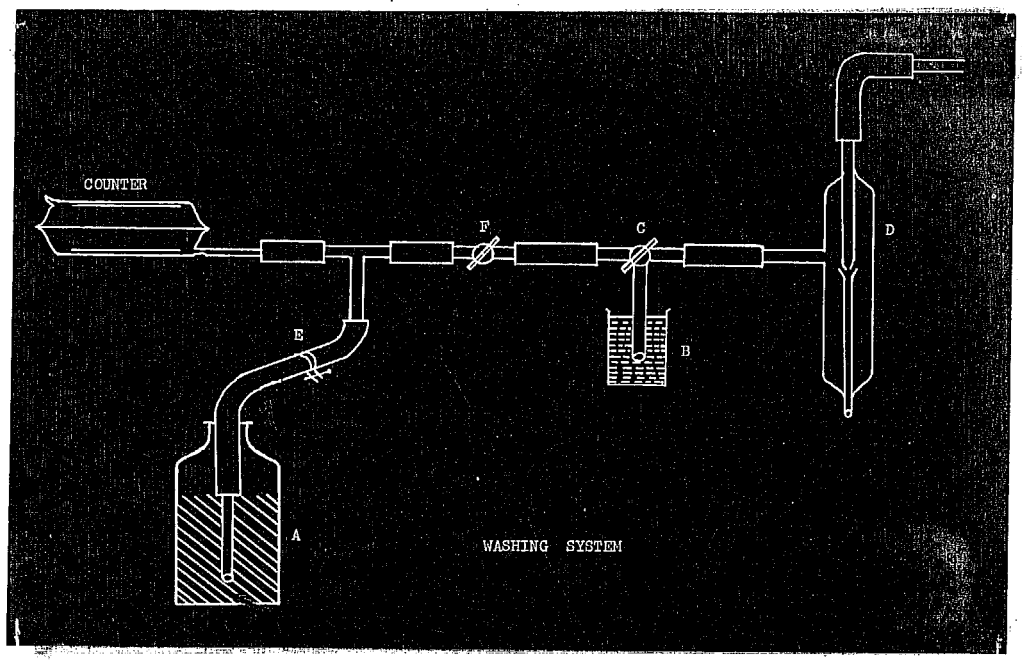

Fig. 12. Washing system.

The bottle A and the beaker B contain distilled water and dilute nitric acid respectively. C is a two-way cock which can connect the counter side either to the beaker B or the filter pump D. The pinch-cock E is opened when distilled water is to be admitted. A cock is provided at F also.

All the connections are first made air tight by putting sealing wax on all the rubber to glass joints. The counter is evacuated by the filter pump and then cock C is adjusted to admit the dilute nitric adid in the counter side. The acid rushes in and fills the counter tube. The counter is now connected to the filter pump. This accelerates the action of the acid and the counter cylinder gets a bright appearance. The acid is now

drained out by raising the counter. Cock F is now closed and the pinch-cock E opened till the counter is filled with distilled water from the flask A. E is closed and the counter is moved up and down till it is thoroughly rinsed. The water is then drained out by opening F. A fresh supply of distilled water is then admitted. The process is repeated five or six times to remove all traces of acid from the counter. The counter is then emptied of water and dried as far as possible by evacuation with the filter pump. It is then separated from the system and connected to a vacuum pump through a U-tube containing $CaCl_2$ lumps. It is simultaneously heated with an electric heating element capable of sliding over the counter. The copper sheet thus gets a thin coating of copper oxide which is found to be very useful for the proper working of a counter. Fig. 13 below gives the plateau characteristics of two counters filled identically but having different conditions of the cathode surface.

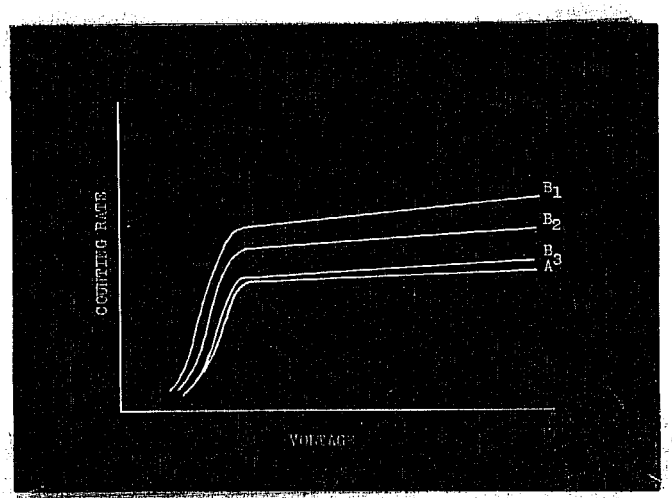

Fig.13. Photo-electric effect in a Geiger counter.

Curve A is for a counter having a thin oxide coating on the cathode while curves B_1, B_2 and B_3 are for counter with a bright shining cathode. The curves have been obtained by allowing different amount of lighting in the room where the counters are tested. Thus B_1 represents the curve when light from a fluorescent tube could penetrate into the interior of the counter through its ends. B_2 is the curve obtained by substituting an ordinary electric lamp. B_3 is the curve obtained with the fluorescent tube on but the ends of the counter covered with thick black paper so that no light could penetrate in. The similiarity of the two curves A and B_3 suggests that the thin coating of Copper oxide on the cathode surface is helpful in reducing the photo-electric effect.

The cleaned counter is next connected to the filling system which is shown in the following diagram :

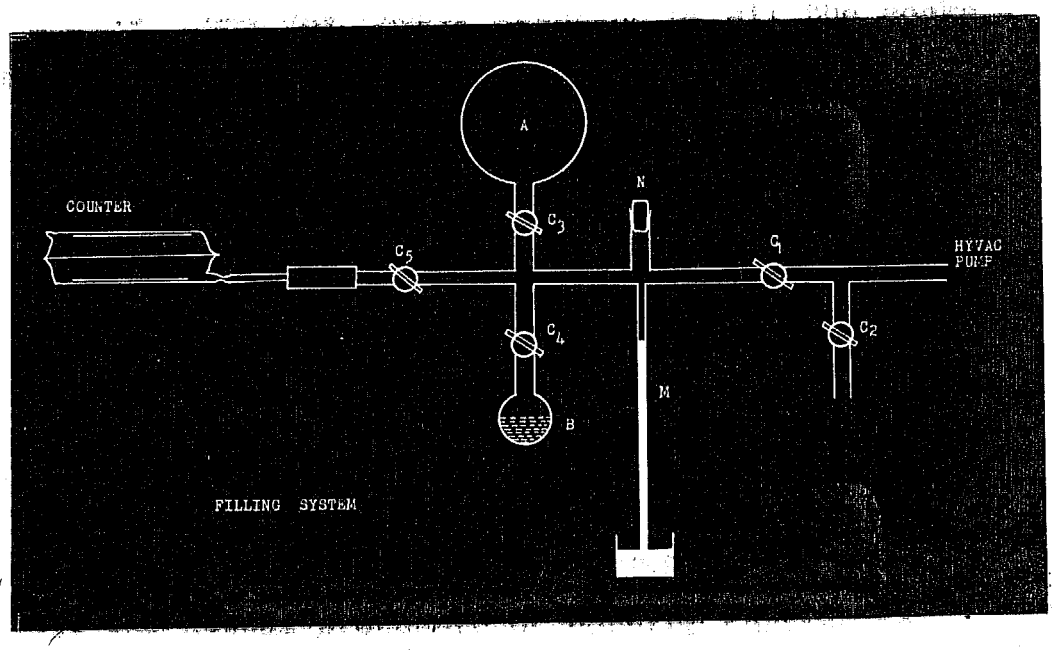

Fig. 14. Filling system.

A is a big flask of capacity 2 litres and contains Argon kept in contact with Calcium chloride which absorbs all traces of moisture from the gas. The bulb B contains ethyl acetate of a refined variety. M is a mercury manometer. The cock C_1 connects the system to a Cenco high vacuum pump. Cock C_2 is for leaking air in the system whenever needed. Cocks C_3 and C_4 are opened whenever argon or ethyl acetate is to be admitted in the system. Cock C_5 when closed separates the counter from the main system.

The counter connection is made air-tight by putting Apiezon wax and the system is evacuated with the counter. To test the vacuum a small Tesla-coil which is essentially a high frequency probe, is used. The order of vacuum is judged from the colour of the gaseous discharge. A slight leakage of air turns the colour of the discharge to brick red, whereas a pale blue colour indicates a vacuum of the order of 10^{-4} mm. Hg. Proper greasing of all the cocks is very essential to attain a vacuum of this order.

After proper evacuation, the main cock C_1 is closed and ethyl-acetate vapour is let in by opening cock C_4 till the mercury level in the manometer M descends by 10 mm. Cock C_4 is then closed and cock C_3 opened to admit argon till the manometer shows a total pressure of 10 cms. The gas mixture is allowed to mix up thoroughly for an hour or so and then cock C_5 is closed. The counter is now ready for testing. The actual procedure of counter testing is described in section 4.

Whenever the argon in the flask A is exhausted, it is refilled from an Argon cylinder containing 99 % pure argon gas. Cock N is meant for this purpose. The ethyl acetate used is free from water. However, when newly filled, the empty portion in the bulb B contains air. It is removed by evacuation by the pump through the cock C_4. The ethyl acetate vapour drives out all the air from the bulb in a few minutes and leaves the section free from air.

2.4 Counter testing :-

The arrangement used for counter testing is schematically shown in the following diagram :

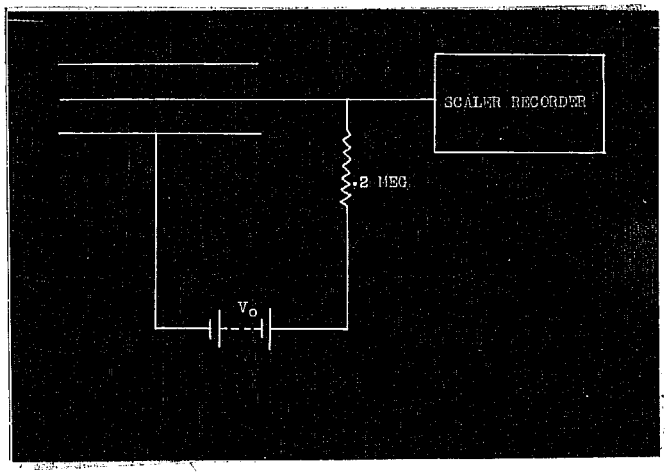

Fig. 15. Arrangement for counter testing.

The pulse developed on the central wire (anode) of the counter is fed to the grid of a multivibrator scaler-recorder circuit. The high voltage across the counter is slowly increased from about 800 volts. At about

1200 volts, the recorder unit starts counting. The counts are measured by a stop-watch for a minute. The voltage is then raised by 25 volts and the counts measured again. The process is repeated, increasing the voltage by 25 volts steps till the total voltage is about 200 volts over the threshold. The counting rates at different voltages are rechecked by decreasing the voltage. The mean of the two readings at each voltage is evaluated and plotted against the voltage. If there is a satisfactory indication of a flat plateau (not more than 3 % change of counting rate per 100 volts) extending for about 200 volts, the counter is sealed at the constriction in the neck.

The counter is now operated in the middle of its plateau region for a period of 12 hours. The plateau characteristics are then rechecked. Counters which show good plateau after this process of aging are selected for use.

3. Electronic units :-

In this section, we shall describe in brief the various electronic circuits used for this investigation.

3.1 Power supplies :-

3.11 The high voltage power supply : Following is the circuit diagram of the high voltage power supply used for giving high voltage to the Geiger counters.

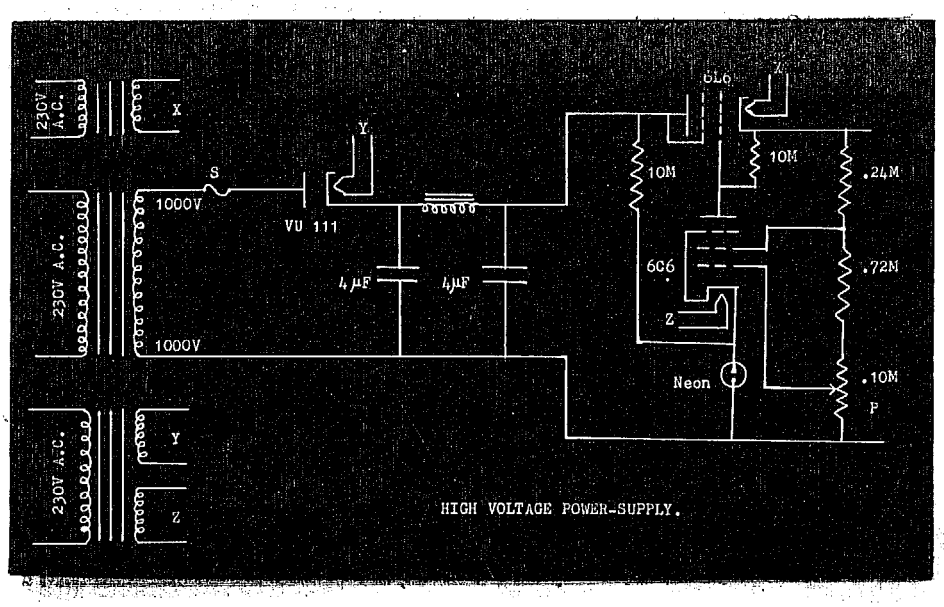

Fig. 16. The high voltage power supply.

The output voltage can be varied over a large range viz. 600 to 1500 volts by adjusting the potentiometer P. To get voltage tappings differing by 50 volts, resistances (one resistance of 2 Meg. and eight resistances of .1 Meg. each) are put in series across the output terminals of the power supply, the 2 Meg. resistance coming first from the positive terminal which is also earthed. For avoiding spurious coincidences due to feed-back of the counter pulse, it was necessary to put a small capacity to earth from each of the negative high voltage tappings.

The degenerative type of voltage regulator, which is incorporated in the power-supply , gives very good voltage regulation. For a change of mains voltage from

150 to 250 volts, the output voltage alters by less than 5 volts at 1200 volts.

3.12 The + B power supplies :- The 420 volts, 210 volts and 150 volts power supplies are all alike and are electronically regulated. The circuit diagram is given below :

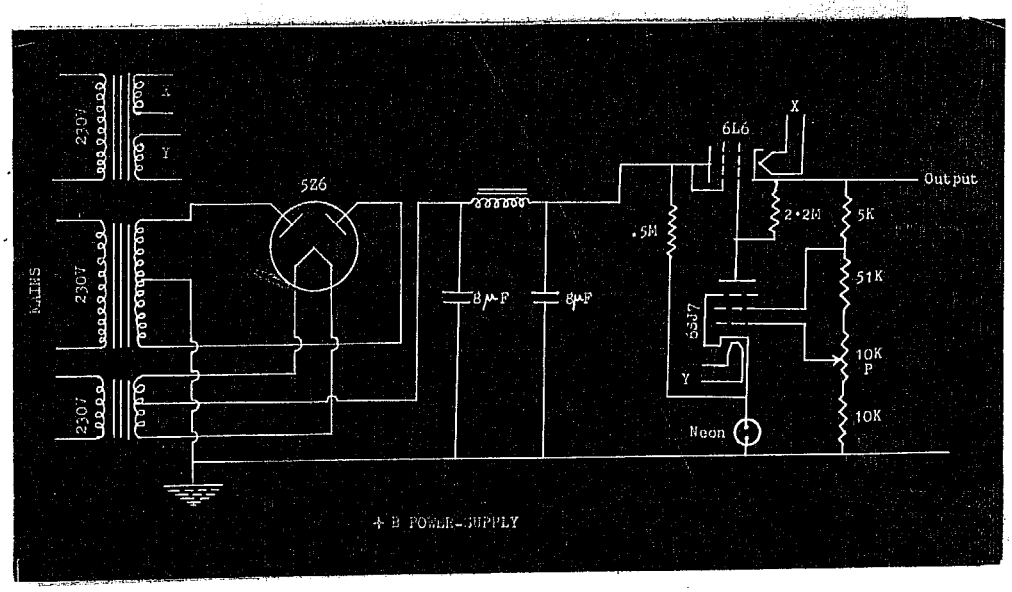

Fig. 17. + B power supply.

The output voltage is variable and can be adjusted to any desired value by adjusting the potentiometer P. The circuit has a very good voltage regulation against varying input voltage and output load.

3.13 The negative bias voltage power supply : The bias voltage of -75 V. is obtained from a V-R tube arranged in a circuit as follows :

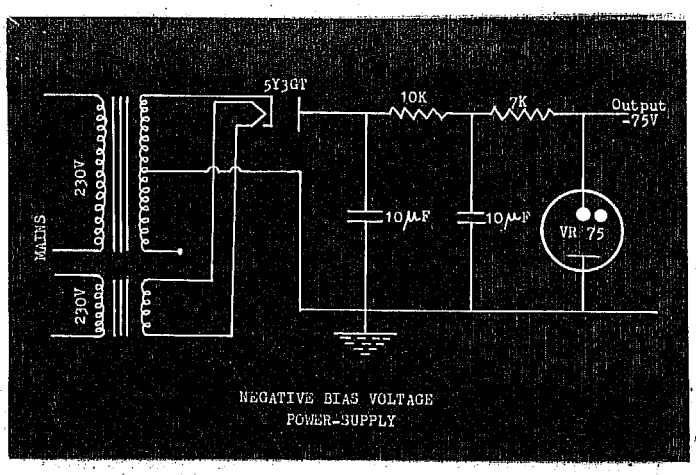

Fig. 18. The negative bias voltage power-supply.

The output from the secondary of a step-up transformer is fed to the 5Y3 (G.T.) rectifier. The rectified voltage is applied across the V-R tube through a high wattage resistor. The V-R 75 tube is a gaseous discharge tube giving constant output voltage of 75 volts. If the positive terminal is earthed, the negative terminal can be used as a bias voltage of -75 volts.

3.14 Filament supply : The filament voltages are obtained from suitable filament transformers.

3.2 The quenching unit :

Following is the circuit diagram of the quenching unit used with the Geiger counters:

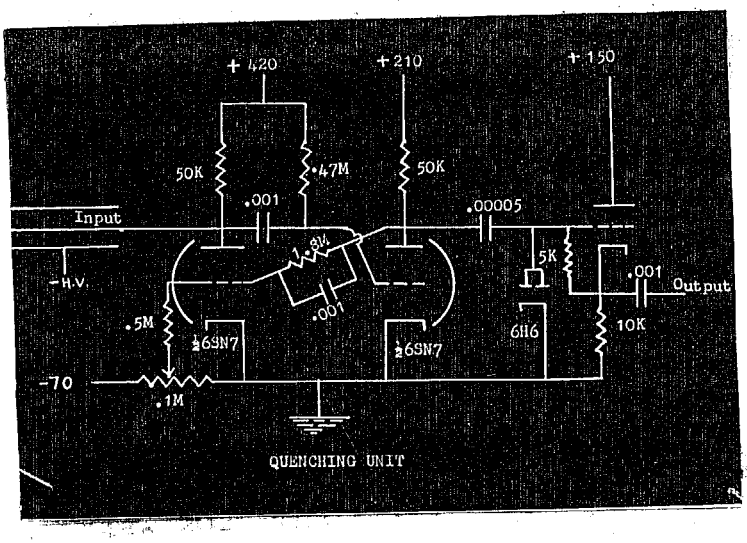

Fig. 19. The quenching unit.

Every time the Geiger counter discharges, the quenching unit imposes a square negative pulse of approximately 300 volts and 5×10^{-4} sec. duration. The unit operates as a one shot multivibrator, with variable bias for sensitivity control. The bias value is adjusted to avoid any interfeeding between two counter trays.

The various voltages are supplied from the power supplies already described.

3.3 The coincidence unit :-

The coincidence unit is constructed on the basis of the Rossi coincidence circuit. The circuit is given below :

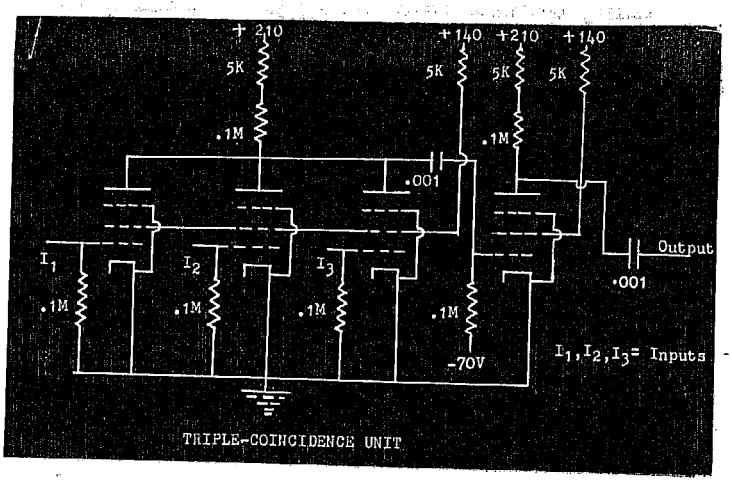

Fig. 20. The triple-coincidence unit.

This circuit has a resolving time of about 10^{-5} sec.

3.4 The scaler-recorder unit :-

The scaler-recorder unit consists essentially of three Eccle-jordan scale-of-two stages connected in cascade and followed by a recording stage. Following is the circuit diagram of a scale-of-two stage.

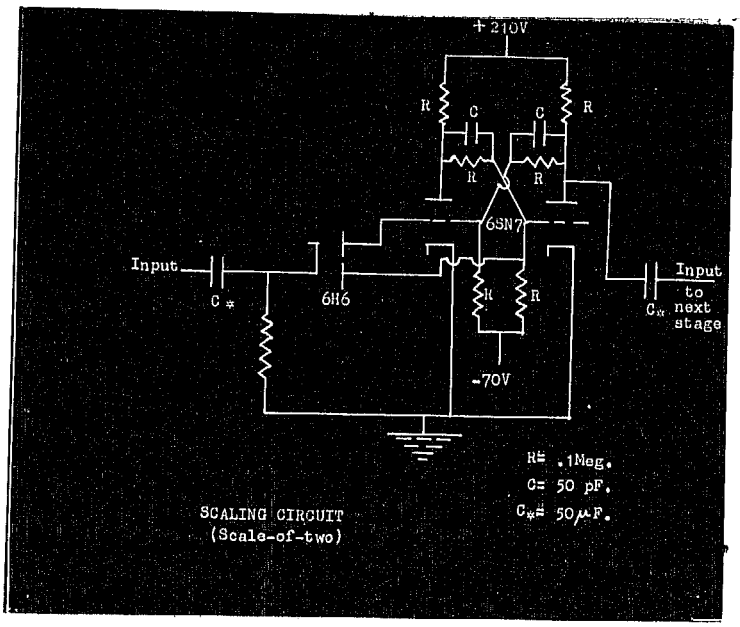

Fig.21. The scaling circuit (Scale-of-two).

Each stage has two stable states and the arrival of a coincidence pulse triggers the first pair from one state to another. The second pair (not shown in the figure) is triggered by the first pair whenever the latter reverts to its original state. Similarly, the third pair is triggered by the second. The original counting rate is thus scaled by a factor of $2^3 = 8$. Neons are used as indicators of the three scaling stages.

III. PRESENTATION OF DATA.

We have described till now the complete experimental arrangement that was used for the present investigation. In section 1 of the present chapter, we describe the methods of analysis of data and in section 2, the data are presented.

1. Methods of analysis :-

1.1 Tabulation of primary data :-

As has been already stated, the data were obtained in the form of hourly photographs of the mechanical recorders. Though the data were available for every hour, it was decided to note down only bi-hourly readings since for the purpose of the daily variation curve, it did not mean much loss of accuracy and helped to reduce the statistical fluctuations because of the doubling of the number of counts for each reading. Readings for the hours 0100, 0300, 0500, 0700, 0900, 1100, 1300, 1500, 1700, 1900, 2100 and 2300 (I.S.T.) were thus noted down every day and the differences between consecutive values computed. Twelve bi-hourly rates were thus obtained for every day, the values being centered at the hours 0200, 0400, 0600, 0800, 1000, 1200, 1400, 1600, 1800, 2000, 2200 and 2400. In addition, the difference between the readings at 0100 hr. for consecutive days was divided by 12 to give the average bi-hourly value centered at 1300 hrs.

From charts taken on an accurate thermograph and micro-barograph, the ground temperature and pressure values were read for the hours 0200, 0400, 0600, 0800, 1000, 1200, 1400, 1600, 1800, 2000, 2200 and 2400 and the daily averages calculated. Everyday's data thus consisted of 12 values (C_1, C_2, ... C_{12}) for each of the measured components of cosmic ray intensity, and for ground temperature and pressure. In addition, it gave the daily averages for each of them. The data for the various cosmic ray components viz. T', T'' ; M_1', M_1'' ; M_2', M_2'' ; H_c and S was noted separately.

1.2 Classification of data according to sets :-

Since the various rates were greatly dependent upon the individual counting rates of the Geiger counters, a failure of any counter and its replacement would change the coincidence rate, though not always appreciably. To be on the safe side, therefore, a run of days was concluded as soon as there was any such failure in the counters or a known disturbance in the geometrical arrangement. Each run was designated as a set. In the earlier stages, counter failures were very frequent and hence the sets would usually extend from 10 to 15 days. Later on, however, sets could be obtained of duration more than 20 days.

Values for the same bi-hourly interval on different days of a set were then added together and the 12 values

ΣC_1, ΣC_2, ... ΣC_{12} centered at 0200, 0400, ... 2400 hours (I.S.T.) were obtained. These were then expressed as deviations from their mean value

$$\bar{C} = \frac{\Sigma C_1 + \Sigma C_2 + \ldots\ldots + \Sigma C_{12}}{12} .$$

The resultant data of each set thus comprised of 12 values ΔC_1, ΔC_2, ... ΔC_{12} centered at hours 0200, 0400, ... 2400 (I.S.T.) and expressed as deviations from the mean value $\bar{C}$. The standard error for each of these values was thus

$$\sqrt{\frac{\bar{C}}{8}} .$$

The factor 8 in the denominator is due to the fact that the rates as obtained from the mechanical recorders are 1/8 th of the original rates because of the scale of eight units preceding the recording stages.

The same procedure was adopted to get the values of the bi-hourly deviations ΔP_1, ΔP_2, ...ΔP_{12} and $\Delta \theta_1$, $\Delta \theta_2$, ...$\Delta \theta_{12}$ for the ground pressure and temperature from their respective means.

1.3 Daily variation :-

The variation obtained for any one set was not usually statistically significant. The standard error was comparable to the amplitude of the variation itself and little could be said from the data of one set about the

nature of the daily curve or the positions of the maxima and minima. The resultant data from all sets were, therefore, superposed for each bi-hourly interval of the day and a final set of 12 values

$$\sum_{set1}^{n} \Delta C_1, \sum_{set1}^{n} \Delta C_2, \ldots\ldots \sum_{set1}^{n} \Delta C_{12}$$

was obtained as deviations from the overall mean of all sets

$$\sum_{set1}^{n} \bar{C} .$$

Each one of these values was divided by the sum of the number of days in all the sets. The new set of 12 values expressed as deviations from their mean

$$\frac{\sum_{set1}^{n} \bar{C}}{\text{Total No. of days.}}$$

and centered at the hours 0200, 0400, ... 2400 (I.S.T.), thus represents the daily bi-hourly variation of the particular component of cosmic ray intensity. The procedure was adopted for all the cosmic ray components, for the ground pressure and temperature. For facility in physical interpretation, the bi-hourly values were expressed as percentage deviations from mean for each component.

The final curves thus obtained were generally very smooth and the resulting variation was statistically significant. The curves for M_1 and M_2 were almost alike as is to be expected;because the percentage of particles that can traverse 7 cms. of lead but get absorbed in 15 cms. of lead is small (See Table 10 p. 95). We have, therefore, superposed the two giving better statistical significance to each bi-hourly value. This new curve designated by M, when subtracted from the total intensity T, gave the variation of the electron component E .

1.4 Correlation analysis :-

Correlation coefficient gives a measure of the relationship between two or more variables. Thus, if ΔC and ΔP represent the deviations from mean for cosmic ray intensity and ground pressure respectively over a common interval of time, the correlation coefficient between the two is expressed by

$$r_{CP} = \frac{\sum \Delta C \cdot \Delta P}{\sqrt{\left\{ \left(\sum \Delta C \right)^2 \cdot \left(\sum \Delta P \right)^2 \right\}}} \quad \ldots\ldots (1)$$

the summation being carried out for all the pairs of ΔC and ΔP values. The regression equation between the variates is then

$$\Delta C = \beta \cdot \Delta P, \text{ where } \beta = r_{CP} \cdot \sqrt{\frac{\sum (\Delta C)^2}{\sum (\Delta P)^2}} \quad \ldots\ldots (2)$$

For studying the relationship of one variable with two others, the partial correlation coefficients are calculated. These are a measure of the relationship between two variables, the third one remaining constant. Thus, $r_{CP \cdot \theta}$ gives the correlation between cosmic ray intensity and ground pressure, the temperature remaining constant. These coefficients can be evaluated as follows :

$$r_{CP \cdot \theta} = \frac{r_{CP} - r_{C\theta} \cdot r_{P\theta}}{\sqrt{\{(1 - r_{C\theta}^2)(1 - r_{P\theta}^2)\}}} \quad \text{and}$$

$$r_{C\theta \cdot P} = \frac{r_{C\theta} - r_{CP} \cdot r_{P\theta}}{\sqrt{\{(1 - r_{CP}^2)(1 - r_{P\theta}^2)\}}} \quad \ldots\ldots (3)$$

The relationship between the variates can be expressed by the regression equation

$$\Delta C = \beta' \cdot \Delta P + \gamma' \cdot \Delta \theta \quad \ldots\ldots\ldots\ldots (4)$$

and the constants β' and γ' can be evaluated from the equations

$$= \frac{r_{CP} - r_{C\theta} \cdot r_{P\theta}}{(1 - r_{P\theta}^2)} \cdot \sqrt{\frac{\sum (\Delta C)^2}{\sum (\Delta P)^2}}$$

$$= \frac{r_{C\theta} - r_{CP} \cdot r_{P\theta}}{(1 - r_{P\theta}^2)} \cdot \sqrt{\frac{\sum (\Delta C)^2}{\sum (\Delta \theta)^2}} \quad \ldots (5)$$

III.

The constants β' and γ' are called the regression coefficients. The pressure and temperature coefficients of cosmic ray intensity are evaluated from β' and γ' as follows :

$$\text{Pressure coefficient } \bar{\beta} = \frac{100\,\beta'}{C} \% \text{ per cm. Hg. and}$$

$$\text{Temperature coefficient } \bar{\gamma} = \frac{100\,\gamma'}{C} \% \text{ per } {}^{o}\text{C.} \quad \ldots \quad (6)$$

where C represents the mean value of cosmic ray intensity about which the deviations Δ C are expressed.

Partial correlation coefficients can be calculated even when there are more than 3 variables. Duperier[2] has tried to correlate the variation of cosmic ray intensity with three factors operating simultaneously viz. the variations in ground pressure, the changes in height of the 100 mb. level and the variations in the air temperature between 100 and 200 mb. levels. The relationship can be represented by the equation:

$$\Delta C = \mu \cdot \Delta P + \mu' \cdot \Delta H + \alpha \cdot \Delta \theta_H \quad \ldots \quad (7)$$

where μ , μ' and α are the absorption, decay and temperature coefficients respectively. The values can be evaluated from the correlation coefficients by the following relations :

$$\mu = r_{CP \cdot H\theta_H} \cdot \sqrt{\frac{\sum (\Delta C)^2}{\sum (\Delta P)^2}} \cdot \sqrt{\frac{(1 - r^2_{CP \cdot H})}{(1 - r^2_{CP \cdot \theta_H})}}$$

and two similar equations for μ' and α . . . . . (8)

The partial correlation coefficients $r_{CP \cdot H\theta_H}$ etc. can be evaluated as follows :

$$r_{CP \cdot H\theta_H} = \frac{r_{CP \cdot \theta_H} - r_{CH \cdot \theta_H} \cdot r_{PH \cdot \theta_H}}{\sqrt{\left\{(1 - r^2_{CH \cdot \theta_H})(1 - r^2_{PH \cdot \theta_H})\right\}}}$$

and two similar equations for $r_{CH \cdot P\theta_H}$ and $r_{C\theta_H \cdot PH}$ . . (9)

The values of the correlation coefficients obtained by such methods have always a probable error associated with them. It is given by

$$P = \frac{.67 (1 - r^2)}{\sqrt{n}} \quad . . . . . (10)$$

where 'r' is the correlation coefficient and 'n' is the number of pairs from which 'r' is calculated. It is obvious that the values of 'r' will be more and more significant for larger values of 'n'. For any particular value of 'n' there are certain fixed values of 'r' above which the correlation coefficients will be significant on the .5 %, 1 %, 5 % levels. A significance on the .5 % level means

that the probability of getting that value for 'r' by the operation of purely random causes in only 1 in 200. Information about the significance of correlation coefficients for various values of 'n' is given in standard tables.

Levels of significance are taken into consideration before attaching weight to any correlation coefficient. However, very high correlations can always be taken as indicative of the high degree of relationship between any two variables, because high correlation coefficients are fairly significant even for comparatively low values of 'n'. For significant correlation coefficients, the values of ΔC as computed from the corresponding regression equation do not differ much from the actual values. The factor

$$\sum \frac{1}{C}\left\{\Delta C - (\beta'\cdot\Delta P + \gamma'\cdot\Delta \theta)\right\}^2$$

can be taken as a measure of the agreement between the calculated curve and the experimental values, by applying the so-called χ^2 - test. Such statistical tests are, however, always to be interpreted with great caution in physical problems, since they are liable at times to lead one to wrong conclusions.

1.5 Harmonic analysis :-

For an elucidation of a periodic variation and its

relationship with other factors, it is often very useful to perform the Harmonic Analysis. Any variation can be expressed as a Fourier series; but when there is a periodic component in it, an examination of the amplitudes and phases of the successive Fourier components is very illuminating. A primary variation connected with the earth's rotation reveals itself in the first two components of 24 and 12 hourly periods and the amplitudes of these two in relation to those of the higher components indicate the presence of disturbing factors.

The method of resolving a certain periodic curve into its fundamental and higher harmonics has been treated rigorously in various text-books. One can obtain expressions for the amplitudes and phases of the various components as functions of the hourly or bi-hourly values of the variate. For practical purposes, the calculation associated with the harmonic analysis can be greatly simplified by arranging the data in a particular order. The method followed by us is described by Whittaker and Robinson[59] in their book 'The Calculus of Observations' (p.270). The primary bi-hourly data is filled in the appropriate places in the following chart :

Table 3.

Harmonic Analysis of 12 bi-hourly values.

	$(U_0$ to $U_6)$	....	....	....	....	....	....
	$(U_{11}$ to $U_7)$	....	....	....	....	....	
Sums	$(V_0$ to $V_6)$	....	....	....	....	....	....
Diffs.	$(W_1$ to $W_5)$	....	....	....	....	....	

	$(V_0$ to $V_3)$	....	....	....		$(W_1$ to $W_3)$	....	....	
	$(V_6$ to $V_4)$	....	....			$(W_5$ to $W_4)$	....		
Sums	$(P_0$ to $P_3)$	....	....	....	Sums	$(R_1$ to $R_3)$	....	....	
Diffs.	$(Q_0$ to $Q_2)$	....	....		Diffs.	$(S_1$ to $S_2)$	....		

	P_1 =	, P_2 =	, Q_2=	, R_1=	,	Q_1=	, R_2=	, S_1=	, S_2= ,
(½ line above)	H_1 =	, H_2 =	, L_2=	, M_1=	, (0.866 x line above)	L_1=	, M_2=	, N_1=	, N_2= ,

Table 3 (contd.).

	P_0= , P_1=	Q_0= , L_1=	P_0= , H_1=
	P_2= , P_3=	L_2= ,	P_3= , H_2=
Sum of 1st col.	....	....	....
Sum of 2nd col.	....	....	....
Sum	....= $12A_0$	....= $6A_1$	
Diff.	....= $12A_6$	....= $6A_5$	....= $6A_4$

	P_0= , P_3=	M_1= , M_2=	
	H_1= , H_2=	R_3=	
Sum of 1st col.	....	....	
Sum of 2nd col.	....	....	
Sum		....= $6B_1$	
Diff.	....= $6A_2$	....= $6B_5$	

	Q_0= , N_1= ,	R_1=	
	Q_2= , N_2= ,	R_3=	
Sum		...= $6B_2$	
Diff.	...= $6A_3$	...= $6B_4$	...=$6B_3$

The values U_0, U_1, U_2, ... U_{11} represent the 12 bi-hourly values centered at hours 0000, 0200, 0400, ... 2200 respectively. As a result of calculating and filling in the various blanks in the chart we get the original variation expressed as :

$$X = A_0 + (A_1 \text{ Sin } \theta + B_1 \text{ Cos } \theta) + (A_2 \text{ Sin } 2\theta + B_2 \text{ Cos } 2\theta) + (A_3 \text{Sin } 3\theta + B_3 \text{Cos } 3\theta) + (A_4 \text{ Sin } 4\theta + B_4 \text{ Cos } 4\theta) + (A_5 \text{Sin } 5\theta + B_5 \text{Cos } 5\theta) + (A_6 \text{ Sin } 6\theta) \quad \ldots (11)$$

The terms can be combined to give the amplitudes and phases of the various components in the form :

$$X = A_0 + r_1 \text{ Sin } (\theta + \phi_1) + r_2 \text{ Sin } (2\theta + \phi_2) + r_3 \text{ Sin}(3\theta + \phi_3) + r_4 \text{ Sin } (4\theta + \phi_4) + r_5 \text{ Sin}(5\theta + \phi_5) + r_6 \text{ Sin } (6\theta + \phi_6)$$

where $r_1 = \sqrt{A_1^2 + B_1^2}$ etc. and $\phi_1 = \text{Tan}^{-1}(B_1/A_1)$ etc. . . (12)

Since the 12 bi-hourly values substituted for U_0 ..... U_{12} are expressed as deviations from their mean, the term A_0 reduces to zero.

r_1 and ϕ_1 represent the amplitude and phase of the 24 hourly component, r_2 and ϕ_2 those of the 12 hourly component and so on for the 8 hourly, 6 hourly etc. periods. Here the phase angle corresponds to the time at which the deviation from mean of the particular component of the variate becomes zero. The angle ψ corresponding to the

time at which the variate attains the maximum value is calculated from the phase angle ϕ from the relation :.

$$\Psi = 90^{o} - \phi \quad \ldots\ldots\ldots\ldots\ldots (13)$$

1.6 Harmonic dial :-

Having determined the amplitudes and the angles for the times of maxima for the principal harmonic components of a variation, it is convenient to represent them on what are known as 'Harmonic dials', there being one dial for each harmonic component of a particular period.

Thus the first dial represents the diurnal wave of 24 hours period and a clockwise rotation of 15^{o} about the origin is equivalent to one hour. The amplitude and the hour of maximum of any diurnal component of a variation can then be represented on the dial as a vector which starts from the origin of the diagram and makes an appropriate angle with the positive Y-axis taken as 0000 hours.

Similarly a dial of 12 hour period, where a clockwise rotation of 30^{o} corresponds to one hour, can be used for the representation of the semi-diurnal component.

The significance of a component is judged by the size of the circle of standard error at the end of a vector in relation to the length of the vector.

The study of the harmonic dial is particularly helpful when a variety of causes operating simultaneously, confuse the nature of a variation and its true relationship with other variations. The method is also useful for detecting a long period variation superimposed on a daily variation as is so often found to occur in cosmic ray intensity variations. If the variation is of one year's period, the end-points of the daily variation vectors for data grouped for a month or a season trace approximately a closed curve over a period of one year.

1.7 Day-to-day variation :-

As already stated, each set gives a daily average for the intensity of the various cosmic ray components as also for ground pressure and temperature. These values can be correlated with each other and the correlation coefficients for day-to-day variations calculated. The probable error of the coefficients will, however, be large since majority of the sets do not extend for more than a fortnight individually. To get significant values, some sort of superposition was therefore necessary.

To arrive at the correlation coefficients, we have to calculate first the values of $\sum(\Delta C \cdot \Delta P)$, $\sum (\Delta C)^2$ and $\sum (\Delta P)^2$ where ΔC and ΔP represent the deviations of the daily means (centered at 1300 hrs.) from the mean of the set. (ref. 1.4 eq.(1)). These values were calculated separately for each set and then combined together for all

sets. A final set of values

$$\sum_{\text{set 1}}^{n} \sum (\Delta C \cdot \Delta P), \quad \sum_{\text{set 1}}^{n} \sum (\Delta C)^2 \text{ and } \sum_{\text{set 1}}^{n} \sum (\Delta P)^2$$

was thus obtained. The correlation coefficients were then calculated from these values by equation (1). This procedure is perhaps the best way of tackling our data.

Once the values of r_{CP}, $r_{C\theta}$ and $r_{P\theta}$ are thus calculated, the rest of the procedure for evaluating the regression coefficients is the same as before.

2. Experimental results :-

2.1 Daily variation at Kodaikanal :-

The results obtained at Kodaikanal for the total intensity T and meson intensities M_1 and M_2 are grouped in seven intervals or sets in all. For set 1, there are no results for the meson intensity as no lead absorber was then inserted between any of the trays.

The results are entered in Tables 4(a), 4(b), 5(a), 5(b), 5(c) and 5 (d). Thus Tables 4(a) and (b) give the results for the total intensities T' and T". Tables 5(a), (b), (c) and (d) give the results for the meson intensities M_1', M_1'', M_2' and M_2'' respectively. In each table are entered the mean bi-hourly rates expressed as deviations from their respective means given in the last row. The figures

entered in the tables are 1/8 th of the true counting rates on account of the scale of 8 units which preceded the mechanical recorders. Data is given for each particular set as specified at the top of each column with its period of duration and the number of days. The values in any row are centered at the hour (I.S.T.) given in column one of the table.

Table 4(a) — Total intensity T'.

Set.	1	2	3	4	5	6	7
Interval.	26 Jun.-9 July.	14 Jul.-2 Aug.	5 Aug.-20 Aug.	21 Aug.-1 Sep.	7 Sep.-29 Sep.	30 Sep.-23 Oct.	23 Oct.-4 Nov.
No.of days.	(16)	(7)	(14)	(11)	(19)	(22)	(9)
Hr.00	3	- 1	-10	-12	- 5	- 8	-12
02	7	4	0	12	2	4	0
04	15	6	6	15	1	6	1
06	9	10	20	12	- 2	8	7
08	5	5	10	3	3	3	9
10	-11	9	7	7	10	3	5
12	- 5	- 3	- 1	3	2	5	12
14	-11	- 3	- 6	- 2	3	1	3
16	- 9	-13	- 2	- 6	1	1	3
18	- 8	- 3	- 2	- 7	0	- 4	2
20	- 3	-11	-12	-13	- 7	-12	-18
22	8	0	- 9	-12	- 6	- 8	-12
Mean	906	901	926	888	931	926	950

Table 4(b) — Total intensity T".

Set.	1	2	3	4	5	6	7
Interval	26 Jun.- 11 July.	14 Jul.- 2 Aug.	5 Aug.- 20 Aug.	21 Aug.- 1 Sep.	7 Sep.- 29 Sep.	30 Sep.- 23 Oct.	23 Oct.- 4 Nov.
No.of days.	(25)	(8)	(14)	(10)	(18)	(22)	(11)
Hr. 00	8	2	- 8	- 6	- 4	- 5	- 1
02	9	8	2	- 1	7	1	2
04	12	3	4	- 4	11	6	6
06	4	- 1	10	- 3	8	5	0
08	8	9	11	9	- 2	5	3
10	- 3	5	9	11	2	7	5
12	- 9	- 5	7	11	5	6	1
14	- 5	- 3	0	6	6	7	9
16	- 9	2	- 5	2	- 6	- 5	3
18	- 6	- 3	- 8	- 8	- 8	- 7	- 5
20	- 8	-11	-15	- 6	- 9	-10	- 8
22	3	- 7	- 7	-11	-11	- 8	-15
Mean.	867	828	806	770	750	741	752

Table 5(a) — Meson intensity M_1'.

Set.	2	3	4	5	6	7
Interval.	14 July - 2 Aug.	5 Aug.- 20 Aug.	21 Aug.- 1 Sep.	7 Sep.- 29 Sep.	30 Sep.- 23 Oct.	23 Oct.- 4 Nov.
No.of days.	(5)	(14)	(11)	(19)	(22)	(12)
Hr. 00	5	- 6	- 8	- 3	- 4	- 4
02	- 2	- 2	- 3	- 5	0	3
04	12	- 2	6	0	- 1	- 1
06	1	12	1	2	5	1
08	- 4	9	6	- 2	5	1
10	- 6	6	13	10	4	7
12	- 3	1	10	13	4	2
14	- 3	- 1	4	4	3	2
16	2	1	- 3	- 8	- 3	- 1
18	- 5	- 3	-10	- 4	- 2	- 4
20	- 8	-11	-10	- 5	- 7	- 2
22	9	- 6	- 7	- 2	- 3	- 6
Mean.	637	654	641	678	662	672

Table 5(b) — Meson intensity M_1'' .

Set.	2	3	4	5	6	7
Interval.	14 July– 2 Aug.	5 Aug.– 20 Aug.	21 Aug.– 1 Sep.	7 Sep.– 29 Sep.	30 Sep.– 23 Oct.	23 Oct.– 4 Nov.
No.of days.	(8)	(14)	(12)	(16)	(22)	(9)
Hr. 00	0	- 4	- 6	- 7	- 3	- 2
02	5	2	3	- 1	- 5	2
04	- 1	2	- 1	0	0	3
06	- 6	6	4	7	3	- 1
08	6	9	9	2	4	4
10	5	11	7	11	7	7
12	- 2	2	6	6	6	0
14	0	- 2	3	6	4	1
16	- 1	- 4	0	0	- 1	2
18	- 3	- 9	- 6	- 5	- 2	- 5
20	- 4	-12	-11	-10	- 5	0
22	1	- 2	- 6	-10	- 9	-11
Mean.	539	539	513	530	543	522

Table 5(c) — Meson intensity M_2'.

Set.	2	3	4	5	6	7
Interval.	14 July - 2 Aug.	5 Aug.- 20 Aug.	21 Aug.- 1 Sep.	7 Sep.- 29 Sep.	30 Sep.- 23 Oct.	23 Oct.- 4 Nov.
No.of days.	(6)	(15)	(8)	(19)	(22)	(11)
Hr. 00	- 1	6	14	- 4	3	- 3
02	0	12	16	- 1	3	- 2
04	12	12	16	5	8	0
06	12	11	19	5	3	5
08	4	-14	- 6	1	4	0
10	- 2	-10	- 7	4	2	4
12	6	1	-12	6	2	- 1
14	7	- 2	-14	6	1	5
16	-12	-15	-25	- 3	-10	- 1
18	- 1	- 4	- 8	- 7	- 8	- 3
20	- 6	2	1	- 9	1	1
22	0	2	7	- 3	- 3	- 5
Mean.	603	585	559	642	615	518

Table 5(d) — Meson intensity M_2''.

Set.	2	3	4	5	6	7
Interval.	14 July - 2 Aug.	5 Aug.- 20 Aug.	21 Aug.- 1 Sep.	7 Sep.- 29 Sep.	30 Sep.- 23 Oct.	23 Oct.- 4 Nov.
No.of days.	(8)	(15)	(11)	(17)	(21)	(9)
Hr. 00	2	- 5	0	- 8	- 6	- 5
02	0	- 3	11	0	- 2	5
04	- 4	2	7	6	6	- 2
06	- 5	6	4	7	2	- 2
08	7	11	6	4	6	7
10	5	10	3	10	3	11
12	1	3	0	10	8	- 1
14	0	0	- 2	0	5	- 1
16	- 2	1	- 5	- 7	0	- 2
18	- 3	- 5	- 6	- 8	- 5	- 3
20	0	-11	-13	- 7	- 5	- 5
22	- 2	- 7	- 4	- 7	-11	- 5
Mean.	557	568	547	585	626	605

As can be seen from these tables, the general trend of the daily variation at Kodaikanal is mainly diurnal iwith the maximum in the early part of the day and minimum some time late in the evening. A better impression of the whole data can be obtained from the following few tables which give for each set (i) the hour of transition i.e. the hour after which the positive trend of the morning hours vanishes and (ii) the maximum and minimum expressed as % deviations from mean with their hours of occurance.

Table 6(a) — T'.

Set.	1		2		3		4	
Hour of transition.	08 Hr.		10 Hr.		10 Hr.		12 Hr.	
Maximum.	+1.7	04 Hr.	+1.1	06 Hr.	+ 2.2	06 Hr.	+1.7	04 Hr.
Minimum.	-1.2	12 Hr.	-1.4	16 Hr.	-1.3	20 Hr.	-1.5	20 Hr.

Set.	5		6		7	
Hour of transition.	18 Hr.		16 Hr.		18 Hr.	
Maximum.	+1.0	10 Hr.	+ 0.9	06 Hr.	+1.3	12 Hr.
Minimum.	-0.8	20 Hr.	-1.3	20 Hr.	-1.9	20 Hr.

Table 6(b) — T".

Set.	1		2		3		4		5		6		7	
Hr.of transi.	08 Hr.		10 Hr.		12 Hr.		16 Hr.		14 Hr.		14 Hr.		16 Hr.	
Max.	+1.4	04Hr.	+1.1	08Hr.	+1.4	08Hr.	+1.4	10Hr.	+1.5	04Hr.	+0.9	10Hr.	+1.2	14Hr.
Min.	-1.0	14Hr.	-1.3	20Hr.	-1.9	20Hr.	-1.4	22Hr.	-1.5	22Hr.	-1.3	20Hr.	-2.0	22Hr.

Table 7(a) — M_1'.

Set.	2		3		4		5		6		7	
Hr.of transi.	06 Hr.		16 Hr.		14 Hr.		14 Hr.		14 Hr.		14 Hr.	
Maximum.	+1.9	04 Hr.	+1.8	06 Hr.	+2.0	10 Hr.	+1.9	12 Hr.	+0.8	06 Hr.	+1.0	10 Hr.
Minimum.	-1.3	20 Hr.	-1.7	20 Hr.	-1.6	20 Hr.	-1.2	16 Hr.	-1.1	20 Hr.	-0.9	22 Hr.

Table 7(b) — M_1''.

Set.	2		3		4		5		6		7	
Hr.of transi.	10 Hr.		12 Hr.		14 Hr.		16 Hr.		14 Hr.		16 Hr.	
Maximum.	+1.1	08 Hr.	+2.0	10 Hr.	+1.8	08 Hr.	+2.1	10 Hr.	+1.3	10 Hr.	+1.3	10 Hr.
Minimum.	-1.1	06 Hr.	-2.2	20 Hr.	-2.1	20 Hr.	-1.9	22 Hr.	-1.7	22 Hr.	-2.1	22 Hr.

Table 7(c) — M_2'.

Set.	2		3		4		5		6		7	
Hour of transition.	14 Hr.		06 Hr.		06 Hr.		14 Hr.		14 Hr.		14 Hr.	
Maximum.	+2.0	06 Hr.	+2.1	04 Hr.	+3.4	06 Hr.	+0.9	12 Hr.	+1.3	04 Hr.	+1.0	06 Hr.
Minimum.	-2.0	16 Hr.	-2.6	16 Hr.	-4.5	16 Hr.	-1.4	20 Hr.	-1.6	16 Hr.	-1.0	22 Hr.

Table 7(d) — M_2''.

Set.	2		3		4		5		6		7	
Hour of transition.	14 Hr.		12 Hr.		12 Hr.		14 Hr.		14 Hr.		10 Hr.	
Maximum.	+1.3	08 Hr.	+1.9	08 Hr.	+2.0	02 Hr.	+1.7	10 Hr.	+1.3	12 Hr.	+1.8	10 Hr.
Minimum.	-0.9	06 Hr.	-1.9	20 Hr.	-2.4	20 Hr.	-1.4	18 Hr.	-1.8	22 Hr.	-0.8	22 Hr.

III.

The values of the meson intensities seem to be fairly consistent from set to set except for set 2 for which the values are rather erratic. Thus for M_1' (Table 7(a)), the hour of transition for set 2 is 0600 hrs. in contrast to 1400 to 1600 hrs. for all other sets. For M_1'' and M_2'' (Tables 7(b) and 7(d)), the hour of minimum is 0600 hr. in contrast to about 2000 hr. for all other sets. For M_2' (Table 7(c)) the values are quite consistent. The number of days in set 2 is only six. The value of M_2' cannot therefore be taken as representative of the meson intensity of set 2 as a whole. Set 2 is therefore neglected for all the meson intensities.

Also for the meson intensity M_2' the values for sets 3 and 4 are unreliable. Because of fluctuations in mains voltage during the morning hours, the particular mechanical recorder was found to be losing counts. The values for the hours between 8 A.M. and 11 A.M. are thus abnormally low and unreliable (see Table 5(c)). Sets 3 and 4 are therefore rejected for meson intensity M_2'.

Tables 6(a) and 6(b) indicate that for the total intensity curves T' and T", there is a trend towards later hours for the hour of transition as also for the hour of minimum. The variation of the electronic component E is evaluated by subtracting the variation of the meson intensity from the variation of the total intensity, hour to hour. Sets 1 and 2 are therefore neglected from the total

intensity as there is no corresponding data for the meson intensities and the data for set 2 for M_1', M_1'', M_2' and M_2'' is not taken into consideration for reasons given in the previous paragraph.

The final data thus consists of sets 3, 4, 5, 6 and 7 for the intensities T', T'', M_1', M_1'' and M_2'' and sets 5, 6 and 7 for M_2'. The raw values for a particular cosmic ray component for different sets are added up as already described in section 1.3 of this chapter. Table 8 gives the final mean bi-hourly rates expressed as % deviations from their respective means (given at the bottom of each column) and centered at the hours (I.S.T.) given in the first column.

Table 8. Daily variations of the total and the meson intensities as measured by independent telescopes.

Hour.	T'	T''	M_1'	M_1''	M_2'	M_2''
00	-0.9	-0.7	-0.7	-0.8	-0.6	-0.9
02	0.2	0.3	-0.2	-0.1	0.1	0.2
04	0.6	0.7	0.0	0.1	0.9	0.7
06	0.9	0.7	0.7	0.7	0.8	0.7
08	0.5	0.6	0.6	1.0	0.3	1.1
10	0.7	0.8	1.1	1.6	0.5	1.2
12	0.4	0.7	0.9	0.9	0.5	0.9
14	0.0	0.7	0.4	0.5	0.7	0.1
16	-0.0	-0.4	-0.5	-0.1	-1.0	-0.4
18	-0.2	-0.9	-0.6	-1.0	-1.2	-1.0
20	-1.3	-1.3	-1.0	-1.5	-0.5	-1.3
22	-0.9	-1.3	-0.6	-1.4	-0.6	-1.3
Mean.	924.5	760.8	662.8	531.8	604.0	590.0

The rates T', M_1' and M_2' have been obtained independently of the rates T", M_1'' and M_2''. Table 9 gives the correlations between the corresponding bi-hourly rates.

Table 9. Correlation between the rates obtained by the independent telescopes.

	T' and T"	M_1' and M_1''	M_2' and M_2''
Correlation coefficients.	+ .90	+ .96	+ .83

The high values of the correlations indicate a very good agreement between the two. The corresponding bi-hourly rates are therefore combined together to give the final curves for the total and meson intensities.

In spite of the fact that all the trays contain the same number of counters and the trays are separated by a uniform distance, the counting rates of the telescopes are not directly comparable. The small differences in the effective dimensions of counters and the inaccuracies of alignment of the trays are responsible for this.

To know, therefore, the exact proportions of the various cosmic ray components in the total intensity, an absorption experiment was carried out for a few days. The procedure was to measure the counting rate of the

triple coincidence unit meant for measuring the hard component (H_c) for different lead thicknesses in between the trays. The geometrical arrangement thus remained constant and the rates for various lead thicknesses were comparable.

The coincidence rate was measured for one day for each value of lead thickness. The day-to-day variation was neglected for rates which changed by more than 5 % from one value of lead thickness to the other. The rates were measured for lead thicknesses of 0, 3, 7, 15, 20, 28 and 36 cms.

As the difference in the values for 7 cm. and 15 cm. of lead was small, these values were evaluated to a greater accuracy from readings of six days using alternate days for the two thicknesses.

Table 10 gives the results obtained in the absorption experiment.

Table 10. Absorption of cosmic rays in lead.

Lead thickness.	Rate per hour.	Standard error.
0 cm.	196.6	± 1.0
3 cm.	154.5	± 0.9
7 cm.	123.9	± 0.6
15 cm.	117.9	± 0.6
20 cm.	110.0	± 0.9
28 cm.	102.0	± 0.9
36 cm.	99.0	± 0.9

The percentage of the number of particles which are absorbed between 7 cm. and 15 cm. of lead is thus 3.1 % of the total intensity. This is very small as compared to the percentage of the component absorbed in 7 cm. of lead which is 37 % . The meson intensities M_1 and M_2 can therefore be assumed to be one and the same.

The raw values for the meson intensities M_1', M_1'', M_2' and M_2'' are now superimposed and the resultant is designated by M^*. The resultant of T' and T" is designated by T. If the geometry of the telescopes was identical, M^* which corresponds to the intensity penetrating through a mean thickness of 11 cm. of lead should be 61.5 % of the total intensity (see Table 10). Actually the mean rates of T and M^* are 842.7 and 597.8 respectively. The values of M^* are therefore normalised to a value 519.8 which is 61.5 % of the total intensity rate. The normalised values of M^* are designated as M.

The final daily variation curves for the total intensity T, meson intensity M, electronic component E, ground pressure P and ground temperature θ (all expressed as percentage deviations from their respective means) are given in Table 11 and plotted in Fig. 22.

Table 11. Daily variations of the various cosmic ray intensities and ground pressure and temperature at Kodaikanal.

Hour.	T ± 0.10	M ± 0.08	E ± 0.6	P	θ
00	-0.80	-0.73	-0.9	0.09	-.35
02	0.27	-0.05	0.8	-.05	-.42
04	0.65	0.36	1.1	-.10	-.50
06	0.74	0.72	0.9	-.06	-.56
08	0.57	0.77	0.3	.06	-.15
10	0.73	1.13	0.1	.16	.52
12	0.56	0.82	0.1	.10	.80
14	0.33	0.38	0.3	-.05	.73
16	-0.22	-0.47	0.2	-.14	.48
18	-0.55	-0.88	0.0	-.10	.04
20	-1.28	-1.10	-1.6	.01	-.25
22	-1.09	-0.97	-1.3	.12	-.31
Mean.	842.7	519.8	322.9	578.0 mm.	286.8°A.

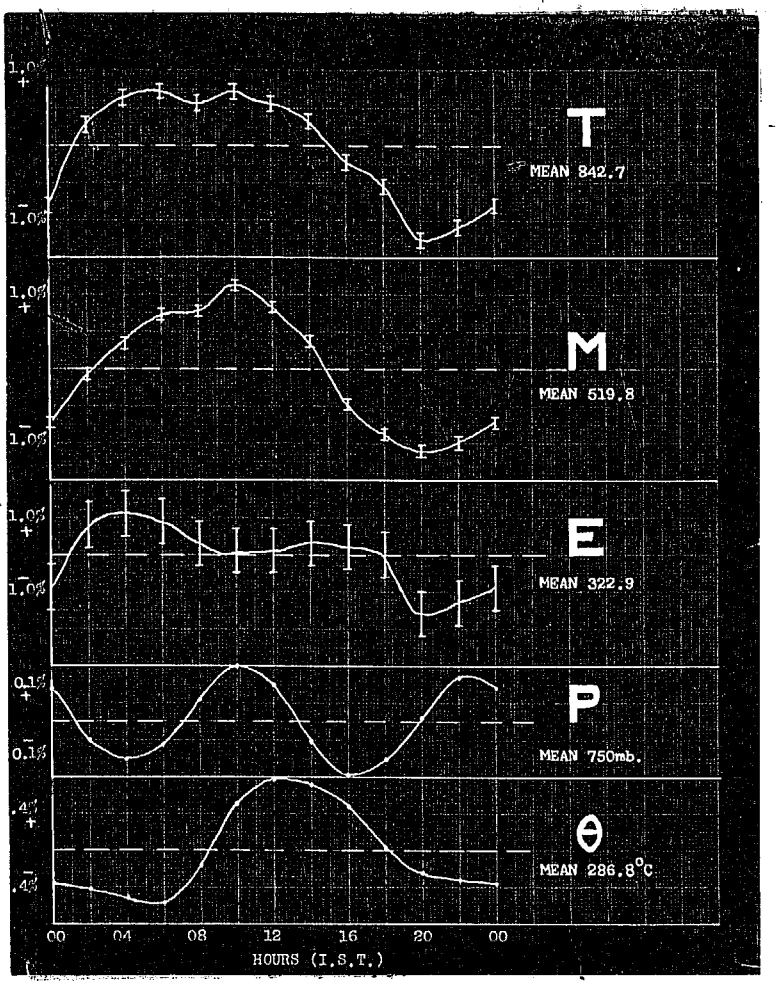

Fig. 22. Daily variation curves for the total intensity T, meson intensity M, electron component E, ground pressure P, and ground temperature θ at Kodaikanal.

2.2 The nature of the daily variation from set to set:-

With a view to study the nature of the daily variation from set to set, the variations obtained from the two independent telescopes for any set are combined together. Tables 12, 13, 14, 15 and 16 give the bi-hourly values for T (average of T' and T"), M (average of M_1', M_1'', M_2' and M_2''), E (T - M), P (ground pressure) and θ (ground temperature) respectively. Values for the cosmic ray components are expressed as % deviations from mean. Those for pressure and temperature are the deviations from mean in millibar and degrees fahrenheit respectively.

The standard error for each set is given in the top row.

Table 12. Total intensity from set to set.

Set.	1	2	3	4	5	6	7
Std. error.	0.2	0.3	0.2	0.3	0.2	0.2	0.3
Hr.00	0.8	0.0	-1.0	-1.1	-0.5	-0.8	-0.7
02	0.9	0.7	0.1	0.7	0.2	0.3	0.1
04	1.4	0.5	0.6	0.7	0.7	0.7	0.5
06	0.6	0.5	1.7	0.6	0.4	0.8	0.3
08	0.5	0.8	1.2	0.7	0.1	0.5	0.7
10	-1.1	0.8	0.9	1.6	0.7	0.6	0.6
12	-0.6	-0.4	0.4	0.8	0.4	0.6	0.7
14	-0.9	-0.4	-0.4	0.2	0.6	0.5	0.7
16	-1.0	-0.6	-0.4	-0.2	-0.3	-0.3	0.4
18	-0.8	-0.3	-0.6	-0.9	-0.4	-0.6	-0.2
20	-0.5	-1.3	-1.5	-1.2	-0.9	-1.3	-1.5
22	0.7	-0.4	-0.9	-1.4	-1.0	-0.9	-1.7
Mean.	879.7	861.7	865.9	831.2	843.3	833.6	841.3

Table 13. Meson intensity from set to set.

Set.	2	3	4	5	6	7
Std. error.	0.2	0.2	0.2	0.2	0.2	0.2
Hr.00	0.2	-0.9	-0.8	-0.8	-0.6	-0.6
02	0.2	-0.2	0.6	-0.3	-0.2	0.3
04	0.6	0.1	0.7	0.4	0.5	0.0
06	-0.1	1.4	0.5	0.8	0.5	0.3
08	0.7	1.7	1.3	0.2	0.8	0.4
10	0.2	1.5	1.3	1.4	0.6	1.2
12	0.1	0.4	1.0	1.4	0.8	0.0
14	-0.5	-0.2	0.3	0.7	0.5	0.3
16	-0.6	-0.1	-0.4	-0.7	-0.6	-0.1
18	-0.4	-1.0	-1.3	-1.0	-0.7	-0.6
20	-0.7	-1.9	-2.0	-1.2	-0.7	-0.3
22	0.2	-0.9	-1.0	-0.8	-1.1	-1.1
Mean.	530.0	531.0	511.0	518.0	512.0	517.0

The means have been normalised so as to be about 61.5 % of the corresponding means of the total intensity.

Table 14. Electron component from set to set.

Set.	2	3	4	5	6	7
Std. error.	1.1	1.2	1.4	1.2	1.2	1.4
Hr.00	-0.3	-1.3	-1.5	0.0	-1.0	-1.0
02	1.5	0.6	0.8	1.1	0.9	-0.2
04	0.4	1.3	0.8	1.1	1.0	1.0
06	1.4	2.3	0.8	-0.4	1.1	0.3
08	1.1	0.4	-0.3	-0.1	0.0	1.1
10	1.7	-0.1	0.7	-0.3	0.4	-0.4
12	-1.3	0.4	0.6	-1.3	0.3	1.9
14	-0.2	-0.7	0.1	0.4	0.5	1.4
16	-0.6	-0.9	0.1	0.4	0.2	1.1
18	-0.3	0.1	-0.3	0.6	-0.6	0.5
20	-2.2	-0.9	0.0	-0.5	-2.4	-3.4
22	-1.4	-1.0	-2.0	-1.1	-0.7	-2.5
Mean.	332.0	335.0	320.0	325.0	322.0	324.0

The values have been obtained by subtracting the normalised values of meson intensity from the corresponding values of total intensity.

Table 15. Pressure variation from set to set.

Set.	1	2	3	4	5	6,7
	mb.	mb.	mb.	mb.	mb.	mb.
Hr.00	0.5	0.4	0.7	0.7	0.6	0.8
02	-0.1	-0.2	-0.4	-0.3	-0.3	-0.6
04	-0.6	-0.5	-0.3	-0.8	-1.1	-1.0
06	-0.6	-0.7	-0.1	-0.5	-0.6	-0.7
08	0.3	0.1	0.3	0.5	0.6	0.6
10	1.0	1.0	0.8	1.0	1.4	1.4
12	0.9	0.9	0.8	0.7	0.9	0.7
14	0.1	0.1	0.0	-0.4	-0.5	-0.6
16	-0.7	-0.7	-0.8	-1.1	-1.2	-1.2
18	-0.8	-0.8	-0.7	-0.6	-0.9	-0.8
20	-0.1	-0.3	0.0	0.0	0.2	0.3
22	0.4	0.4	0.8	0.8	0.9	1.0
Mean.	769.8	768.4	769.8	771.5	770.2	771.1

Table 16. Temperature variation from set to set.

Set.	1	2	3	4	5	6,7
Hr.00	-2.3	-0.9	-2.0	-1.8	-1.6	-2.1
02	-2.9	-1.3	-2.1	-1.8	-2.0	-2.5
04	-2.9	-1.7	-2.5	-2.0	-2.8	-2.9
06	-3.2	-1.8	-2.7	-2.5	-2.9	-3.4
08	-0.6	0.0	-1.3	-0.8	-1.5	-0.6
10	3.2	2.5	1.9	2.4	2.2	3.3
12	4.6	2.2	4.1	3.3	4.3	4.6
14	4.4	2.5	4.4	3.1	3.7	4.1
16	3.2	1.5	3.0	2.0	2.5	2.5
18	0.7	-0.5	0.4	0.7	0.3	-0.1
20	-1.8	-1.4	-1.5	-1.2	-1.2	-1.1
22	-2.3	-1.3	-1.3	-1.5	-1.1	-1.3
Mean.	56.9°F	55.0°F	57.2°F	56.7°F	57.3°F	56.9°F

Tables 17(a) and (b) give the percentage amplitudes and the hours of maxima (in degrees) for the first and the second harmonics respectively. As before, for pressure and temperature, the amplitudes are in millibars and degrees F. respectively.

Table 17(a). First harmonics of T, M, E, P and θ for different sets.

	T		M		E		P		θ	
Set.	Amp.%	Hr.of max.	Amp.%	Hr.of max.	Amp.%	Hr.of max.	Amp. (mb.)	Hr.of max.	Amp. (^{o}F)	Hr.of max.
1	1.1	40^{o}					.24	115^{o}	4.0	$\pi + 25^{o}$
2	0.8	95^{o}	0.5	80^{o}	1.3	70^{o}	.27	115^{o}	2.1	$\pi + 15^{o}$
3	1.2	115^{o}	1.4	125^{o}	0.9	65^{o}	.21	70^{o}	3.3	$\pi + 30^{o}$
4	1.2	130^{o}	1.4	125^{o}	0.8	105^{o}	.14	105^{o}	2.7	$\pi + 25^{o}$
5	0.7	130^{o}	1.1	140^{o}	0.3	0^{o}	.21	125^{o}	3.1	$\pi + 30^{o}$
6	0.9	125^{o}	0.9	130^{o}	1.0	85^{o}	.14	80^{o}	3.6	$\pi + 25^{o}$
7	1.0	145^{o}	0.7	135^{o}	1.5	125^{o}				

III.

Table 17(b). Second harmonics of T, M, E, P and θ for different sets.

Set.	T		M		E		P		θ	
	Amp.%	Hr.of max.	Amp.%	Hr.of max.	Amp.%	Hr.of max.	Amp. (mb.)	Hr.of max.	Amp. (°F)	Hr.of max.
1	0.1	90°					0.82	π + 145°	1.3	25°
2	0.1	75°	0.2	π+145°	0.4	70°	0.77	π + 155°	0.9	10°
3	0.3	175°	0.2	π + 35°	0.6	95°	0.72	π + 140°	1.4	35°
4	0.3	70°	0.4	35°	0.6	65°	0.93	π + 135°	0.9	20°
5	0.3	80°	0.3	10°	0.8	55°	1.14	π + 135°	1.4	20°
6	0.3	90°	0.1	100°	0.8	30°	1.18	π + 130°	1.5	10°
7	0.5	95°	0.1	75°	1.2	35°				

The two harmonics are plotted on separate harmonic dials given in Fig.23(p.104).

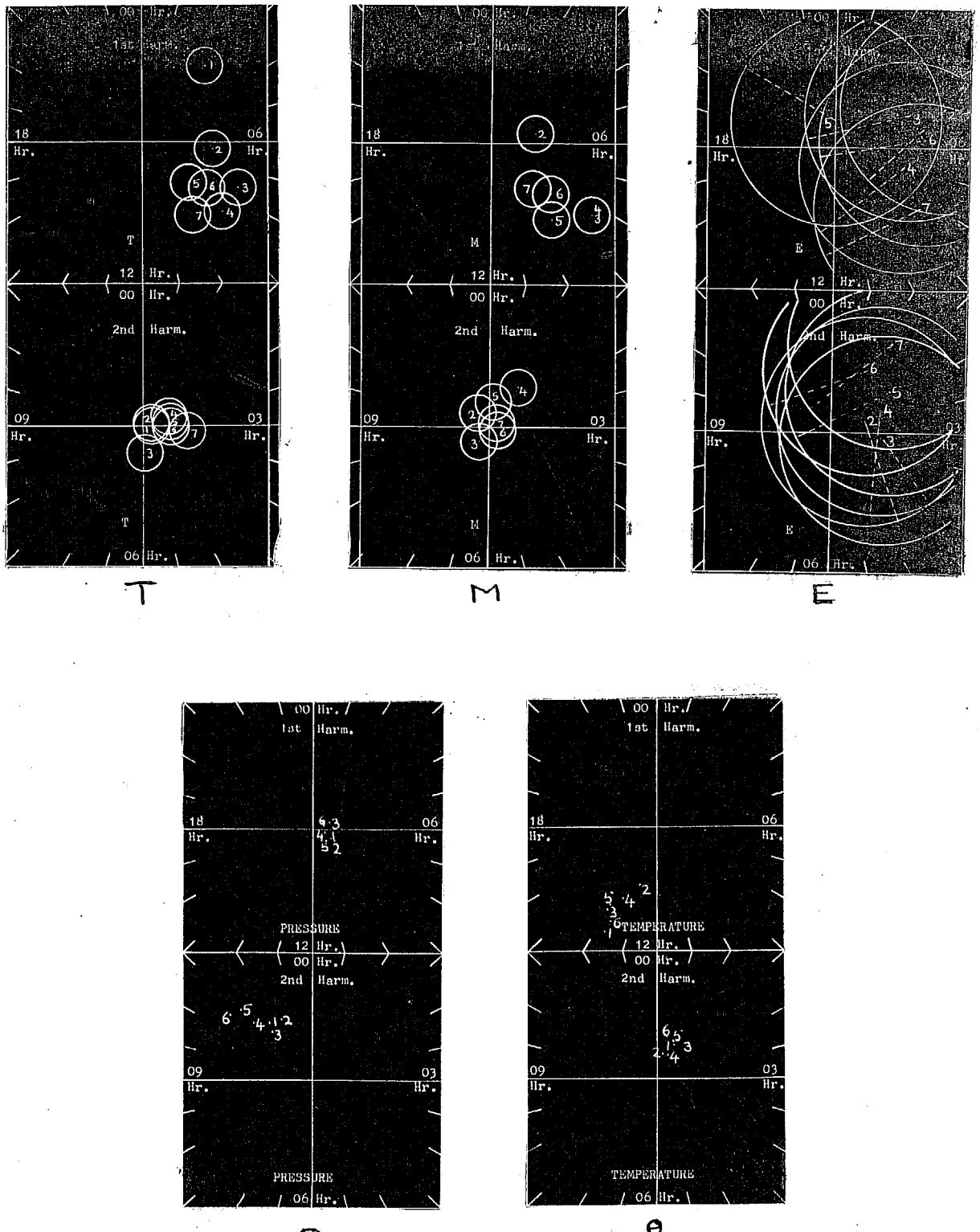

Fig. 23. Harmonic dials for the daily variation from set to set.

As can be seen from the harmonic dials (Fig.23), the total intensity shows a shift of the hour of maximum towards later hours as we pass from set 1 to set 7. No such trend can be seen for the meson intensity. The ground pressure and temperature have almost similar phases from set to set though the amplitude alters appreciably.

2.3 Day-to-day variation :-

As already stated, the daily means of the various cosmic ray components and the ground pressure and temperature can be evaluated from the bi-hourly primary data. The temperatures and heights of the various pressure levels in the atmosphere are obtained from the daily Radio-sonde ascents at nearby stations of Madras and Trivendrum. It was found that the data for Madras was very scanty especially for the 300 and 200 mb. levels. Hence only the data for Trivendrum was taken into consideration.

For any particular period, the trend of the day-to-day variation of the daily means for similar telescopes on the two sides of the instrument should be similar. A straight comparison between the values did not, however, reveal great similarity in all sets due to their statistical errors. A smoothening procedure was applied by adopting the method of moving averages where the average value of three consecutive days was taken as the value for the middle day. This is well illustrated by consi-

deration of the data of set 5 (14-20 Sept. 1951). Table 18 gives the values for the total and meson intensities for set 5 expressed as deviations from their respective means. The values for the moving averages are also given.

Table 18. Original values and moving averages for the day-to-day variation of set 5.

	Original values.						Moving averages.					
Date	T'	T''	M'_1	M''_1	M'_2	M''_2	T'	T''	M'_1	M''_1	M'_2	M''_2
14	1	-3	-2	-0	-3	3						
15	-2	1	-2	4	3	-1	1	1	-1	1	1	2
16	7	6	7	3	4	7	3	2	3	4	4	3
17	5	-1	8	8	5	0	2	1	3	2	0	-1
18	-4	-2	0	-3	-9	-12	-2	-2	-1	-1	-2	-3
19	-5	-1	-5	-6	0	1	-4	-1	-5	-6	-3	-2
20	-2	0	-6	-7	1	3						
Mean	916	747	671	522	644	566	916	747	671	522	644	566

Improvement in the agreement after taking moving averages can be easily seen from the following table which gives the intercorrelations between the corresponding rates before and after taking the moving averages:

Table 19. Correlations between the corresponding rates before and after taking the moving averages.

	T' and T"	M_1' and M_1''	M_2' and M_2''
Original values,	+.56	+.82	+.73
Moving averages,	+.90	+.94	+.90

The procedure adopted was therefore to evaluate the moving averages of all the intensities separately and then compare the values of T' with T" and of M_1', M_1'', M_2' and M_2'' between themselves. In all cases where data was available for both T' and T" for the same period, the trend of variation was similar. Hence the two were combined together. In cases where data for any one of them was missing, the moving average of the other was taken as representative of the total intensity. For meson intensity, the trends of at least two of the four components were always found to agree. The dissimilar trends were neglected and the rest were combined together. The values for the total and meson intensities thus obtained were then normalised so as to correspond to the mean bi-hourly rates of 900 and 555 for the total and meson intensities respectively for any particular set. The number 900 is arbitrarily chosen while 555 is just about

61.5 % of the total intensity rate, as is to be expected from the absorption for a mean thickness of 11 cm. of lead. Values of T and M so obtained were expressed as deviations from their means (viz. 900 and 555 respectively) and the values for the electron component E were evaluated by subtracting the meson intensity from the total intensity. The values of E had thus a mean value of 345.

Moving averages were also evaluated for the ground pressure and temperature, the height and temperature of the 200 mb. level and the daily sunspot number at Kodaikanal.

The cosmic ray components that have been neglected in any set due to insufficient data or dissimilar trends, are given in Table 20.

Table 20. Selection of cosmic ray components in any set for day-to-day variations.

Set.	No.of days.	Components neglected due to		Components considered.
		Insufficient data.	Dissimilar trends.	
3 (a)	4	T', M_1', M_2'	None	T'', M_1'', M_2''
(b)	5	" " "	"	" " "
4	8	T', M_2'	M_1'	" " "
5 (a)	5	None	None	T', T'', M_1', M_1'', M_2', M_2''
(b)	4	"	M_1'	" " , " " "
6	21	"	M_2'	" " M_1', " , "

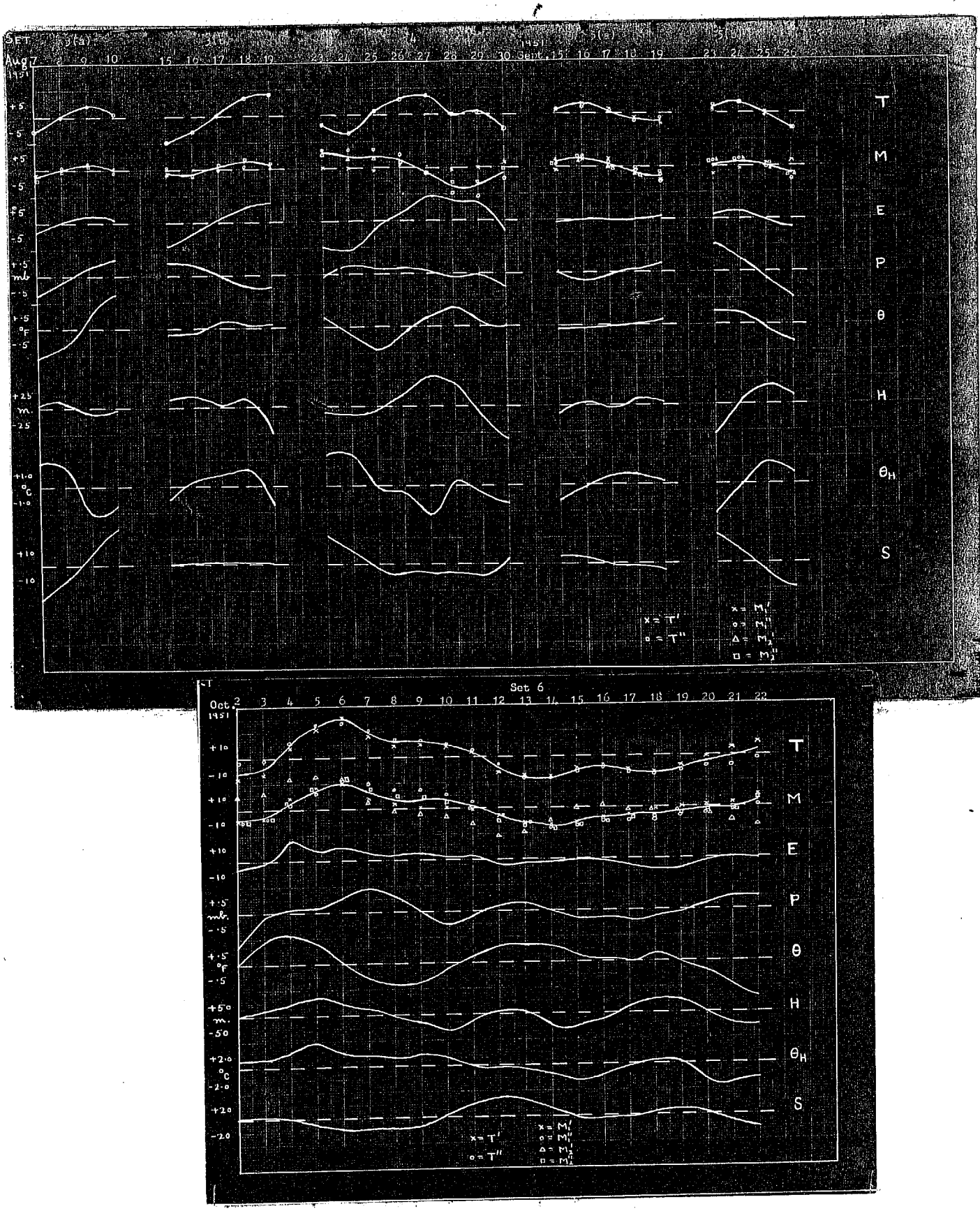

Fig. 24. Moving averages for different periods.

The moving averages for different periods are plotted in Fig. 24 (p.109). The abbreviations used are :-

T = Total intensity,

M = Meson intensity,

E = Electron component,

P = Ground pressure,

θ = Ground temperature,

H = Height of the 200 mb. level,

θ_H = Temperature at the 200 mb. level and

S = The daily sun-spot number.

Correlations have been calculated between the various cosmic ray intensities and the different meteorological factors and daily sunspot number for each set. It was found that the correlations varied widely from set to set and were even different in sign. Some sort of grouping of the data was therefore necessary. This was done by consideration of the 'standard variance' of the meson and electron intensities in the different sets. The values are given in Table 21.

Table 21. Standard variances of the electron and meson intensities for different sets.

Set.	M	E
3 (a)	3	5
(b)	3	43
4	24	62
5 (a)	9	1
(b)	3	7
6	86	36

As can be seen, the value of the standard variance for sets 4 and 6 is abnormally high as compared to the value of the other sets, for both M and E. The sets are therefore grouped together as normal and abnormal groups as follows :

Normal group :- Sets 3 (a), 5 (a) and 5 (b).

Abnormal group :- Sets 4 and 6.

Set 3 (b) is neglected as it gives an abnormal variance for E as compared to that of M which is negligibly small.

The superposition is carried out as already described in Section 1.7 of this chapter. The correlations obtained for the two groups are given in Tables 22 (a) and (b).

Table 22 (a). Correlations between cosmic ray intensities and meteorological factors.

Group.	r_{MP}	$r_{M\theta}$	r_{MH}	$r_{M\theta_H}$	r_{MS}	r_{EP}	$r_{E\theta}$	r_{EH}	$r_{E\theta_H}$	r_{ES}
Abnormal.	.43	-.36	.22	.53	-.47	.25	.04	.19	.20	-.54
Normal.	.23	.28	-.26	-.44	.48	.86	.78	-.36	-.57	.74

Table 22 (b). Inter-correlations between meteorological factors.

Group.	$r_{P\theta}$	r_{PH}	$r_{P\theta_H}$	r_{PS}	$r_{\theta H}$	$r_{\theta\theta_H}$	$r_{\theta S}$	$r_{H\theta_H}$	r_{HS}	$r_{S\theta_H}$
Abnormal.	-.06	.14	.01	-.30	.42	.27	-.17	.44	-.09	.00
Normal.	.84	-.65	-.73	.86	-.41	-.76	.93	.78	-.61	-.87

IV. DISCUSSION OF RESULTS.

It is evident from Fig. 22 (p.98) that the daily variation of the various cosmic ray components at Kodaikanal is mainly diurnal. The percentage amplitudes with the angles corresponding to the time of maxima for the different harmonics of the cosmic ray intensities, ground pressure and temperature at Kodaikanal are given in Table 23.

Table 23. Percentage amplitudes and the hours of maxima for the different harmonics.

	1 st		2 nd		3 rd		4 th		5 th		6 th
T ± .10	0.96	128°	.30	96°	.10	51°	.03	π+84°	.04	π+31°	.08 +π
M ± .08	1.07	132°	.12	25°	.09	174°	.03	π+32°	.03	32°	.05 +π
E ± .6	0.8	119°	.8	112°	.2	90°	.1	π+127°	.2	π+42°	.1 +π
P %	0.02	110°	.13	π+132°	...	...	.01	π+112°	...	...	...
θ %	0.63	π+24°	.25	16°	.05	105°	.05	π+63°	...	...	...

For calculating the percentage amplitude of the temperature variation, the mean temperature and its deviations from the mean are first converted into degrees 'absolute'. For the first harmonic, one solar hour is equivalent to 15°, whereas for the second harmonic, it is

represented by 30^0. The hours are counted from 12 midnight onwards.

It can be seen that in general, the components which are predominant in the variations are the first and the second. Thus for T, E and θ, the first and the second harmonics are important while the third and higher components are negligible. For mesons, even the second harmonic is very small and is comparable to the higher components. For P, the 1st, 3rd, 4th, 5th and 6th harmonics are all small as compared to the second one.

Since our analysis is made according to the solar time, which is connected with the earth's rotation round its axis in 24 hours, it is to be expected that the variates would show an important first harmonic with a period of 24 hours. The atmosphere, however, has a free period[49,50] of oscillation corresponding to approximately 12 hours and the resonance excitation of this oscillation by solar thermal and tidal actions is responsible for significant second harmonic components, directly for the pressure and indirectly for the other variates. A close analysis of the first two harmonics is therefore revealing for understanding the physical causal relationships between the variates.

Fig. 25 (a) and (b) (p. 114) show the harmonic dials for the first and second harmonics respectively. The error circle for any cosmic ray component is drawn at the end of its radius vector.

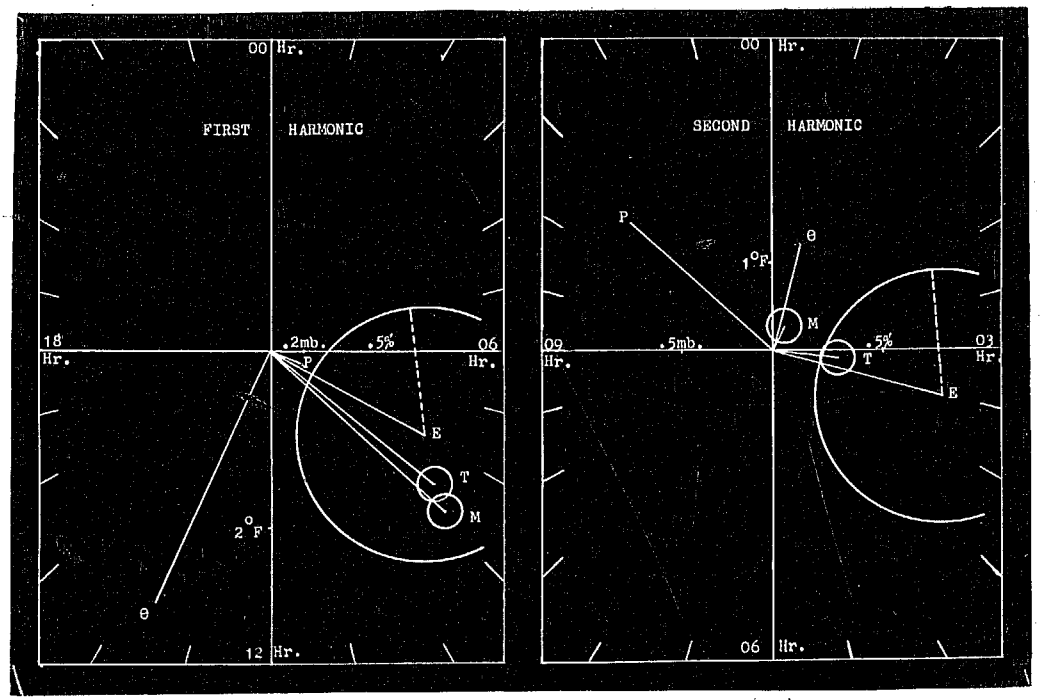

(a) (b)

Fig. 25. Harmonic dials for the first and the second harmonics.

It is seen that in the first harmonic, all the cosmic ray components lie in a narrow cone and agree in phase with the pressure component. However, the latter is of negligible amplitude and hence is not significant. The first harmonic of temperature is quite substantial but is almost completely out of phase with the cosmic ray components and is therefore uncorrelated with them.

For the second harmonic, the total intensity and the electron component have significant amplitudes and

the vectors lie in a narrow cone almost in opposition to the corresponding pressure vector with a phase difference of nearly 180°. The second harmonic of pressure represents the predominent component in the total variation of pressure. Since the second harmonic of temperature is almost out of phase with the second harmonics of T and E, the semi-diurnal variations of T and E can be supposed to be mainly caused by the changes in pressure. The second harmonic of M does not agree in phase with the other two cosmic ray intensities (viz. T and E), but its amplitude is extremely small and not statistically significant. Table 24 gives the correlation coefficients of the second harmonics of T and E with the second harmonics of P and θ.

Table 24. Correlations of the second harmonics of T and E with the second harmonics of P and θ.

r_{TP}	r_{EP}	$r_{T\theta}$	$r_{E\theta}$
-.81	-.94	+.17	-.10

Regression coefficients can now be calculated for those pairs of variates where the correlation coefficients are high and significant (viz. T : P and E : P). Thus one gets the two pressure coefficients

$$\left.\begin{aligned}\beta_T &= -3.3\ \% \\ \beta_E &= -9.6\ \%\end{aligned}\right\} \text{ per cm. Hg. . . . . (1)}$$

IV.

It is at first sight surprising why β_M has not turned out significant. For M, Duperier[2] has demonstrated that the coefficient β may be considered to be made up of two and probably three factors. There is the usual factor μ which is due to pure mass absorption. There is a factor μ' which is due to changes in the height of the meson formation layer with a consequent alteration in the probability of decay of the meson. Lastly, there may be a factor α dependent upon the density of the atmosphere below the average height of formation of π -mesons. Duperier has suggested that α is due to changes in the probability of nuclear capture of π -mesons which is a process in competition with the decay process giving rise to μ-mesons. This last factor is still not properly understood. Nevertheless, the pressure coefficient that is measured is dependent on all these factors and would depend on the meteorological processes governing them. The overall pressure coefficient β is given by an equation of the type

$$\Delta C = \beta \cdot \Delta P \quad \ldots\ldots\ldots (2)$$

where ΔC and ΔP are the variations in cosmic ray intensity and ground pressure respectively. According to Duperier, the modified form of the equation is

$$\Delta C = \mu \cdot \Delta P + \mu' \cdot \Delta H + \alpha \cdot \Delta \theta_H \quad \ldots\ldots (3)$$

where ΔH is the variation of the height of the meson

formation layer and $\Delta\theta_H$ is the variation of the temperature just below this layer. μ, μ' and α thus represent the mass absorption coefficient, decay coefficient, and the so called positive temperature coefficient respectively. If the R. H. S.s of equations (2) and (3) are equated, we get

$$\beta = \mu + \mu' \cdot \frac{\Delta H}{\Delta P} + \alpha \cdot \frac{\Delta \theta_H}{\Delta P} \quad \ldots\ldots \quad (4)$$

Thus the overall coefficient β differs from the actual mass absorption coefficient μ by the two terms $\mu' \cdot \frac{\Delta H}{\Delta P}$ and $\alpha \cdot \frac{\Delta \theta_H}{\Delta P}$ which are governed by purely meteorological factors. They vary according to whether the changes considered are daily, day-to-day or seasonal and also with the variations of the processes causing the day-to-day changes. Table 25 below gives the correlation coefficients between pairs of variates consisting of the day-to-day values of ground pressure P, ground temperature θ, height of the 200 mb. level H and temperature of the 200 mb. level θ_H for the various sets. Here the values for P and θ are those taken from the Kodaikanal Observatory records and the upper air data are those obtained from daily radiosonde flights made at the nearby station of Trivendrum.

Table 25. Inter-correlations between the meteorological factors for different sets.

Set.	Period (1951).	$r_{P\theta}$	r_{PH}	$r_{P\theta_H}$	$r_{\theta H}$	$r_{\theta\theta_H}$	$r_{H\theta_H}$
3	6-17 Aug.	.67	.06	-.54	.07	-.38	.34
4	23-30 Aug.	-.48	.53	.28	.30	-.03	-.17
5	15-27 Sep.	.68	-.75	.55	-.59	.55	-.88
6	4-12 Oct.	-.30	.53	.23	.55	.17	.66
7	18-29 Oct.	.28	-.33	.01	.37	.15	.63

For $r_{P\theta}$, we get a value of + .14 for the daily variations of P and θ at Kodaikanal.

As is easily seen, the values of the correlation coefficients vary widely from set to set and are different even in sign. Values of r_{PH} and $r_{P\theta_H}$ reveal that the factors $\frac{\Delta H}{\Delta P}$ and $\frac{\Delta \theta_H}{\Delta P}$ change appreciably from set to set.

The first factor μ is expected to be constant at a place and is independent of meteorological factors. Also it will act equally for daily and day-to-day changes. Inspite of this, the value of β from day-to-day data will vary from set to set depending upon the variations of $\frac{\Delta H}{\Delta P}$ and $\frac{\Delta \theta_H}{\Delta P}$.

Tables 26 (a), (b) and (c) give the values of the pressure coefficients and the absorption and decay coefficients obtained by various workers for the total intensity, meson intensity and electron component from daily and day-to-day variations.

Table 26 (a). Coefficients for the total intensity.

Author.	Experimental arrangement.	Nature of variation.	Pressure coefficient. β	Absorption coefficient. μ	Decay coefficient. μ'
Baranothy[44] & Forro.	Counter telescope.	Day-to-day	-3.5%/cm.Hg.		
Stevenson[60] & Johnson.	"	"	-3.8%		
Kolhorster[61]	"	"	-2.7%		
Smith[62]	"	"	-3.9%		
Duperier[63]	"	"	-3.5%	-2.3%/cm.Hg.*	-5.4%/Km.*
Messerschmidt[64]	Ionisation chamber.	"	-1.9%		
Duperier[63]	Counter telescope.	Daily.	...	-1.1%/cm.Hg.*	-3.9%/Km.*

* The total intensity has been interpreted by Duperier, as consisting of mesons only.

Table 26 (b). Coefficients for the meson intensity.

Author.	Experimental arrangement.	Absorber.	Nature of variation.	Pressure coefficient. β	Absorption coeff. μ	Decay coeff. μ'
Baronothy[31] & Ferro.	Counter telescope.	36cm.Pb.	Day-to-day	-3.1%/cm.Hg.		
Kolhorster[61]	"	140gm./cm^2	"	-1.6%	"	
Smith[62]	"	20.5cm.Pb.	"	-3.4%	"	
"	"	30.0cm.Pb.	"	-1.5%	"	
Duperier[2]	"	25cm.Pb.	"	-2.0%	"	-1.0%/cm.Hg. -3.9%/Km.
"	"	"	"	-1.0%	"	" "
Dolbear[24] & Elliot.	"	35cm.Pb.	"	...		-1.6% " -5.7% "
Messerschmidt[64]	Ion.cham.	10cm.Pb.	"	-1.8%	"	
"	"	20cm.Pb.	"	-1.1%	"	
Steinmaurer[37]	"	10cm.Pb.	"	-2.7%	"	
Compton[65] & Turner.	"	12cm.Pb.	"	-1.6%	"	
Hogg[18]	"	10cm.Pb.	"	-2.8%	"	

Table 26 (c). Pressure coefficient for the electron component.

Author.	Nature of variation.	Pressure coefficient.
Baronothy[31] & Forro.	Day-to-day	-4.2%/cm.Hg.
Stevenson[60] & Johnson.	"	-5.5% "
Johnson.[60]	"	-6.3% "

As can be seen, the value of the pressure coefficient β for the meson intensity is not quite consistent. On the other hand, the values for μ show better agreement.

In our investigation, the meson intensity has a very low positive correlation with pressure in the daily values and hence the very low value of + 0.4 % per cm.Hg. for the pressure coefficient. If μ alone were operative, β_M should have been about -1.0 % per cm.Hg. and this would require not only an appreciable change of phase, but also a larger amplitude than is obtained for the second harmonic of M. The absence of a significant semi-diurnal component for M, suggests that even in the daily variation, the factors μ' and α are operative in such a way as to produce an effect contrary to that of μ and a resultant variation almost uncorrelated with the pressure variation.

The electron-photon component found in the cosmic radiation is primarily created by the following processes:-

(1) The decay of the π°-mesons into photons in the very high atmosphere. The photons then give rise to cascade showers which are mainly responsible for the shape of the height-ionisation curve for total intensity at higher levels. This electronic component was erroneously believed some years ago to be due to a primary electron component coming to the earth from outside space. At sea-level, very little of the electron component is due to this process.

(2) The decay of μ-mesons. This is the predominant process for the creation of the electronic component at low levels of the atmosphere near the ground and at levels underground below sea-level.

(3) The knock-on electrons generated by the μ mesons.

When the first process becomes negligible, the soft component attains equilibrium with the μ-meson component as is observed at sea-level. At the elevation of Kodaikanal, the electron component increases to about $3\frac{1}{2}$ times the value at sea-level, compared to an increase of about $1\frac{1}{4}$ times for the meson component. Therefore at Kodaikanal, the total soft component is made up of approximately two parts of electrons formed by the process (1)

and one part by the processes (2) and (3) considered jointly.

For an electron formed by any of these processes, the main variation would be that due to the direct influence of the change in the mass of air between the points of creation and of observation. The variation of E due to the variation of π°- and μ-mesons caused by the meteorological factors would certainly be a second order effect.

For the pressure coefficient of the electronic component, therefore, while there is little complication created by factors such as μ' and α, the value of the mass coefficient is not expected to be constant under all conditions. According to the cascade theory, the number of electrons N found at a thickness of 't' radiation lengths, due to a primary electron of energy E_0 depends on both 't' and E_0. Bhabha[66] and Chakrabarty have calculated the total number of particles that are found at a penetration depth of 't' radiation lengths produced by primary electrons of energy equivalent to $y_0 = \log (E_0 / \beta)$, where E_0 is equal to the energy of the electron, and 'β' is the critical energy. The radiation length 't' is calculated in terms of a characteristic length'l' defined by

$$l^{-1} = 4 \frac{Z^2 N}{137} \left(\frac{e^2}{mc^2} \right)^2 \log 183\, Z^{-1/3}, \quad \ldots\ldots (5)$$

IV.

where Z is the atomic number and $\bar{N}$ the number of atoms per unit volume. The other symbols have their usual meaning. Table 27 gives the values of N for different values of 't' and y_o.

Table 27. Values of N for different values of y_o and 't'.

t \ y_o	3	4	5	6	7	8	9	10	12
2	3.1	6.2	10.6	17.1	25.6	36	50	67	120
4	1.2	4.8	13.8	33.2	69.9	137	241	423	1117
6	0.4	2.1	8.6	28.7	80.6	198	460	970	3735
8	0.1	0.8	4.0	16.7	58.8	181	499	1284	6898
10		0.3	1.6	7.9	33.3	121	392	1176	8073
12		0.1	0.6	3.3	16.1	68	252	859	8018
15			0.1	0.8	4.5	22	98	396	5080
20				0.1	0.4	2	12	63	1268
25							1	7	198
30								1	22

The values of the characteristic unit of length 'l' and the critical energy 'β' for different substances are given in Table 28. (p.125).

Table 28. Values of 'l' and 'β' in different substances.

Substance	Air	H_2O	Al	Fe	Pb
'l' in cm.	34200	43.4	9.80	1.84	0.525
'β' in M.e.V.	103.0	114.6	55.56	25.88	6.927

As can be seen from Table 27, the value of N first increases with 't', attains a maximum at some value of 't' (depending upon the value of y_o) and then decreases for higher values of 't'. During the growth of the shower, therefore, (dN/dt) will be positive and during its decay it will be negative. The apparent pressure coefficient would thus start by being positive, reduce to zero at the maximum of the showers and then become negative. The experimentally observed pressure coefficient would depend upon the location of the point of observation with respect to the mean electron transition curve in the atmosphere. It would perhaps be more logical to consider separately the position of the point of observation vis a vis the electron transition curve produced by the first process of π^o decay and the electron transition curve produced by the second and third processes. In general, for a place near sea-level the effective 't' value would

be greater for the π° cascades than for the remainder of the electron component which is produced in closer proximity of the point of observation. Therefore, the value of β_E will change according to the altitude of the station.

The value of β_E obtained at Kodaikanal is -9.6 % per cm.~~Hg~~. It agrees approximately with the values given in Table 26 (c) (p. 121). The value obtained at Ahmedabad (at sea-level) from an investigation similar to the present one, is -22.0 %. Since, for stations at lower depths in the atmosphere, the contribution due to process (1) is less, the effective value of 't' is lower and hence the pressure coefficient is expected to be higher. It seems reasonable therefore, that the value of the pressure coefficient is higher at Ahmedabad than at Kodaikanal.

As far as the total intensity is concerned, an examination of β_T is not particularly revealing, since T is made up of M and E which have different pressure coefficients. Since β_M is negligible, the pressure coefficient of T is mainly contributed by the electron component. The variations of the total intensity and electron component can be corrected for the pressure effect by their respective coefficients. For the meson component, a correction is not appropriate since the amplitude of

the second harmonic of H is not significant. The values of T and E corrected for the pressure effect are designated as T' and E'. The bi-hourly values are given in Table 29.

Table 29. Daily variation of the total intensity and the electron component corrected for the pressure effect.

Hour.	T' .10	E' .6
00	-0.62	-0.4
02	0.17	0.5
04	0.45	0.5
06	0.61	0.5
08	0.70	0.7
10	1.03	1.0
12	0.76	0.7
14	0.23	0.0
16	-0.50	-0.6
18	-0.75	-0.6
20	-1.25	-1.5
22	-0.86	-0.7
Mean.	842.7	322.9

These pressure-corrected values of T and E and the original values of H are now correlated with the ground temperature. The correlation coefficients are given in Table 30 (p. 128).

Table 30. Correlation of the pressure corrected variations with ground temperature.

$r_{T'\theta}$	$r_{M\theta}$	$r_{E'\theta}$
+ .24	+ .30	+ .13

The correlation coefficients are all very low and positive in sign. Several workers (e.g. Hess[17], Hogg[18]) have found out the temperature coefficient by utilising the daily means of cosmic ray intensity and ground temperature. The values obtained are not very consistent, but the coefficient is always negative and its average value is about -.15 % per ^{0}C. Blackett[19] has offered an explanation of the seasonal temperature effect on the basis of the meson decay process. An increase in ground temperature during the summer corresponds to a warming of the atmosphere in general and hence an elevation in the height above ground of the region where mesons are produced. The mesons have thus to travel a greater distance before arriving at the ground and the probability of decay is increased. Thus, an increase of temperature causes a decrease in cosmic ray intensity, giving a negative correlation between the two. Our results show that a similar process is not operative for the daily variation.

It is worth-while reviewing the results in terms of the 'positive temperature effect' reported by Duperier[2].

rw

If we assume that the daily variation we obtain is caused by corresponding temperature changes near the meson formation layer, the phase of the daily variation of temperature at that level is required to be earlier than the phase of ground temperature by about 4 hours. Also, taking Duperier's value $\alpha = +.10$ % per ^{o}C for the temperature coefficient, an amplitude of about $10^{o}C$ is necessary to explain a variation of meson intensity of 1.0 % amplitude at ground. There is no meteorological evidance[67] for a temperature variation of such a phase and amplitude at the 100 to 200 mb. level which is supposed to be the level of meson formation. Moreover, no agency is known to be located at that level which can absorb or release radiation and cause the required temperature variation. If, therefore, temperature variations of the required magnitude do take place, they have to be due to heating by turbulence or release of latent heat by water-vapour in the lower atmosphere or to heating from above by radiation from the ozone layer. Both these processes would occur over an extended portion of the atmosphere and hence would produce variation in the heights of the different isobar levels. An increase in temperature would cause an expansion of the atmosphere and the different isobar levels would rise up. The meson intensity would, therefore, tend to decrease and the positive temperature effect would be effectively reduced. To explain the observed positive temperature effect, the

amplitude of the temperature variation will have to be still higher. It seems therefore, that the observed variation of meson intensity cannot be explained on the basis of the positive temperature effect.

The values given in Table 29 are harmonically analysed. The percentage amplitudes and the hours of maxima for the first and second harmonics are entered in Table 31.

Table 31. First and second harmonics of the pressure corrected curves.

Harm.	1 st		2 nd	
T'	1.00	127°	.19	35°
M or M'	1.07	132°	.12	25°
E'	1.00	118°	.30	30°

The pressure corrected curves are thus predominantly diurnal with the hoursof maxima at about 9 A.M.(I.S.T.). The percentage amplitude is about 1.0 % and is the same for the total and the meson intensity. Since the standard error is only 0.1 %, the amplitude is quite significant.

It is worth-while in this connection to take into consideration the daily variation of cosmic ray intensity at Ahmedabad, which is studied by my colleague Mr.U.D.Desai

by an experimental arrangement similar to the present one and which forms a part of the subject matter of his Ph.D. thesis. The variations at Ahmedabad, when harmonically analysed, show a high negative correlation between the second harmonics of cosmic ray intensities and ground pressure. The pressure coefficients for T, M and E are

$$\left.\begin{aligned} T &= -6.4\ \% \\ M &= -3.1\ \% \\ E &= -22.0\ \% \end{aligned}\right\} \quad \text{per cm. Hg.} \quad \ldots \quad (6)$$

When the variations are corrected with these coefficients, the residual curves for T and M show low correlations with the ground temperature. The electron component shows a high negative correlation (-.66) with ground temperature. The temperature coefficient for the electron component is -.29 % per ^{o}C. The T and M curves corrected for pressure effect and the E component corrected for both pressure and temperature effects, are harmonically analysed. The percentage amplitudes and hours of maxima for the first and the second harmonics are given in Table 32, (p. 132).

Table 32. First and second harmonics of the daily variations at Ahmedabad, corrected for meteorological effects.

Harm.	1 st		2 nd	
T	0.5	124°	.11	45°
M	0.5	165°	.02	90°
E	2.3	70°	.60	55°

The final residual curves for both Kodaikanal and Ahmedabad are plotted in Fig. 26.

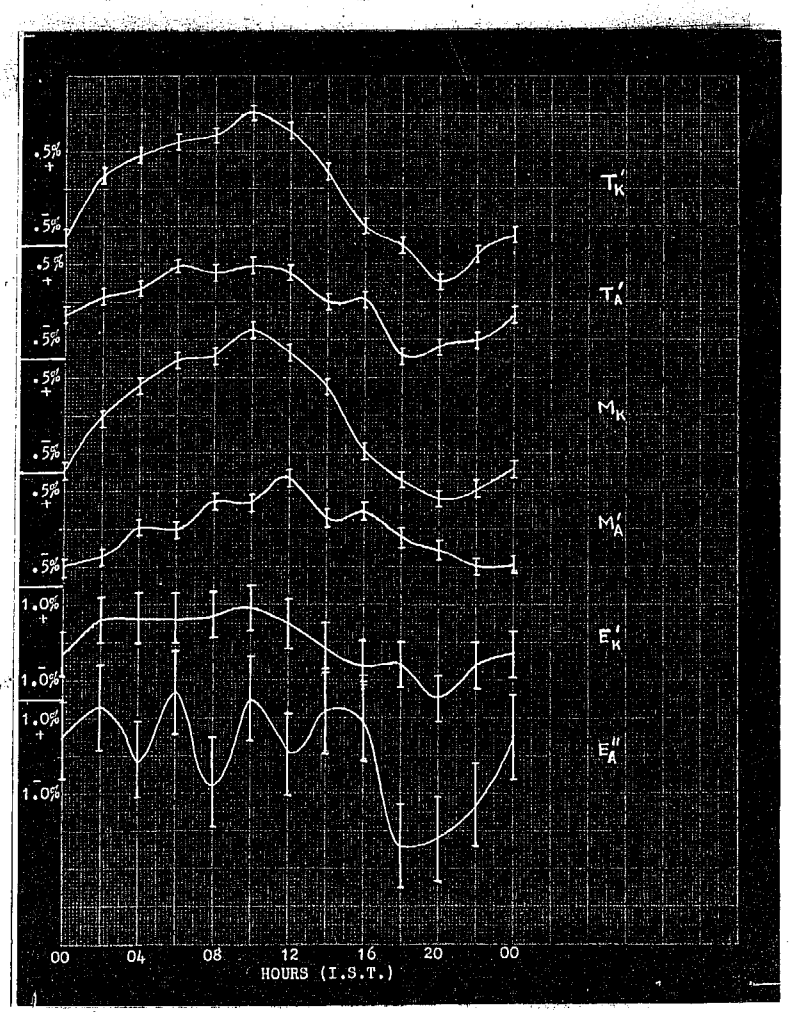

Fig. 26. The final residual curves for Kodaikanal(K) and Ahmedabad (A).

The curves given in Fig. 26 are smoothened by taking moving averages for three consecutive values. The smoothened curves thus obtained are plotted in Fig. 27.

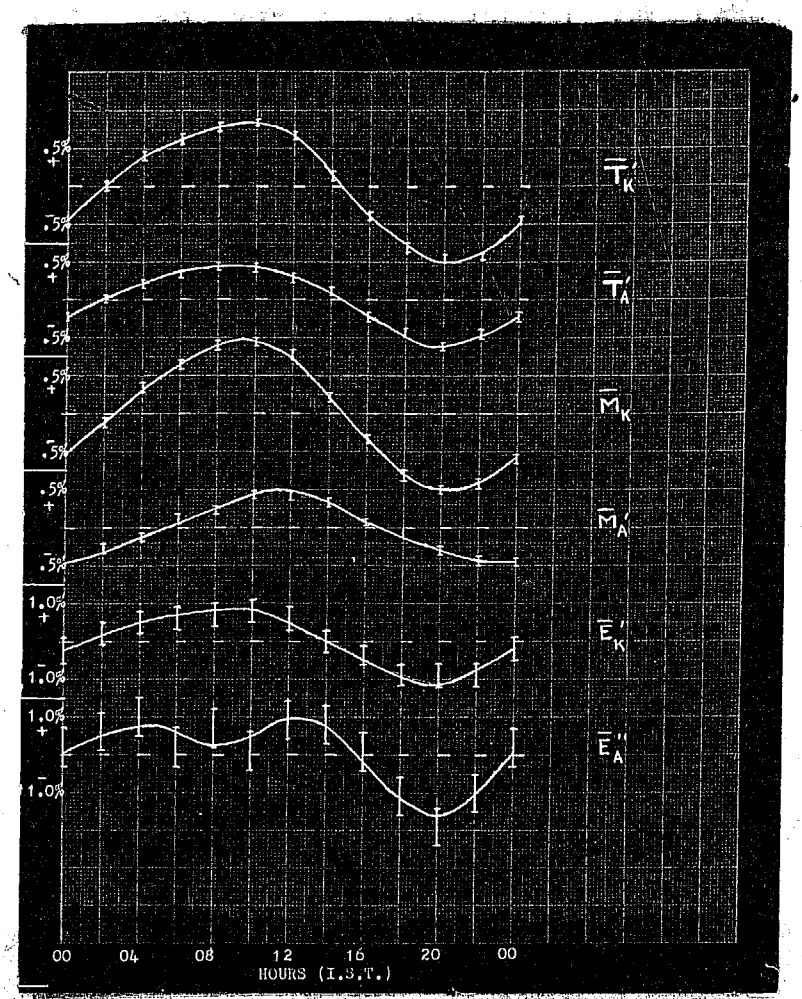

Fig. 27. Residual curves after taking moving averages.

The smoothened curves are harmonically analysed. The percentage amplitudes and hours of maxima for the first and the second harmonics are given in Table 33(p.134).

TW

Table 33. First and second harmonics of the smoothened residual curves at Kodaikanal and Ahmedabad.

	Kodaikanal.				Ahmedabad.			
Harm.	1 st		2 nd		1 st		2 nd	
T	.91 .05	127°	.12 .05	37°	.49 .05	124°	.08 .05	45°
M	.97 .04	131°	.09 .04	26°	.43 .04	168°	.02 .04	90°
E	.90 .30	117°	.10 .30	45°	.93 .60	119°	.77 .60	60°

The harmonic dials for the first and second harmonics of these variations are shown in Fig. 28.

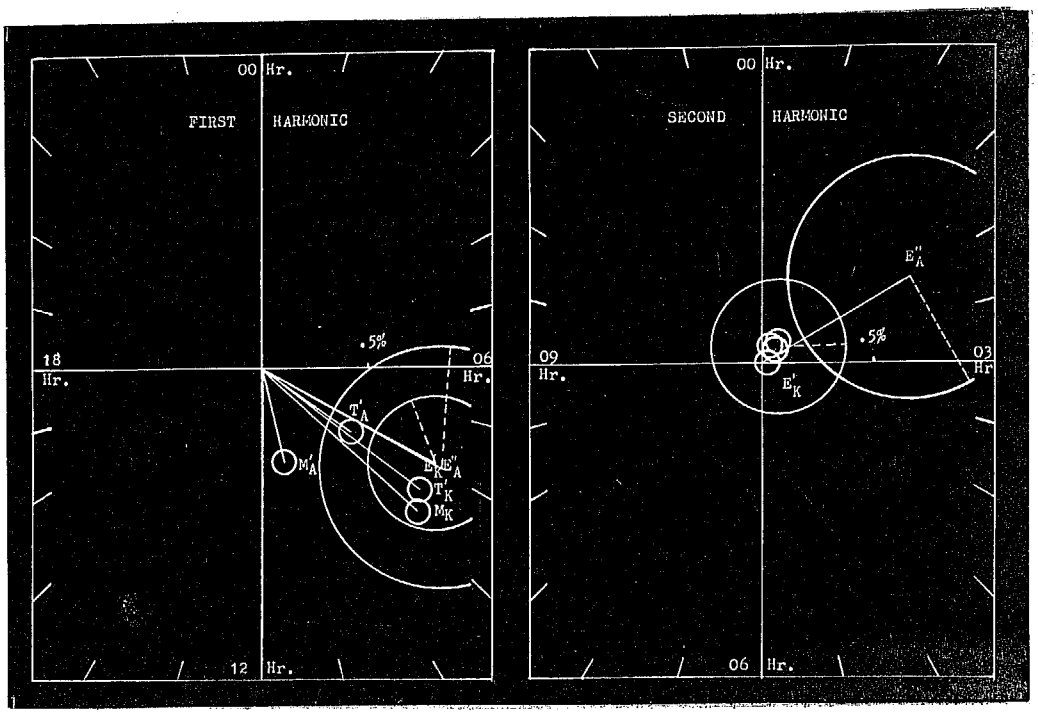

Fig. 28. Harmonic dials for the residual curves at Kodaikanal and Ahmedabad.

TV

The similiarity between the Kodaikanal and Ahmedabad curves is very striking. The hours of maxima are almost the same. The electron curves cannot be relied upon since the statistical errors (especially at Ahmedabad) are appreciable.

It is evident therefore that a non-meteorological variation is present in the daily variation at Ahmedabad also, though the amplitude is much smaller (viz. about .5 %). The phase of the variation is however the same as at Kodaikanal.

Kodaikanal is a hill station situated almost on the geomagnetic equator and has an altitude of about 7700 ft. Ahmedabad, on the other hand, has a geomagnetic latitude of about 13°N and height of only 180 ft. above sea level. It is rather difficult to imagine that a latitude change of only 13° can cause so much amplitude change in the residual variation. The meteorological effects are different at the two places, the correlation coefficients with meteorological elements as well as the pressure and the temperature coefficients being higher at Ahmedabad. It seems therefore, that the difference between the variations at the two places might be due to the difference in altitude. At lower depths in the atmosphere, the meteorological factors are expected to be more effective. At higher altitudes, on the other hand, the pressure and temperature effects are small except for the electron component which is regarded as generated in

the first few kilometers above any station. The amplitude of the residual effect seems to be more for higher altitudes.

The results can be proved conclusively if data is available for different altitudes and similar latitudes. Experiments are being planned to be conducted at the sea level near the geomagnetic equator and also at different altitudes away from the geomagnetic equator.

The results obtained from the day-to-day variation at Kodaikanal can be considered to throw some more light on this aspect. As can be seen from the Table 22 (a)(p.111) the correlations of the meson intensity with ground pressure and temperature are very low, both in the normal as well as abnormal sets. The meson intensity shows a low positive correlation with ground pressure. The data for the normal set is not sufficient to draw any definite conclusions. In fact, the high positive correlation of ground pressure with ground temperature and the sunspot number (Table 22 (b) p.111) may not represent a consistent feature. Similarly the high negative correlation of the ground temperature and pressure with the temperature and height of the 200 mb. level, may be just casual. Table 34 gives the total and partial correlations of the two cosmic ray intensities M and E with ground temperature and pressure for the normal and the abnormal sets.

Table 34. Total and partial correlations between cosmic ray intensities and ground pressure and temperature.

Set.	r_{MP}	$r_{M\theta}$	$r_{MP.\theta}$	$r_{M\theta.P}$	r_{EP}	$r_{E\theta}$	$r_{EP.\theta}$	$r_{E\theta.P}$	$r_{P\theta}$
Abnorm.	.43	-.36	.44	-.25	.25	.04	-.25	.06	-.06
Norm.	.23	.28	-.01	.18	.86	.78	.65	.20	.84

The high correlationsof the electron intensity for the normal set with ground pressure and temperature (viz. +.86 and +.78) reduce to +.65 and +.20 when partial correlations are taken. It would therefore seem that the electron component at Kodaikanal is affected more by pressure changes than by ground temperature changes.

On the whole, the correlations for the meson intensity are very low which confirms the conclusion previously arrived at, that the cosmic ray intensity at high altitude is little affected by variations in the meteorological elements.

The large variation from day-to-day in the cosmic ray intensity, would require a non-meteorological cause just as in the case of the daily variation. In the daily variation, the intensity during day-time is more than that during night-time. It was felt worth-while, therefore, to see whether the day-to-day changes were more for the

day-time values as compared to those of the night-time values. For this purpose, the data of set 6, which shows large fluctuations in day-to-day values, was utilised. The data for each day was divided into day-time and night-time values reckoned from 7 A.M. to 7 P.M. and 7 P.M. to 7 A.M. respectively. The day-time and night-time values for different days in the set were then expressed as deviations from their respective means. The standard deviations for the meson intensity were found to be

(5.7 ± 0.2) % for day-time values and

(4.9 ± 0.2) % for night-time values.

The standard deviation for the day-time values is significantly different from that for the night-time values. Therefore, during day-time, there is an additional factor contributing to the variation of the cosmic ray intensity or, the contribution of the disturbing factor is greater during the day-time than in the night-time. This suggests that the factor causing the diurnal increase of cosmic ray intensity during day-time, is probably responsible also for the increased deviations of the day-time values in day-to-day variations.

V. HARD COMPONENT AND THE SHOWER INTENSITY.

Besides the variations of the total intensity T, the meson intensity M and the electron component E, the variations of two other cosmic ray components were studied. The first was the hard component which could penetrate 36 cm. of lead and was designated by H_c. The second was the intensity of showers in the atmosphere, designated by S. The experimental arrangement used in the two cases has already been described in Chapter II.

The results for the hard component are presented and discussed in Section 1 below. Those for the shower intensity are given in Section 2. The reason for presenting these separately is that for H_c the data is rather confusing and for S it is very limited. Hence, both of these require further verification.

1. The hard component (H_c) :-

The data for the hard component is divided into five sets, the criteria for selection being the same as was adopted for T and M. The bi-hourly values for different sets are given in Table 35(p.140).

Table 35. Hard component (H_c) from set to set.

Set.	1	2	3	4	5
Interval	5 Aug.- 20 Aug.	21 Aug.- 1 Sep.	5 Sep.- 28 Sep.	3 Oct.- 10 Oct.	16 Oct.- 31 Oct.
No. of days.	(14)	(11)	(20)	(11)	(15)
Hr. 00	5	5	2	6	6
02	8	9	10	16	8
04	2	6	10	17	11
06	3	3	7	15	10
08	- 4	- 5	- 4	-14	- 5
10	- 6	- 6	- 8	-20	-10
12	- 3	- 5	- 1	- 5	- 3
14	- 3	- 5	1	3	0
16	- 6	- 7	- 5	-14	- 9
18	- 2	- 1	0	- 3	- 7
20	3	3	- 4	- 2	- 6
22	2	4	- 5	1	5
Mean.	287	284	291	298	227

The hour of transition i.e. the hour at which the positive trend of the morning hours vanishes, and the maximum and the minimum values expressed as percentage deviations from the mean with their hours of occurence are given in Table 36 (p.141).

Table 36. Hours of transition, maxima and minima for the hard component for different sets.

Set.	1	2	3	4	5
Hour of transi.	06 Hr.	06 Hr.	06 Hr.	06 Hr.	06 Hr.
Max.	2.8 02Hr.	3.2 02Hr.	3.4 02Hr.	5.7 04Hr.	4.8 04Hr
Min.	2.1 10Hr.	2.4 10Hr.	2.7 10Hr.	6.7 10Hr.	4.4 10Hr

The data for the various sets seems to be consistant so far as the hours of transition and maxima and minima are concerned. However, the percentage amplitude of the variation has a large fluctuation from set to set and is, in all cases, much greater than the percentage amplitudes for the total and meson intensities described in the previous chapter. The final bi-hourly values expressed as percentage deviations from mean after the superposition of all these sets, are given in Table 37 (p.142).

Table 37. Daily variation of the hard component.

Hour	H_c ·2
00	1.6
02	3.7
04	3.2
06	2.7
08	-2.2
10	-3.5
12	-1.2
14	-0.3
16	-2.8
18	-0.9
20	-0.6
22	0.3
Mean.	276.4

The amplitude of the variation is abnormally high (about 3.5 %) as compared to the other cosmic ray intensities and varies considerably from set to set. It is, therefore, desirable to continue the observations over a much longer period in order to ascertain whether the variation is genuine or spurious.

2. The atmospheric shower intensity (S) :-

The experimental arraugement measuring showers was run for a period of 24 days in November 1951. The average bi-hourly values expressed as percentage deviations from the mean are given in Table 38. The values of the electron component E are given in column 3 for comparison.

Table 38. Daily variation of the atmospheric shower intensity.

Hour.	S ±.4	E ±.6
00	0.4	-0.9
02	0.7	0.8
04	1.1	1.1
06	0.6	0.9
08	0.1	0.3
10	0.3	0.1
12	0.5	-0.1
14	0.1	0.3
16	0.8	0.2
18	-1.6	0.0
20	-1.9	-1.6
22	-1.2	-1.3
Mean.	101.0	322.9

The two variations seem to agree well within the standard errors of each. There is a suggestion of a shift in S by about two hours as compared to the electron component. This is brought out more clearly by taking the moving averages for three consecutive values, centered at the middle hour. The values so obtained are given in Table 39 (p. 144).

Table 39. Daily variations of S and E after taking moving averages.

Hour.	S ± .2	E ± .3
00	0.0	-0.5
02	0.7	0.3
04	0.8	0.9
06	0.6	0.8
08	0.3	0.4
10	0.3	0.2
12	0.3	0.2
14	0.5	0.2
16	-0.2	0.2
18	-0.9	-0.5
20	-1.6	-1.0
22	-0.9	-1.3
Mean.	101.0	322.9

The percentage amplitudes and the hours of maxima for the first and the second harmonics are given in Table 40. The corresponding values for ground pressure and temperature are also given.

Table 40. First and second harmonics of the smoothened curves for S and E.

Harm.	1 st		2 nd	
S	.83 ± .20	110^{0}	.58 ± .20	68^{0}
E	.75 ± .30	120^{0}	.52 ± .30	113^{0}
P	.02	110^{0}	.13	132^{0}
θ	.63	24^{0}	.25	16^{0}

It is seen that the first harmonics of the shower intensity and electron component are almost the same while the second harmonic of the former is 45° (1½ hours) earlier in phase as compared to the second harmonic of the latter. The second harmonic of shower intensity has therefore a low correlation (-.44) with the second harmonic of ground pressure, in contrast to the value (-.95) for the electron component.

For temperature, both the first and the second harmonics have low correlations with the first and second harmonics of the shower intensity and the electron component.

It seems, therefore, that the shower intensity at Kodaikanal, is not much affected by the meteorological factors. The variation has an important diurnal component comparable to the meson intensity M, both in phase and amplitude. Before one can make a close analysis of the variation of S and its relationship with other components of cosmic radiation, it is necessary to accumulate much more experimental data. Further work in this connection is in progress.

VI. CONCLUSION.

The daily variations of the total cosmic ray intensity and meson intensity at Kodaikanal (geomag. lat. 1°N, altitude 7688 ft.) are predominently diurnal with a maximum at about 1000 hr. local time. The electron component which is obtained as a difference curve between the total and the meson intensity, shows a semi-diurnal component as well. The pressure variation at Kodaikanal is mainly semi-diurnal and has a high negative correlation with the semi-diurnal components of the total and the electron intensities. The pressure coefficients are $\beta_T = -3.3$ % per cm. Hg. for the total intensity and $\beta_E = -9.6$ % for the electron component. On the other hand, the semi-diurnal component of the meson intensity has a very low positive correlation with the semi-diurnal pressure variation. The absence of a mass absorption coefficient for mesons indicates that during the atmospheric oscillations responsible for the semi-diurnal pressure variation at Kodaikanal, there are changes in the height of the meson formation layer or temperature in the upper atmosphere, which mask this effect. The small positive effect experimentally observed is not significant and does not give a clue to the precise nature of the mechanism due to which the mass absorption effect is obliterated.

Compared to what is observed at Ahmedabad which is nearly at sea-level and at a somewhat higher geomagnetic

latitude (13°N.), the effects of the meteorological factors at Kodaikanal on the total, meson and the electron components are smaller and contribute less to the daily variations. When the cosmic ray data at both these places are corrected for the variations of the atmospheric pressure and the ground temperature wherever a significant correlation has been found, there remains a strongly diurnal residual variation at both places. For Kodaikanal, the variation of mesons has an amplitude of about 1.0 % and the hour of maximum is at about 0930 hr. At Ahmedabad, it has an amplitude of about 0.5 % and the hour of maximum is at about 1100 hr.

The results can be compared to those obtained at Hafelekar (geomag.lat. 47°N, altitude 2300 m.), Huancayo (geomag. lat. 1°S, altitude 3350 m.), Christchurch (geomag. lat. 49°S, altitude 8 m.), Cheltenham (geomag. lat. 50°N, altitude 72 m.) and Godhavn (geomag.lat.80°N, altitude 9 m.), where the measurements were made with ionisation chambers and showed a predominently diurnal trend in the daily variation. Fig. 29 (p. 148) gives the harmonic dial for the first harmonics of the variations of the meson intensity at these places together with the first harmonics of the residual variations obtained by us at Kodaikanal and Ahmedabad.

VI.

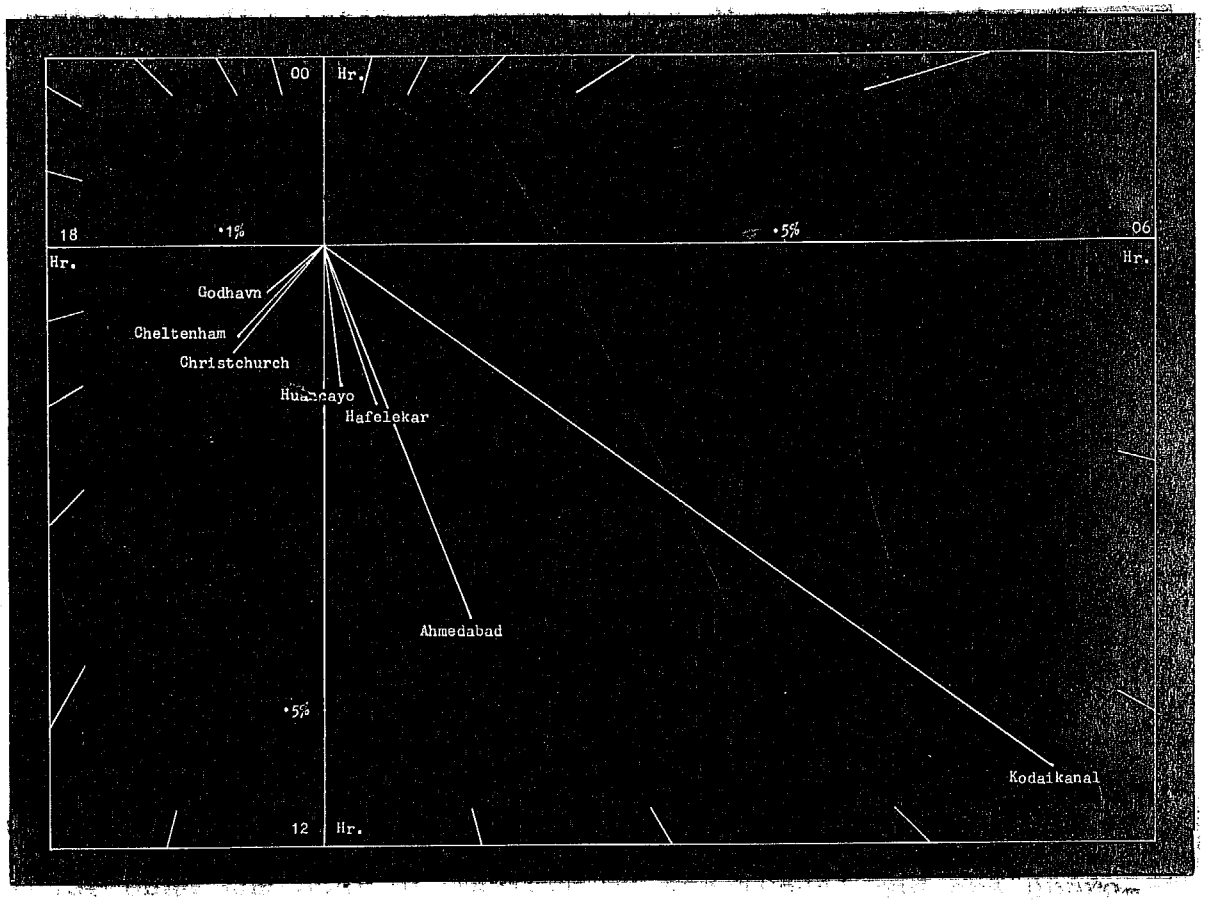

Fig. 29. Harmonic dial for the first harmonics of the pressure corrected daily variations at Kodaikanal, Ahmedabad, Hafelekar, Huancayo, Christchurch, Cheltenham and Godhavn.

The pronounced residual diurnal variation which remains after correcting for the meteorological elements near the ground, is unlikely to be caused by meteorological changes in the upper atmosphere which have a totally insufficient amplitude of diurnal variation according to existing meteorological knowledge. The diurnal changes in geomagnetic elements are also unlikely to cause the residual

variation. The nature of the magnetic variations changes radically with latitude whereas the diurnal variation of cosmic ray intensity has a similar form at places as far separated as Kodaikanal, Ahmedabad, Hafelekar, Huancayo, Christchurch, Cheltenham and Godhavn.

The increase in the percentage amplitude of the residual diurnal variation of the total and the meson intensities in going from Ahmedabad to Kodaikanal is most probably an effect of altitude rather than of change of latitude. This is in agreement with the increase of amplitude found at the two high level stations of Hafelekar and Huancayo as compared to the low level stations of Christchurch, Cheltenham and Godhavn. The hours of maxima for the first two stations are approximately three hours later than the hour of maximum at Kodaikanal and are approximately three hours in advance of the hours of maxima for the last three stations. This shift of the hour of maximum to later hours at low level stations is also seen between Kodaikanal and Ahmedabad, the latter station having a maximum about two hours later than the former. In comparing the hours of maxima obtained with our apparatus with those with ionisation chambers, the difference in the aperture of the two types of apparatuses should be kept in mind.

The lower percentage amplitude of the diurnal variation observed with ionisation chambers at Huancayo,

Christchurch, Cheltenham and Godhavn as compared to the percentage amplitude found with vertically pointing counter telescopes at Kodaikanal and Ahmedabad, must be attributed to the difference in the apparatus. Ionisation chambers which can register intensity from all directions of the sky, are expected to reveal a lower amplitude of the variation than telescopes measuring intensity coming through a restricted solid angle from the vertical. This is particularly true for variations of non-meteorological origin due to anisotropy in space of the primary cosmic radiation.

The dependence of the residual diurnal variation on local time, its low correlation with terrestrial meteorological and magnetic elements, and the increase of its percentage amplitude with elevation, lead one to believe that the variation may be connected with a direct emission of moderate and low energy cosmic rays from the sun. This is also supported by the observation that the day-to-day changes of cosmic ray intensity at Kodaikanal are more pronounced for the day-time values than for the night time values. If there is an emission of low energy cosmic rays from the sun, the following consequences would follow, which can be experimentally tested.

(1) The percentage amplitude of the diurnal variation would depend on the altitude of the station and would increase further for stations higher than Kodaikanal.

(2) The amplitude would alter with the sun's zenith angle, and would have a seasonal variation with maximum amplitude in the summer.

(3) For telescopes pointing East and West, there would be an alteration of the phase of the diurnal curve. Whether the hour of maximum is before or after local noon, would depend on the sign of the particles causing the anisotropy in the primary cosmic rays.

Experiments have been planned to test these consequences. However, the present tentative conclusion for the ascribing of the residual diurnal variation to low and medium energetic particles from the sun, is supported by

(a) occasional large increases in cosmic rays, associated with solar flares,

(b) recent work by Simpson[68] associating variations of cosmic ray neutrons with solar prominences,

(c) large diurnal variation of star intensity reported by Schein[69] for the upper atmosphere.

TABLES.

FIGURES.

REFERENCES.

1. Duperier. Proc. Phys. Soc., 57, 468, 1945.
2. " " 62, 684, 1949.
3. " Nature, Lond., 167, 312, 1951.
4. Hogg. Memoirs of the Commonwealth Observatory, Canberra, No.10, 1949.
5. Chapman. Nature, Lond., 140, 423, 1937.
6. Forbush. Terr. Magn. Atmos. Elect., 43, 207, 1938.
7. Johnson. Rev. Mod. Phys., 10, 193, 1938.
8. Alfven. Nature, Lond., 158, 618, 1946.
9. " Phys. Rev., 75, 1732, 1949.
10. Lange and Forbush. Terr. Magn. Atmos. Elect. 47, 331, 1942.
11. Ehmert. Z. NaturForsch. 39, 264, 1948.
12. Clay. Proc. K. Ned. Akad. Wet. 52, 906, 1949.
13. Menzel and Salisbury. Nucleonics 2, No.4, 67, 1948.
14. Forbush, Gill and Vallarta. Rev. Mod. Phys. 21, 44, 1949.
15. Forbush. Phys. Rev. 54, 975, 1938.
16. " Rev. Mod. Phys. 11, 168, 1939.
17. Hess. Terr. Magn. Atmos. Elect. 41, 345, 1936.
18. Hogg. Proc. Roy. Soc. A 192, 128, 1947.
19. Blackett. Phys. Rev. 54, 973, 1938.
20. Vallarta and Godart. Rev. Mod. Phys. 11, 180, 1939.
21. Thiessen. Z. Astrophys. 26, 16, 1949.
22. " The Observatory, 69, 228, 1949.

23. Kluber. Mon. Not. R. Astr. Soc. Vol.III, No.1,2, 1951.

24. Elliot and Dolbear. J. Atmos. Terr. Phys. 1,205, 1951.

25. Duperier. Nature, Lond. 158, 196, 1946.

26. Hogg. J. Atmos. Terr. Phys. 1, 114, 1950.

27. Nicolson and Sarabhai. Proc. Phys. Soc. 60, 509, 1948.

28. Lindholm. Gerl. Beitr. Z. Geophys. 20, 12, 1928.

29. Rau. Z. Phys. 114, 265, 1939.

30. " . " " 116, 105, 1940.

31. Barnothy and Forro. Phys. Rev. 55, 868, 1939.

32. Kolhorster. Z. Phys. 42, 55, 1941.

33. Alfven and Malmfors. Ark. Mat. Astr. Fys. 29, No. 24, 1943.

34. Sarabhai. Proc. Ind. Acad. Sc. A 21, 66, 1945.

35. Elliot and Dolbear. Proc. Phys. Soc. A 63,137, 1950.

36. Compton, Bennett and Stearns. Phys. Rev. 41,119,1932.

37. Steinmaurer. Gerl. Beitr. Z. Geophys. 45, 148, 1935.

38. Hess and Graziadei. Terr. Magn. Atmos. Elect. 41, 9, 1936.

39. Doan. Phys. Rev. 49, 107, 1936.

40. Forbush. Terr. Magn. Atmos. Elect. 42, 1, 1937.

41. Schonland, Delatizky and Gaskell. Terr. Magn. Atmos. Elect. 42, 137, 1937.

42. Thompson. Phys. Rev. 54, 93, 1938.

43. Lange and Forbush. Carnegie Institution of Washington Publication 175, 1948.

44. Barnothy and Forro. Z. Phys. 100, 742, 1936.

45. " " " . 104, 534, 1937.

46. Regener and Rau. Naturwiss. 27, 803, 1939.

AUTHOR INDEX.

The numbers given in brackets refer to the pages of this thesis where the reference occurs.

Dolbear,
see Elliot.

Duperier,
1944 ——— Terr. Magn. Atmos. Elect. 49, 1. (119).

1945 ——— Proc. Phys. Soc. 57, 468. (2,4,10,16,18,19).

1946 ——— Nature London, 158, 196. (8).

1949 ——— Proc. Phys. Soc. A62, 684. (2,8,73,116,120, 128,129).

1951 ——— Nature London, 167, 312. (3).

Ehmert,
1948 ——— Z. Naturforsch, 3(a), 264. (4, 5).

Elliot,
1950 ——— and Dolbear, Proc. Phys. Soc. A 63, 137. (10, 12, 14).

1951 ——— " J. Atmos. Terr. Phys. 1, 205. (7, 8, 13, 15, 120).

Forbush,
1937 ——— Terr. Magn. Atmos. Elect. 42, 1. (11).

1938 ——— Phys. Rev. 54, 975. (6).

1938 ——— Terr. Magn. Atmos. Elect. 43, 207. (4).

1939 ——— Rev. Mod. Phys. 11, 168. (6).

1949 ——— Gill and Vallarta, Rev. Mod. Phys. 21, 44. (6).

Forro,
see Barnothy.

Freier,
1948 ——— et al. Phys. Rev. 74, 213. (18).

Gaskell,
see Schonland.

Gill,
see Forbush.

Godart,
see Vallarta.

Go Pok Oen,
see Woltjer.

Graziadei,
see Hess.

Greisen,
1942 ——— and Nereson, Phys. Rev. 62, 316. (25).

Hess,
1936 ——— and Graziadei, Terr. Magn. Atmos. Elect. 41, 9. (11).

1936 ——— Terr. Magn. Atmos. Elect. 41, 345. (6,7,128).

Hogg,
1947 ——— Proc. Roy. Soc. A 192, 128.(6,7,120,126).

1949 ——— Memoirs of the Commonwealth Observatory, Canberra, No. 10. (4, 11).

1950 ——— J. Atmos. Terr. Phys. 1, 114. (8).

Johnson,
1938 ——— Rev. Mod. Phys. 10, 193. (4).

see Stevenson.

Kay,
1952 ——— Meteorological Magazine, 81, 21. (129).

Kluber,
1951 ——— Mon. Not. R. Astr. Soc. Vol.III, No.1,2.(7).

Kolhorster,
1939 ——— Z. Phys. 40, 142. (119, 120).

1940 ——— " 42, 55. (10, 12).

Korff,
——— Electron and Nuclear counters - Theory and Use. (40 to 51).

Lange,
1942 ——— and Forbush, Terr. Magn. Atmos. Elect. 47, 331. (4).

1948 ——— " Carnegie Institution of Washington Publication, 175, (11, 13).

Lindholm,
1928 ——— Gerl. Beitr. Z. Geophys. 20, 12. (10).

Lord,
see Schein.

MacAnuff,
1951 ——— Ph.D. Thesis London. (11).

Malmfors,
1945 ——— Ark. Mat. Astr. Phys. 32 A, No.8. (13, 14).

see Alfven.

Menzel,
1948 ——— and Salisbury, Nucleonics 2, No.4, 67. (5).

Messerschmidt,
1932 ——— Z. Phys. 78, 688. (119).

Montogomery,
1940 ——— and Montogomery, Phys. Rev. 57, 1030. (41).

1941 ——— " J. Franklin Inst. 231,447.(39).

Nereson,
see Greisen.

Nicolson,
1948 ——— and Sarabhai, Proc. Phys. Soc. 60, 509. (8, 16, 17).

Pekeris,
1937 ——— Proc. Roy. Soc. A 158, 650. (16).

1939 ——— " A 171, 631. (16).

Rau,
1939 ——— Z. Phys. 114, 265. (10, 11).

1940 ——— " 116, 105. (10, 11).

see Regener.

Regener,
1939 ——— and Rau, Naturwiss. 27, 803. (11, 15, 19).

Robinson,
see Whittaker.

Salisbury,
see Menzel.

Sarabhai,
1945 ——— Proc. Ind. Acad. Sc. A 21, 66. (10, 11).

see Nicolson.

Schein,
1950 ——— and Lord, Phys. Rev. 80, 304. (151).

Schonland,
1937 ——— Delatizky and Gaskell, Terr. Magn. Atmos. Elect. 42, 137. (11).

Simpson,
1951 ——— Phys. Rev. 81, 639. (151).

Smith,
1945 ——— Intensity coefficients of Cosmic ray components (Uni. of Washington Thesis). (119, 120).

Stearns,
see Compton.

Steinmaurer,
1935 ——— Gerl. Beitr. Z. Geophys. 45, 148. (11, 120).

Stevenson,
1935 ——— and Johnson, Phys. Rev. 47, 578. (119, 121).

Stever,
1942 ——— Phys. Rev. 61, 38. (43).

Swann,
1933 ——— Phys. Rev. 43, 217. (5).

Thiessen,
1949 ——— Zeits. Astrophys. 26, 16. (7).

1949 ——— The Observatory. 69, 228. (7).

Thompson,
1938 ——— Phys. Rev. 54, 93. (11).

Turner,
see Compton.

Vallarta,
1939 ——— and Godart, Rev. Mod. Phys. 11, 180. (7,13).

see Forbush.

Whittaker,
——— and Robinson, The Calculus of Observations.(76).

Woltjer,
1950 ——— and Go Pok Oen, Physica. 16, 122. (11).